DEPARTMENT OF BIOMOLECULAR SCIENCES

PH.D. COURSE IN:

LIFE SCIENCES, HEALTH AND BIOTECHNOLOGIES

CURRICULUM:

BIOCHEMICAL AND PHARMACOLOGICAL SCIENCES AND BIOTECHNOLOGY

XXXIII° CYCLE

UBIQUITIN EXPRESSION IN PRIMARY 23132/87 AND METASTATIC MKN45 GASTRIC CANCER CELL LINES AND DIFFERENTIAL RESPONSE TO POLYUBIQUITIN *UBB* AND *UBC* GENE SILENCING

SSD: BIO/11

Supervisor

Prof. Marzia Bianchi

Ph.D. Student

Dr. Filippo Tasini

ACADEMIC YEAR 2019-2020

Abstract

Gastric cancer is one of the most lethal tumors worldwide; it ranks as the 5th most common malignancy and the 3rd most lethal, with over 1 million new diagnoses and over 780'000 deaths in 2018 alone. The outcome of the disease is greatly influenced by tumor stage at the time of diagnosis; unfortunaterly, most patients are diagnosed only after the tumor has already metastasized, which dramatically reduces their chances of survival. Therefore, additional knowledge regarding gastric cancer is needed to define possible biomarkers and therapeutic targets that may respectively improve early detection protocols and treatment.

To this end, we compared the asset and regulation of ubiquitin pools in two gastric cancer cell lines: the primary line 23132/87 and the metastatic MKN45. The two cell lines were analyzed in various aspects, such as the relative ubiquitin content and the expression patterns of the four ubiquitin genes *UBC, UBB, UBA52* and *RPS27A*; the mRNA and protein levels of three transcription factors, HSF1, YY1 and SP1, were also measured in light of their involvement in the regulation of some of the ubiquitin genes.

Then we performed a series of siRNA-mediated knockdown experiments targeting the two polyubiquitin genes *UBB* and *UBC* to investigate if and how different alterations of the ubiquitin content would affect the two cell lines. To briefly summarize our results, the primary gastric cancer cell line 23132/87 exhibits a higher reliance on its endogenous ubiquitin production for survival than the metastatic line MKN45, identifying *UBB* and *UBC* as pro-survival genes in 23132/87 primary cells.

Chapters 1 and 2 respectively contain an introduction to gastric cancer and the ubiquitin system, the major topics addressed in this thesis.

Chapter 3 lists the research objectives.

Chapter 4 includes the rationale, methods and results concerning the characterization and comparison of the two gastric cancer cell lines 23132/87 and MKN45, regarding the expression of ubiquitin genes and their reliance on the intracellular content of ubiquitin. The article reported therein summarizes the greater part of the research work I have done during my Ph.D.

Chapter 5 comprehends the knowledge base that constituted the foundations of our investigation of gastric cancer. My contribution to the displayed manuscript consisted in performing a series of transfection experiments in several cell lines (both normal and tumor-derived), in order to find out if the downregulation of *UBC* caused by the ectopic expression of ubiquitin could be found in cell lines other than HeLa. Mycoplasma detection was also performed by me in all cell lines tested.

Chapter 6 and 7 contain the concluding remarks and references respectively.

TABLE OF CONTENTS

ORIGINAL PAPERS

This Thesis is based on the following original research articles, which will be referred to by their Roman numerals.

I.   Scarpa ES, Tasini F, Crinelli R, Ceccarini C, Magnani M, Bianchi M. *The Ubiquitin Gene Expression Pattern and Sensitivity to UBB and UBC Knockdown Differentiate Primary 23132/87 and Metastatic MKN45 Gastric Cancer Cells*. Int. J. Mol. Sci. 2020;21(15):5435.

II.   Bianchi M, Crinelli R, Giacomini E, Carloni E, Radici L, Scarpa ES, Tasini F, Magnani M. *A negative feedback mechanism links UBC gene expression to ubiquitin levels by affecting RNA splicing rather than transcription.* Sci. Rep. 2019;9(1):18556. Published 2019 Dec 6. doi:10.1038/s41598-019-54973-7.

CHAPTER 1: AN INTRODUCTION TO GASTRIC CANCER

1.1 Epidemiology

Gastric cancer (GC) is one of the most lethal tumors worldwide. According to the most recent estimates it ranks as the 5th most common malignancy and the 3rd most lethal, with over 1 million new diagnoses and over 780'000 deaths in 2018 alone.

Gastric cancer is the leading cause of cancer death in several Western Asian countries, such as Iran, Turkmenistan and Kyrgyzstan, while its incidence rates are especially elevated in Central and Eastern Asia (e.g. in Mongolia, China, Japan and Republic of Korea, which exhibits the highest incidence in the world). Other high risk zones are Russia and Central and South America (Bray F et al. 2018; Rawla P, Barsouk A. 2019).

1.2 Classification

While more than 90-95% of gastric cancer cases are adenocarcinomas (Balakrishnan M et al. 2017; WCRF/AICR; 2018), which arise from the glands of the most superficial layer of the stomach (the mucosa), they are individually very heterogeneous and their classification into subtypes is not straightforward. Gastric adenocarcinomas are primarily classified as cardia and non-cardia based on their anatomic site. Cancers of the gastric cardia arise in the region adjoining the esophageal-gastric junction and share epidemiological characteristics with esophageal adenocarcinoma. Non-cardia cancer is more common and arises in the lower (or distal) portion of the stomach (Rawla P, Bardouk A. 2019). Over the years several systems have been devised for the classification of non-cardia gastric cancer, but the most widely utilized is Lauren's classification, which divides gastric cancer in two major subtypes, namely intestinal and diffuse.

Intestinal type gastric cancer grows in more shallow fashion, is significantly larger in size before infiltrating the serous membrane and has a higher incidence of blood vessel invasion and liver metastases. It shows a predominance of glandular epithelium with well-differentiated cells, similar to intestinal columnar cells, good cellular cohesion and a pushing margin at the invasive edge (Grabsch HI, Tan P. 2013). Patients with intestinal-type gastric cancer are on average 7 years older at the time of diagnosis (Grabsch HI, Tan P. 2013) and the disease generally arises from premalignant lesions, such as atrophic gastritis followed by intestinal metaplasia and dysplasia. The progression into cancer may take several years or even decades and is aided by the chronic inflammatory state induced by *Helicobacter pylori* infection, often found in patients affected by intestinal-type GC (McLean MH, El-Omar EM. 2014).

Diffuse type GC tends to spread more commonly via the lymphatics to the pleura and peritoneum. The tumor mass is composed of scattered poorly cohesive cells or small clusters of cells with little or no gland formation and a diffuse infiltrative margin. Tumor cells are

undifferentiated, may contain mucus and can have a signet ring cell appearance (Grabsch HI, Tan P. 2013). Diffuse type GC does not seem to follow any neoplastic progression but arises from normal gastric mucosa with no definite pre-malignant stage. *H. pylori* infection is often negative (McLean MH, El-Omar EM. 2014).

There are also GC cases that exhibit mixed or unidentifiable features and cannot therefore be classified as diffuse or intestinal. The relative frequencies are approximately 54% for intestinal type, 32% for diffuse, and 15% for indeterminate type, although this distribution varies in different geographical regions, age groups and socioeconomic conditions.

Intestinal types are more common in males and older adults, whereas diffuse types may occur in all age groups with equal sex distribution and show more rapid progression and poorer prognosis.

It is important to underline that all information and experimental data contained in this thesis regard only the non-cardia subtype of gastric cancer.

1.3 Environmental Risk factors

Gastric cancer pathogenesis shows a strong environmental component. *Helicobacter pylori* infection has been proposed as one of the causes of GC since the 1990s (Forman D et al. 1991), when it was declared a class I carcinogen (IARC. 1994), and is now considered the main risk factor, as the risk of developing gastric cancer was found to be 20-fold, or even higher, in the presence of *H. pylori* infection (Lazăr DC et al. 2016; Sitarz R et al. 2018). In particular, the infection has a very strong association with intestinal-type gastric cancer, while it is less likely to be found in diffuse-type cases. The chronic inflammatory background induced by *H. pylori* infection fosters premalignant changes in the gastric epithelium, starting with atrophic gastritis, followed by intestinal metaplasia and dysplasia, which in turn develops into gastric tumor. This progression is typical of intestinal-type gastric cancer (McLean MH, El-Omar EM; 2014). According to recent estimates, 84% of all GC patients test positive for *H. pylori* infection (WCRF/AICR; 2018) and as many as 90% of all cases can be attributed to *H. pylori* (Balakrishnan M et al. 2017).

H. pylori is a gram-negative bacterium able to colonize the human stomach; the infection is predominantly acquired in early infancy, remains present indefinitely if not treated with antibiotics (Correa P. 2013), and elicits life-long inflammatory responses, including the release of various bacterial and host-produced cytotoxic substances (Feldman M et al. 2020).

The infection is usually asymptomatic, but it is also widely spread: *H. pylori* prevalence has demonstrated great variability determined by factors such as geographic location, age, ethnicity and socioeconomic conditions. For these reasons, it is usually high in developing regions, where *H. pylori* infection represents a public health issue, and lower in developed countries. Its prevalence can show variability within regions of different countries and between more crowded urban and rural areas, mostly due to socioeconomic differences between the inhabitants (Lazăr DC et al. 2016). Globally, *H. pylori* infects 50% of the population and prevalence

increases with age (Ando T et al. 2006; Singh K, Ghoshal UC. 2006). Average *H. pylori* prevalence is 35% in high-income countries and 85% in low-income countries (Ang TL, Fock KM. 2014). The highest prevalence is in Asia; in South Korea, the infection reaches 90% at age 20 years (Youn HS et al. 1998). Regions with high stomach cancer incidence rates tend to have high seroprevalence rates for *H. pylori* infection. However, in some regions of Africa and South Asia, particularly India, *H. pylori* infection rates are high, but stomach cancer incidence rates remain low (Singh K, Ghoshal UC. 2006). This could be explained by studies on genomic sequencing and post-genomic analyses *of H. pylori*, which hyphothesize that the bacterium might once have been a symbiotic component of the human biome.

While *H. pylori* infection increases the risk of non-cardia gastric cancer, it also reduces acid secretion in the proximal portion of the stomach, thus having protective effects on gastro-esophageal reflux, esophageal adenocarcinoma and cardia GC, as it reduces risk of esophageal inflammation (Rawla P, Barsouk A. 2019).

Although international variation in *H.pylori* prevalence correlates reasonably with that of stomach cancer incidence, other risk factors have been proposed (Bray F et al. 2018); among these are consumption of salt-preserved foods, Epstein-Barr virus (EBV) infection, active tobacco smoking, alcohol consumption, obesity and certain occupations (WCRF/AICR, 2018; IARC, 2012). Evidence from preclinical studies suggests that *H. pylori* interacts with dietary factors such as salt to affect cancer risk (Gaddy JA et al. 2013). Research mainly relates to high-salt foods and salt-preserved foods, including pickled vegetables, processed meat and salted or dried fish (WCRF/AICR, 2018).

Epstein-Barr virus, member of the Herpesviridae family, is mainly known as the cause of infectious mononucleosis and for its association to various lymphoproliferative diseases such as Burkitt's and Hodgkin's lymphomas, but may also have a causal role in gastric carcinogenesis (Sitarz R et al. 2018). According to recent estimates, about 10% of all GC cases present EBV infection. The association between EBV and gastric cancer is highest in Germany and USA (16-18%) and lowest in China (4,3%) (Iizasa H et al. 2012).

Regarding tobacco smoking, both current and former smokers have an increased risk of gastric cancer compared with people who have never smoked, with estimates of increased risk ranging from 1.5–2.5 times that of never-smokers. The risk increase is larger in men than in women, but a dose-response relationship is apparent in both (Freedman ND et al. 2007; Sjodahl et al. 2007; Tredaniel J et al. 1999).

Occupational exposure to dusty and high-temperature environments, such as in wood processing and food machine-operating occupations, has been associated with increased risk of stomach cancer, particularly diffuse type cancer (Santibañez M et al. 2012). Exposure to other dusty environments, such as in rubber manufacturing, coal mining and metal processing, has also been implicated (Raj A et al. 2003). Finally, male sex is also a risk factor: males exhibit a 2-fold higher risk of developing gastric cancer than females (Karimi P et al. 2014).

1.4 Inheritable Genetic components

Gastric cancer carcinogenesis and progression result from a combination of both environmental factors and accumulation of specific genetic alterations, including activation of oncogenes,

overexpression of growth factors and receptors, inactivation of tumor suppressor genes, DNA repair genes and cell adhesion molecules. Most of these alterations are acquired randomly in the population, while only few have been documented to be hereditary. It follows that the majority of GC cases arise sporadically and show no apparent inherited component.

Familial clustering is observed in 10 to 15% of gastric cancer cases and most of these are not associated with a definite germline mutation.

Only less than 3% of gastric carcinomas arise from inherited gastric cancer predisposition syndromes, such as Hereditary Diffuse Gastric Carcinoma (HDGC), familial adenomatous polyposis, Hereditary Nonpolyposis Colorectal Carcinoma (HNPCC or Lynch syndrome), juvenile polyposis syndrome, Peutz-Jeghers syndrome, Li-Fraumeni syndrome and gastric hyperplastic polyposis (Hu B et al. 2012).

The most frequent is Hereditary Diffuse Gastric Cancer (Carneiro F. 2012; Oliveira C et al. 2013), an automosomal dominant pathology characterized by high penetrance and a heterozygous germline mutation. Approximately 30% of HDGC patients and 45% of the identified HDGC families harbor germline mutations of CDH1, the tumor suppressor gene that encodes cadherin 1 (or E-cadherin), a protein with an essential role in cell-cell adhesion (Hu B et al. 2012; Paredes J et al. 2012).

The mutation in CDH1 can take many forms (such as a deletion, frameshift, splice-site or missense mutations) that may involve a variety of sites in the gene and is not only restricted to coding regions but could include untranslated regions as well. A loss-of-function mutation in the remaining allele can be caused by a number of mechanisms, such as loss of heterozygosity or promoter hypermethylation, and can lead to gastric cancer (McLean M, El-Omar EM. 2014). The estimated lifetime risk for HDGC in proven mutation carriers is more than 80% in both men and women by age 80 (Oliveira C et al. 2013). Given the high penetrance of CDH1 mutation, prophylactic total gastrectomy after confirmation through CDH1 molecular testing is the only recommended way to save patients' lives (Hu B et al. 2012).

CDH1 mutations have only been found in hereditary and sporadic diffuse type, but not in intestinal type GC (Grabsch HI, Tan P. 2013).

Patients with hereditary nonpolyposis colon cancer suffer an increased risk of intestinal-type gastric cancer, which arises from mutations in DNA mismatch repair genes such as MSH2 or MLH1. These events in turn increase the mutation rate in oncogene and tumour suppressor genes, which leads to cancer initiation and progression. Microsatellite instability is also a key characteristic of this pathology. Gastric cancer seems to be a common extracolonic manifestation of HNPCC, with a 2 to 19-fold increased risk of GC in patients with this syndrome compared to the general population; geographical location correlates with the level of increased risk (McLean MH, El-Omar EM. 2014). According to a study conducted in Northern Europe and the USA, the lifetime risk of gastric cancer in families with HNPCC is around 7%, occurring primarily in subjects over 50 years of age (Watson P et al. 2008).

In contrast, GC patients with germline mutations in one of the DNA mismatch repair genes (hereditary nonpolyposis colon cancer patients) show intestinal type morphology in 79% of cases (Grabsch HI, Tan P. 2013; Gylling A et al. 2007).

1.5 Acquired genetic factors

As most cases of GC are sporadic, acquired mutations play a great role in GC carcinogenesis. These genetic abnormalities can result from several mutagenic events, such as chromosomal and microsatellite instability (CSI and MSI; respectively), alterations in the epigenetic landscape and somatic gene mutations (McLean M, El-Omar EM. 2014). Given the highly variable nature of genetic mutations and the fact that many can occur and be accumulated by a single individual or even by a single tumor, gastric cancer, as all other malignant pathologies, exhibits intrapatient and interpatient heterogeneity (Renovanz M, Kim EL. 2014).

Chromosomal instability is defined by a change in the DNA content, with loss or gain of whole or large portions of chromosomes leading to altered DNA copy number and consequentially to loss or gain of function of oncogenes and tumor suppressors (McLean M, El-Omar EM. 2014). Chromosomal Instability has been detected as the most common feature of sporadic gastric cancers and has been reported in up to 84% of gastrointestinal tumours (Hudler P. 2012). A large variety of chromosomal aberrations have been identified in GC patients and different anomalies have been associated to patient age, geographical background and prognosis; particularly relevant in this context is the association of certain aberrations to GC histology: for example, intestinal type GC is associated with copy number gains at 8q, 17q and 20q, while diffuse type GC has been linked with copy number gains at 12q and 13q (Hudler P. 2012; Tomioka N et al. 2010; Tsukamoto Y et al. 2008).

Microsatellite instability is a condition arising from deficiency or inactivation of one or more DNA mismatch repair genes (Li K et al. 2020) of the DNA mismatch repair genes, such as MLH1, MSH2, MSH6 and PMS2, which in turn renders the naturally occurring DNA replication errors impossible to repair. In this scenario, hundreds of thousands of somatic mutations (e.g. insertions or deletions) accumulate in microsatellite DNA, which consists of short, repeated sequences randomly interspersed in the human genome. GC tumors can be categorized into those with high or low levels of MSI, depending on the frequency of mutations within a specific set of microsatellite markers. Tumors that show no instability in any of the markers are defined as stable.

MSI can lead to genetic anomalies in hundreds to thousands of genes and cause the appearance of new alleles not normally present: this condition takes the name of "MSI phenotype" or "DNA replication phenotype" (Oliveira C et al. 1998; Grabsch HI, Tan P. 2013). The reported frequency of MSI for GC varies between 11,68 and 33,82%, strongly depending on the number of loci examined (Zhu L et al. 2015).

GC tumors can be categorized into those with high or low levels of MSI, depending on the frequency of mutations within a specific set of microsatellite markers. Surprisingly, according to a meta-analysis study conducted in 2015, gastric cancer patients with a high rate of MSI show improved prognosis and reduced risk of lymphnode metastasis, tumor invasion and mortality (Zhu L et al. 2015).

The most common cause of MSI in GC cases is the hypermethylation of the MLH1 gene promoter, with consequent impairment of its transcription (Fleisher AS et al. 1999). As a matter

fact, aberrant methylation of CpG regions and silencing of tumor suppressor genes can be found in up to 50% of all GC cases (Grabsch HI, Tan P. 2013), and takes the name of CpG Island Methylator Phenotype (CIMP). In addition to MLH1, many other genes are silenced due to aberrant methylation, such as CDK2A and APC (Liu JB et al. 2012; Toyota M et al. 1999). Tumors that test positive for *H. pylori* infection also show a generally higher CpG methylation rate compared to *H. pylori* negative tumors, as do EBV-positive tumors (Cancer genome atlas research network, 2014; Liu JB et al. 2012).

There any many genes known to be subject of somatic mutations in gastric cancer. A comprehensive list would be beyond the scope of this thesis, thus the ones reported below will be limited to the most relevant examples.

Human Epidermal Growth Factor Receptor 2 (HER2) is a tyrosine kinase without any known direct activating ligand and is classified as an oncogene. *HER2* overexpression has been reported in up to 27% of intestinal type GC cases, but only rarely in diffuse type GC cases (Gravalos C, Jimeno A. 2008). While *HER2* amplification has been proposed as a marker of poor prognosis in GC patients, the relation is still regarded as controversial, with several studies reporting contradicting findings (Grabsch H et al. 2010; Okines AF et al. 2013).

K-Ras is GTPase mainly known for its role in the RAS/MAPK pathway and its high mutation rates in various cancers, including colorectal, pancreatic and lung cancer; the most common mutation sites in K-ras are codons 12 and 13. However, *KRAS* mutations are not as common in gastric cancer, in fact several studies report low percentages of cases with *KRAS* mutations ranging from 1,6 to 17,5% and a single study (conducted in Northeast Iran, a high risk area for GC) with a peak of 40% (Ayatollahi H et al. 2018; van Grieken NC et al. 2013). *KRAS* mutations are preferentially present in well-differentiated intestinal type GCs and are more frequently associated with microsatellite instability.

KRAS mutations on codons 12 and 13 have been found on average in 5% of GC and were preferentially present in well-differentiated intestinal-type GC (Corso G et al. 2011; Lee KH et al. 1995). In contrast to colorectal cancer, *KRAS* mutations in GC are more frequently seen in GC with MSI (Corso G et al. 2011; Wu M et al. 2004).

P53 is a nuclear protein involved in cell cycle control, DNA repair and programmed cell death, which is frequently inactivated in tumors by loss of heterozygosity (LOH) or point mutations of its encoding gene (*TP53*); more than one mutation may be present in a single tumor, resulting in heterogeneity of the p53 mutational status. *TP53* mutation is one of the most frequent genetic alterations in GC: there are conflicting results regarding the prevalence of *TP53* mutations and their relationship to histological type or tumor stage of GC. Some studies show that mutations tend to affect mainly intestinal-type tumors, while others found that the incidence of mutation is similar in both intestinal and diffuse-type tumors, ranging between 25% and 40% of the cases presented. Regarding tumor stage, p53 abnormalities appear to occur early in intestinal-type cancers, but some studies have shown that the frequency of *TP53* mutation in both early and advanced intestinal-type is consistent around 40% each, similar to that observed in the advanced diffuse-type, while *TP53* mutations are rare in early diffuse-type (Fenoglio-Preiser CM et al. 2003; Iwamatsu H et al. 2001; Liu XP et al. 2001).

APC (Adenomatous Polyposis Coli) is a multidomain protein with binding sites for numerous proteins including the Wnt pathway components β-catenin and Axin. APC plays a major role in cell adhesion, cell migration, spindle formation, and chromosome segregation. *APC* mutations are the second most frequent mutations in GC and have been observed in 30–40% of well- and moderately differentiated intestinal type GC and in up to 13% of diffuse type GC (Fang DC et al. 2002; Horii A et al. 1992). *APC* mutations have also been described in adenomas of the stomach and intestinal metaplasia, indicating that they occur during early stages of GC development (Nishimura K et al. 1995).

1.6 Importance of prevention
Globally, the incidence of gastric cancer has been steadily declining in the past 50 years, a trend that has been attributed to changes in lifestyle and environment, such as increasing smoking cessation, adoption of healthier dietary habits and, above all, *H. pylori* eradication (McLean M, El-Omar EM. 2014). In turn, the decline in prevalence of *H. pylori* infection is linked to improved food preservation practices such as refrigeration, which also directly favor consumption of fresh produce and reduce consumption of salt-preserved foods (WCRF/AICR 2018).

1.7 Importance of early detection
The 5-year survival rate is defined as the percentage of cancer patients that survive for at least 5 years after diagnosis; it is a very useful index to determine the trend over time of cancerous diseases. There have been great improvements in the 5-year survival rates for GC since the 1970s, but only minor progress has been made in recent years: for example, in the United States it went up from 15% in 1975 to 29% in 2009, to 32% in 2020 (Karimi P et al. 2014; ACS. Cancer facts & figures 2020). This statistic is heavily influenced by the fact that most GC patients are diagnosed after the cancer has already spread to other parts of the body. If the diagnosis happens before tumor metastatization, the 5-year survival rate is higher, but it depends on cancer stage. According to the most recent American estimates, the 5-year survival rate is 69% if the cancer is found and treated when it is still localized, 31% if it has spread to the surrounding tissues and organs, and 5% if it has already undergone distant metastatization (ACS Cancer facts & figures 2020). In most areas of the world, the average 5-year survival rate is currently around 20%. Survival rates are generally higher in high-income countries and other parts of the world where there are established services for screening and early detection of cancer as well as well-established treatment facilities (WCF/AICR 2018). A bright example is set by Japan, where rates above 70% have been reported; these results are attributed to the effectiveness of the mass screening programs employed by Japan (Katai H et al. 2018).
It is thus easy to see how early diagnosis of GC greatly improves patient survival, but diagnosis is usually delayed by a lack of early specific symptoms. Most patients are still diagnosed in advanced stages, resulting in poor 5-year survival rates, but also in short median survival times, less than 1 year for metastatic disease (Lazăr DA et al. 2016).

1.8 Treatment

Patient treatment regimens vary according to the stage of the tumor and the presence of metastases. When possible, surgical resection of the tumor mass (partial or total gastrectomy) and of the nearby lymphnodes is the main approach to gastric cancer treatment, supported by adjuvant chemotherapy or chemoradiation (Sitarz R et al. 2018).

Stage 0 and IA cancers can be treated by surgery alone and chemo- or radiotherapy is usually not required. Cancers that range from stage IB to III are similarly treated with surgical resection and chemo- or radiotherapy can be administered before and/or after the surgical procedure, depending on the severity of the disease, to reduce the size of the tumor and lower the chances of recurrence. Stage IV cancers, by definition, have spread to distant locations, such as the liver, lungs, brain or the peritoneum, and are usually incurable. In these cases, surgery and cycles of chemo- and/or chemoradiation therapy can still be administered, but treatment is palliative and aims at keeping the disease under control, relieving its symptoms, improving quality of life and extending life expectancy of patients (Smyth EC et al. 2016; ACS. Cancer Facts & Figures 2020).

However, even after complete resection, gastric cancer exhibits high rates of recurrence, ranging from 20 to even 50%; in most cases (60-70%) recurrence manifests within 2 years after surgery (Barchi LC et al. 2016; D'Angelica M et al. 2004; Marrelli D et al. 2005; Shin CH et al. 2016).

Targeted therapy is also being explored in the treatment of gastric cancer and a number of preclinical studies and clinical trials investigated several possible therapeutic targets, such as Vascular Endothelial growth Factor Receptor (VEGFR), Epidermal Growth Factor Receptor (EGFR), Poly-ADP-Ribose-Polymerase (PARP) among others (Lazăr DA et al. 2016). Trastuzumab (also known as Herceptin) is a monoclonal antibody specific for the Human Epidermal Growth Factor Receptor Type2 (HER2); originally employed for breast cancer therapy, its use is now permitted for gastric cancer, but only in cases that exhibit HER2 overexpression. Trastuzumab is usually administered in combination with capecitabine or 5-fluorouracil and cisplatin (Lazăr DA et al. 2016; Sitarz R et al. 2018). Another application of moleclular biology to the treatment of gastric cancer is the testing of the CDH1 gene status to screen high risk patients for Hereditary Diffuse Gastric carcinoma (Hu B et al. 2012).

CHAPTER 2: AN INTRODUCTION TO THE UBIQUITIN SYSTEM

2.1 Ubiquitin, a complicated molecule

Ubiquitin (Ub) is a small 8,6 kDa regulatory protein composed of 76 aminoacids. Discovered in 1975 by Goldstein et al. (Goldstein et al. 1975), it takes its name from its "ubiquitous" and abundant presence in all eukaryotic cells, where it constitutes 0,1-5% of the total protein content (Ryu KY et al. 2006).

The attachment of one or more ubiquitin molecules to a protein substrate is called ubiquitination (also known as ubiquitylation or ubiquitinylation) and it consists in a series of sequential reactions catalyzed by enzymes belonging to 3 (or even 4) different classes.

Ubiquitin is also highly conserved among different species: for example, the yeast and human analogues of ubiquitin only differ in 3 aminoacids. This remarkable grade of conservation is attributed to a strong selective pressure on the entire molecule as a result of the many functions it serves in the cell (Pickart CM, Eddins MJ. 2004) such as cell-cycle progression, DNA transcription and repair, apoptosis, modulation of cell surface receptors, cellular differentiation, response to cellular stresses and proteolysis (Pickart CM, Eddins MJ. 2004).

The attachment of a single ubiquitin molecule to a target substrate is called monoubiquitination, while the addition of two or more ubiquitin monomers to just as many residues of a substrate is defined as multi-monoubiquitination. However, additional ubiquitin moieties can be linked to any of the seven lysine residues or to the aminoterminal methionine of the ubiquitin molecule to form chains through subsequent rounds of conjugation; this process is known as polyubiquitination. Said chains may also be branched or linear and, in the latter case, the nature of the linkages can be homogeneous or heterogeneous. Taking into account the presence of multiple linkage sites on each ubiquitin molecule that is part of a chain and the possibility to attach more than one ubiquitin molecule to a given target, the versatility of this modification becomes apparent and is the reason of ubiquitin involvement in so many cellular functions (Guo HJ, Tadi P. 2020; Kim HC, Huibregtse JM. 2009; Lòpez-Mosqueda J, Dikic I. 2014).

Different kinds of ubiquitin modifications result in different outcomes for the target protein, such as proteosomal degradation, changes in cellular location, enzymatic activity or interactions with other proteins. However, the ultimate fate of a ubiquitylated protein depends not only on chain topology, but also on other factors like activity and availability of ubiquitylating and deubiquitylating enzymes, as well as of ubiquitin-binding proteins (Komander D, Rape M. 2012): whereas other post-translational modifications like phosphorylation produce an on-off binary signal, ubiquitylation could be defined as "analogical", given how tunable and diverse it can be (Mevissen TET, Komander D. 2017).

In the case of polyubiquitin chains, the specific linkages connecting the single ubiquitin monomers determine the spatial conformations of the chain. K29- K33-, K63- and M1-linked chains exhibit "open" linear and highly flexible conformations, where the ubiquitin molecules do not interact with each other except for the isopeptide bonds linking them. K6-, K11- and K48-linked chains have "closed" conformations which allow interaction between ubiquitin moieties. These conformations hide and expose different portions of the ubiquitin molecules, and constitute a vast array of geometries that can be specifically recognized by ubiquitin-conjugating enzymes, deubiquitinases (DUBs) and proteins that contain Ubiquitin-Binding Domains (UBDs) (Komander D, Rape M. 2012; Ye Y et al. 2012).

In the cell, the total ubiquitin pool is divided into free and conjugated ubiquitin pools which coexist in a dynamic equilibrium that adjusts in accordance to cellular needs (Park CW, Ryu KY. 2014). Indeed, due to the variety of its functions and large number of ubiquitylated substrates, ubiquitin is not constantly produced in excess, but its *de novo* synthesis increases only when cellular demand does, such as during proteotoxic stress. Ubiquitin recycling, mediated by deubiquitinating enzymes, also plays an important part in ubiquitin homeostasis (Kimura Y, Tanaka K. 2010; Bianchi M et al. 2018).

2.2 Ubiquitination and its mechanism

On a chemical standpoint, ubiquitination comprises 3 stages, each catalyzed by a specific class of enzymes, E1 (ubiquitin-activating enzymes), E2 (ubiquitin-conjugating enzymes) and E3 (ubiquitin ligases):

1) Activation – ubiquitin is activated in a two step ATP-dependent reaction. E1 binds to both a ubiquitin and an ATP molecule. The enzyme then catalyses the acyl-adenylation of the C-terminus of the ubiquitin molecule. Then, in the second step, the ubiquitin molecule is transferred to an active site on the E1 enzyme, constituted by a cysteine residue, with release of AMP and the formation of a thioester link between the C-terminal carboxyl group of ubiquitin and the E1 cysteine sulfhydryl group.

2) Conjugation – thanks to the action of an E2 enzyme, the activated ubiquitin is transferred from the E1 enzyme to the cysteine in the active site of E2 via a trans(thio)esterification reaction in which the E2 binds to both the E1 enzyme and the activated ubiquitin.

3) Ligation – at this point an E3 enzyme catalyzes the formation of an isopeptide bond between the C-terminal glycine of the ubiquitin molecule and a lysine residue on the target protein. The exact mechanism of the reaction differs according to the type of E3 involved and the binding domain it possesses: these mainly include the HECT (Homologous to the E6AP Carboxyl Terminus) domain and the RING (Really Interesting

New Gene) domain. HECT domain E3s transiently bind ubiquitin during the reaction, while RING domain E3s do not form a catalytic intermediate with ubiquitin and instead function as a scaffold that allows interaction between E2 and substrate (Kim HC, Huibregtse JM. 2009; Metzger MB et al. 2012). Other types of E3s contain U-Box domains, which function similarly to RING E3s, or RBR (RING in-between RING), which is a RING-type domain capable of forming a catalytic intermediate with ubiquitin in a similar manner to HECT domains (Nakagawa T, Nakayama K. 2015). Ligation is also the limiting step of the entire ubiquitination process.

2.3 Ubiquitination is highly specific

Ubiquitination is an extremely complex, but also highly specific modification; these characteristics depend on several factors:

First, there is great disproportion in the numerosity of E1, E2 and E3 enzymes. In humans, there are only 2 known ubiquitin-specific E1s (UBA1 and UBA6), whereas there are 35 different E2s and hundreds of E3s. However, these enzyme families also differ in their binding specificities: both E1s can bind many E2s, which in turn can bind hundreds of E3s; finally, every E3 can interact with a wide array of protein substrates (Pickart CM, Eddins MJ. 2004). The hierarchic flow of the process and the enormous variety of protein substrates determine the process specificity and also explain the wide array of cell functions that are affected by ubiquitination. The existence of E2 enzymes as a bridge between E1s and E3s also offers an additional layer of regulation, dependent on E2s concentration, activity and specificity for different E3s. Other Ubiquitin-like proteins (UBLs), such as SUMO, ISG15, Atg8 and Nedd8, are also modified through similar E1-E2-E3 cascades (Kerscher O et al. 2006).

E4s are a less known category of ubiquitin-related enzymes. E4s function as ubiquitin-chain elongation factors as, in the absence of E4s, the E1-E2-E3 cascade is capable of assembling only short ubiquitin chains on target substrates; the presence of an E4 is necessary to elongate those chains into longer ones, yielding substantially longer chains than those obtained with E1, E2 and E3 enzymes alone (Koegl M et al. 1999). E4 enzymes share a conserved "U-Box" domain, which is similar to the RING domain, but lacking its characteristic metal-chelating residues (Aravind L, Koonin EV. 2000).

E4-mediated ubiquitin chain elongation is also associated with efficient targeting of protein substrates to proteosomal degradation (Koegl M et al. 1999): for example, Shi D et al. demonstrated that the E3 activity of MDM2 also requires the E4 activity of the p300/CBP protein complex to achieve polyubiquitination and subsequent degradation of p53. The distinction between E3s and E4s however can be blurry, since E4s can posses E3 activity, as in the case of p300 (Shi D et al. 2009).

2.4 Deubiquitinating enzymes

Enzymes capable of removing or editing ubiquitin molecules attached to proteins are known as deubiquitinases or deubiquitinating enzymes (DUBs) and constitute a large group of proteases. The human genome encodes nearly a 100 DUBs, 79 of which are functional. DUBs are divided in 6 families: Ubiquitin C-terminal Hydrolases (UCH), Ubiquitin-Specific Proteases (USP), Ovarian Tumor Proteases (OTU), Machado-Josephin Domain proteases (MJD) and the recently discovered Motif Interacting with Ubiquitin-containing Novel DUB (MINDY) (Rehman ASA et al. 2016) are classified as cysteine proteases, while Jab1/Mov34/Mpr1 Pad1 N-terminal+ proteases (JAMM) are metalloproteases (Reyes-Turcu FE et al. 2009). Cysteine proteases are characterized by the presence of a cysteine residue in the active site which forms a covalent intermediate with ubiquitin during its removal from a protein substrate; JAMM metalloproteases employ a Zn^{2+} ion, stabilized by an aspartate and 2 histidine residues, to form a non-covalent intermediate with ubiquitin (Ambroggio XI et al. 2004; Nijman SM et al. 2005). The USP family, with its 54 members, is the most represented in humans (Mevissen TET, Komander D. 2017).

To regulate ubiquitin modifications, DUBs must be able to recognize ubiquitin; every DUB has at least one ubiquitin-binding site, named S1, that guides the ubiquitin C-terminus and the scissile bond into the active site. Some DUBs also exhibit additional ubiquitin-binding sites that contribute to linkage specificity. Indeed, some DUBs recognize and cleave specific types of ubiquitin chain, but they are often unable to remove the proximal ubiquitin, that is to say, the one that forms an isopeptide bond with the protein itself (Mevissen TET, Komander D. 2017); an example of a linkage-specificic DUB is OTULIN, which only targets linear Met1-linked chains (Keusekotten K et al. 2013). Conversely, other DUBs, like most USPs, lack said additional ubiquitin-binding sites and remove ubiquitin modifications in their entirety aspecifically, regardless of linkage and chain type (Faesen AC et al. 2011).

Another distinction between DUBs is the capability of endo- or exo-proteolysis: endoproteolytic activity results in the production of unanchored chains from substrates, which can be further processed into monoubiquitin, while exoproteolytic activity directly releases single ubiquitin monomers from substrates.

DUBs represent yet another layer of ubiquitin regulation, as they counteract the activity of ubiquitinating enzymes and are able to trim existing ubiquitin modifications without removing them entirely and thus modify their function. In a manner befitting their role in regulating all processes dependent on ubiquitin, the availability, localization and catalytic activity are kept under strict control (Sahtoe DD, Sixma TK. 2015).

2.5 Ubiquitin and substrate degradation

In eukaryotic cells, the 26S proteasome is the major contributor to protein degradation, both in the cytosol and in the nucleus. It allows a strict control of regulatory proteins such as cyclins,

CDK inhibitors, IκB and p53, while also disposing of misfolded and aberrant proteins (Finley D. 2009).

A complete proteasome is formed by three parts: a barrel shaped 20S core particle, in which the proteasome peptidase activity resides, and two 19S regulatory particles placed at both ends of the barrel-like structure of the 20S core (Bard JAM et al. 2018).

Proteosomal degradation is the most frequent result of ubiquitin tagging; this function is prevalently mediated by K48-linked Ub chains, which are the most abundant type of chain since many E3s, like the SCF complex or E6AP, regulate protein turnover through their synthesis (Petroski MD, Deshaies RJ. 2005; Kim HC, Huibregtse JM. 2009). Other chain types can also induce proteasomal degradation: K11-linked chains are required for the degradation of cell cycle regulators during mitosis (Matsumoto ML et al. 2010), while K29- and K63-linked chains have also been reported as capable of inducing substrate degradation (Johnson ES et al. 1995; Saeki Y et al. 2009).

The proteasome generally recognizes proteins targeted to degradation through the ubiquitin chains they are attached to; it is also important to note that the proteasome has a strong preference for polyubiquitin chains rather than monoubiquitin; longer the chain, better the interaction with the proteasome will be (Lee MJ et al. 2011; Thrower JS et al. 2000). After recognition, the substrate is processed by three deubiquitinases associated with the regulatory particle: Rpn11 cuts entire ubiquitin chains at the base, where the linkage with the substrate is (Yao T, Cohen RE. 2002), USP14 works in similar manner, but only removes supernumerary chains (Lee BH et al. 2016), while UCH37 can edit chains by cleaving single K48-, K11- and K6-linked ubiquitin moieties form the distal end (Lam YA et al. 1997; Lee MJ et al. 2011). Importantly, the editing or removal of substrate-attached ubiquitin chains by USP14 and UCH37 seem to have a regulatory role, since it may result in substrate detachment from the proteasome; thus USP14 and UCH37 might antagonize Rpn11 activity, which results only in substrate degradation (Bard JAM et al. 2019). The ubiquitin molecules that have been released from a substrate are for the most part available for utilization in the cell.

After the substrate has been committed to degradation, its tertiary structure is unraveled by six ATP-dependent proteases, organized in a ring structure named the AAA+ ATPase motor. The structure itself is constituted by three heterogenous protein dimers: Rpt1/Rpt2, Rpt6/Rpt3 and Rpt4/Rpt5. A particular feature of the heterohexamer is the N-ring, a pore that acts as a bottleneck through which the AAA+ motor pulls protein substrates to induce their unfolding through a series of conformational changes dependent on ATP hydrolysis (Bard JAM et al. 2019; Navon A, Goldberg AL. 2001). This channel is sufficiently narrow to allow entry to the core particle only to unfolded polypeptides and thus to prevent spurious degradation of cytoplasmic proteins and incorrectly processed substrates (Finley D. 2009; Lee C et al. 2002). Thanks to the AAA+ motor, each unfolded polypeptide is pulled into the 20S core cavity, in an act termed as translocation.

The core particle is formed by 28 subunits, derived from 14 gene products, and arranged into four heteroheptameric rings. Each ring contains three subunits, named β1, β2 and β5, with

endoproteolytic activity and each capable of processing a wide variety of peptide sequences. Based on their cleaving site, the catalytic activities of the subunits have been classified as caspase-like for β1 as it cleaves on the C-terminal site of acidic residues, trypsin-like for β2 as it cleaves after basic residues and chymotrypsin-like for β5 as it cleaves after hydrophobic residues. The cleavage specificity however does not depend solely on amino acid preference (Borissenko L, Groll M. 2007; Goldberg AL et al. 2002; Groll M et al. 1997).

Once inside the cavity, every polypeptide is degraded by the proteolytic β subunits into a mixture of heterogeneous peptides, generally 7-9 residues long, although they can range from 4 to 25 residues depending on substrate and organism (Finley D. 2009; Voges D et al. 1999).

Moreover, mono ubiquitylation and attachment of K63-linked chains to membrane proteins induce their endocytosis, which may result in lysosomal degradation, another mode of protein disposal. However, lysosomes contain many low-specificity proteases, merge with autophagic vesicles and degrade any protein contained therein, a process which stands in stark contrast to proteasome-mediated degradation, where each protein is recognized and processed individually (Duncan LM et al. 2006; Finley D. 2009; Mukhopadhyay D, Riezman H. 2007).

2.6 Ubiquitin and transcription regulation

Ubiquitin influences gene transcription in many ways. To cite a few:

1) Histones can be monoubiquitylated: H2A monoubiquitylation is associated with transcriptional repression, whereas monoubiquitylation of H2B and H1 usually leads to transcriptional activation.

2) Transcription factors can also be regulated through ubiquitylation. For example the activity of NF-κB, an anti-apoptotic and proinflammatory factor, is regulated by ubiquitin on 4 levels: IκBα, one of the inhibitory partners of NF-κB, can be monoubiquitylated to prevent its phosphorilation by the IκB Kinase complex (IKK), thus indirectly suppressing NF-κB activity (Da Silva-Ferrada et al. 2011); one of IKK subunits, NEMO (NF-κB Essential Modulator), requires monoubiquitylation by cIAP1 to be exported from the nucleus and assembled into the functional IKK complex (Jin HS et al. 2009), while another PKCε (Protein Kinase Cε) is monoubiquitylated by the E3 ligase RINCK1 (Yang W et al. 2012). Finally, the NF-κB precursor p105 must be monoubiquitylated at multiple Lys residues by CRL1$^{\beta\text{-TrCP}}$ in order to be matured into p50 (Kravtsova-Ivantsiv Y et al. 2009). Through its regulation of NF-κB activation, ubiquitin plays an important part in inflammation.

3) Mouse Double Minute 2 (MDM2) is a RING E3 that regulates the levels of the tumor suppressor p53, the famous "guardian of the genome". First of all, MDM2 binds the N-terminal trans-activation domain of p53, inhibiting p53 interaction with DNA and

blocking p53-mediated transcriptional activation (Moll UM, Petrenko U. 2003); importantly, MDM2 transcription is activated by p53, thus MDM2 and p53 are regulated through a negative feedback loop.

Secondly, MDM2 ubiquitylates both itself and p53; the latter is monoubiquitylated on several residues on the C-terminus. However, different levels of MDM2 have different effects on p53.

Low levels of MDM2 result in p53 monoubiquitylation, which induces in p53 a conformational change that exposes its nuclear export signal. Conversely, high levels of MDM2 trigger p53 polyubiquitination (Nakagawa T, Nakayama K. 2015); in the nucleus, MDM2 is mostly bound to the p300/CBP (CREB-Binding Protein) complex, which catalyzes polyubiquitination of p53 and ends in its degradation. To achieve this outcome, both the activities of MDM2 and p300 are required (Grossman SR et al. 2003; Moll UM, Petrenko U. 2003).

2.7 Ubiquitin and DNA damage repair

PCNA (Proliferating Cell Nuclear Antigen) is a processivity factor for DNA polymerases and essential for DNA replication. In the event of DNA damage, PCNA is monoubiquitylated on lysine 164; this modification allows recruitment of Y family DNA polymerases, such as Pol η (eta), Pol ι (iota), and Pol κ (kappa), that, unlike other polymerases, can synthesize over and past damaged nucleotidic bases at the cost of fidelity (Freudenthal BD et al. 2010; Jackson SP, Durocher D. 2013). After the DNA lesion has been repaired, Y polymerases are deubiquitylated by USP1, allowing for normal replication to resume (Huang TT et al. 2006).

2.8 Ubiquitin and apoptosis

Apoptosis is a form of programmed cell death normally employed by multicellular organisms for normal development, tissue homeostasis, defense from autoimmunity, persistent viral infections and insurgence of tumors (Green D et al. 2011). The levels of many pro- and anti-apoptotic proteins are regulated through ubiquitylation. For instance, under normal conditions the largest isoform of the pro-apoptotic factor Bim, namely Bim_{EL}, is constitutively phosphorylated, subsequently ubiquitylated and thus degraded to keep its levels low (Broemer M, Meier P. 2009; Ley R et al. 2003).

XIAP and cIAP1 are two RING E3s who are members of the apoptic inhibitor family IAP (Inhibitors of Apoptosis Proteins). XIAP is capable of inhibiting caspases 3, 7 and 9 (Deveraux QL et al. 1997), while cIAP1 ubiquitinates RIP1, stopping its association with FADD and caspase-8, and resulting in apoptosis avoidance (Bertrand MJ et al. 2008; Graber TE, Holcik M. 2011). Caspase-3 in particular has also been reported to be both poly- and mono-ubiquitinated by XIAP and cIAP1, respectively (Bromer M, Meier P. 2009). However, mutation of XIAP RING

domain does not significantly impact apoptosis (Duckett CS et al. 1998). In these as in many cases, it is unclear to what extent the ubiquitination of caspases is necessary for their inhibition and degradation (Bader M, Steller H. 2009).

2.9 Ubiquitin and immunity

The immunoproteasome is a variant of the normal proteasome that is expressed by immune cells, such as Antigen Presenting Cells (APC), but can also be induced even in non-immune cells (Arellano-Garcia ME et al. 2014; Keller I et al. 2015; Kimura HJ et al. 2009); its main function is processing "foreign" proteins, like those of viral origin, and allowing their presentation on Major Histocompatibility Complex I (MHC I) molecules. During inflammatory events, such as viral infections or autoimmune diseases, the inflammation-related cytokine Interferon-γ (IFN-γ) triggers the expression of 5 specialized proteasome subunits that assemble on the core particle and form the immunoproteasome: β1, β2 and β5 are replaced by iβ1, iβ2 and iβ5 respectively, while the 19S regulatory particle is substituted by the 11S regulator (also known as Protein Activator $\alpha\beta$, PA28$\alpha\beta$), formed by 2 subunits PA28α and PA28β, which lack ubiquitin-binding domains and ATPase activity (Kloetzel P. 2001; Finley D. 2009). Importantly, the binding of PA28$\alpha\beta$ on the proteasome dramatically increases its proteolytic activity, thus boosting the efficiency of substrate degradation (Wang J, Maldonado MA. 2006); iβ1, iβ2 and iβ5 have different cleavage preferences than the canonical β subunits and produce small peptides that are further trimmed at their N-termini by cytosolic aminopeptidases into fragments 8-10 residues long, which are suitable for loading into MHC I molecules (Goldberg AL et al. 2002). These Peptides are transported into the endoplasmic reticulum by the specialized Transporter associated with Antigen Processing (TAP) where they bind with MHC I molecules. The MHC I-peptide complexes are then exposed onto the cellular surface where they can be recognized by specific receptors on CD8+ T lymphocytes (Finley D. 2009).

2.10 Ubiquitin and cell cycle regulation

The cell cycle can be defined as a highly controlled series of events that ultimately results in a cell dividing into 2 daughter cells; the process is unidirectional and irreversible. The cell cycle comprises 4 phases:
- The G1 phase, where the cell grows and the biosynthetic activity is high
- The S phase, where chromosome duplication occurs
- The G2 phase, where the cell continues to grow to prepare for mitosis
- The M phase, where the cell undergoes chromosome and cytosol repartition and division into two daughter cells.

Progression through the phases is regulated primarily by the phosphorylation of numerous proteins, catalyzed by a group of kinases known as Cyclin-Dependent Kinases (CDKs), that are

constantly expressed throughout the entire cell cycle. CDK are activated through binding of cyclins, which act as positive regulatory subunits. Different CDK-cyclin complexes form at different stages of the cell cycle to specifically phosphorylate their target substrates, which participate in chromosome replication and segregation, as well as mitotic spindle assembly. The activity of CDK-cyclin complexes is in turn suppressed by the CDK inhibitors (CKIs). Unlike CDKs, cyclins and CKIs are expressed only at well defined points in the cell cycle (Vermeulen K et al. 2003). The temporally controlled degradation of these proteins, orchestrated by the ubiquitin-proteasome system, is crucial to cell cycle control; in particular, the proteasome is tasked with the elimination of CKIs to favor the transition from G1 to S phase and the degradation of cyclin B, to allow chromosomal separation, and of the anaphase inhibitor Securin (Teixeira LK, Reed SI. 2013).

The Anaphase-Promoting Complex/Cyclosome (APC/C) and the Skp/Cullin/F-box-containing (SCF) complexes are both members of the Cullin-RING Ligases (CRLs) subfamily of E3s and are responsible for the ubiquitylation of key cell cycle regulatory proteins. In humans, the core APC/C complex is composed of at least 14 different proteins; Apc2 serves as the complex scaffold, Apc11 is the E3 enzyme that is responsible for the recruitment of the E2s necessary for ubiquitylation, while Cdc20 and Cdh1 are the adaptors that bind to the complex in a mutually exclusive manner, activate it and contribute to substrate specificity. Once activated, the APC/C complex ubiquitylates mitotic cyclins, anaphase regulators, spindle assembly factors and DNA replication-related proteins; in particular APC/C determines mitotic exit by mediating the degradation of cyclin B and securin, an inhibitor of the protease responsible for sister chromatid separation (Gilberto S, Peter M. 2017; Hirano T. 2015; Teixeira LK, Reed SI. 2013). SCF complexes always contain three components: Cul1, Skp1 (S-phase Kinase-associated Protein 1) and Rbx1. Cul1 is the scaffold protein that binds both the RING E3 Rbx1, responsible in turn for E2 recruitment, and the adaptor protein Skp1 which determines substrate specificity through recruitment of additional proteins. The SCF complex controls S phase and mitosis entry by ubiquitylating CKIs like p27 and WEE1 respectively, G1 and S Phase cyclins, and mitotic inhibitors (Gilberto S, Peter M. 2017; Teixeira LK, Reed SI. 2013).

2.11 Ubiquitin genes

In humans, Ubiquitin is encoded by 4 different genes, namely *UBC*, *UBB*, *UBA52* and *RPS27A*, whose transcripts are translated into different ubiquitin precursors: *UBB* and *UBC* are translated as linear polyproteins, respectively formed by 3 and 9 head-to-tail ubiquitin repeats; each repeat has the same aminoacidic sequence except for one additional residue at the C-terminal end: a cysteine for UBB and a valine for UBC. No spacer sequences are present in-between repeats. *UBA52* and *RPS27A* code for a fusion protein constituted by a single ubiquitin molecule attached to a ribosomal subunit, L40 and S27a respectively (Kimura Y, Tanaka K. 2010; Radici L et al. 2013; Wiborg O et al. 1985). These ubiquitin precursors are processed into ubiquitin monomers by DUBs (Kimura Y, Tanaka K. 2010). Under basal conditions, *UBB* and

UBC contribute the most to the ubiquitin cellular pool thanks to the higher number of ubiquitin monomers encoded per transcript (Bianchi M al. 2015).

Even though all ubiquitin produced in this way is functionally identical, the 4 ubiquitin genes do not seem to be redundant in function as impairment of one of the genes is not compensated by overexpression of the others (Ryu KY et al. 2007; Ryu KY et al. 2008). Ryu KY et al. demonstrated that while disruption of a single *UBC* allele does not result in any apparent phenotype, double knockout of *UBC* is lethal in mice embryos, probably due to severe impairment of liver cell proliferation. Moreover, mouse embryonic fibroblasts obtained from said embryos show reduced growth rate, premature senescence, increased apoptosis, delayed cell-cycle progression and a 40% decrease in ubiquitin content. *UBC* -/- fibroblasts are also unable to adequately increase their endogenous Ub levels when challenged with cellular stresses such as heat shock and proteasome inhibitors. Moreover, midgestation embryonic lethality, liver development impairment and delayed cell-cycle progression were partially rescued by providing extra genomic copies of ubiquitin, suggesting that observed defects are likely due to ubiquitin deficiency (Ryu KY et al. 2007). Further work from the same authors also established that impairment of one or both copies of *UBB* results in viable mice, but *UBB* -/- mice of both sexes are infertile due to failure of the germinal cells to progress through meiosis I and subsequent hypogonadism (Ryu KY, Garza JC et al. 2008). Moreover, *UBB* -/- mice exhibit smaller size and adult-onset obesity, attributed to a 30% reduction of the ubiquitin levels in hypothalamic neurons, which control energy balance and feeding behavior (Ryu KY, Sinnar SA et al. 2008), and interestingly, degeneration of the retina, a tissue which originates during embryonic development from the diencephalon, same as the hypothalamus (Lim D et al. 2019).

2.12 *UBC* gene structure

The polyubiquitin gene *UBC* is located on 12q24.3. Its DNA sequence is 3005 base pairs (bp) long and it contains a 64 bp untranslated exon, an 812 bp intron and a second exon encoding 9 tandem repeats of the ubiquitin molecule (RefSeq NG_027722.2; Radici L et al. 2013).

Even though there is extensive evidence of the functional importance of *UBC* (Ryu KY et al. 2007; Ryu KY, Garza JC et al. 2008; Ryu KY, Sinnar SA et al. 2008), the mechanisms responsible for its regulation have not been fully discovered.

2.13 *UBC* transcriptional regulation in basal conditions

Bianchi et al. showed how the 812 bp intron located next to the first untranslated exon is essential for *UBC* expression in basal conditions (Bianchi M et al. 2009). In plants, the polyubiquitin genes are characterized by the presence of introns in the 5'-UTR (untranslated region), which enhance gene expression through a mechanism named Intron-Mediated Enhancement (IME) that partially depends on splicing (Akua T et al. 2010; Sivamani E, Qu R. 2006).

To determine if the same mechanism could affect the human *UBC* gene, luciferase-expressing reporter constructs were prepared with several different portions of the *UBC* promoter and transfected in HeLa cells; a drastic reduction in luciferase expression was detected in constructs which lacked the intron compared to those that had it. Similarly, moving the intron upstream of the proximal promoter region, inverting its orientation or replacing it with a chimeric intron yielded the same results, thus demonstrating that *UBC* expression relies on the presence of its specific intron sequence, in the correct location and orientation. To investigate the relevance of splicing capability, site-directed mutagenesis was again employed to obtain splicing-impaired constructs; HeLa cells expressing the splicing-defective constructs showed an almost null luciferase expression, proving that intron splicing is a significant contributor of *UBC* expression (Bianchi M et al. 2009; Bianchi M et al. 2013).

Electrophoretic Mobility Shift Assay (EMSA) analysis also revealed the presence, within the intron, of multiple binding sites for three ubiquitously expressed transcription factors: SP1, SP3 and YY1. Knockdown of YY1 levels through use of small interfering RNA (siRNAs) and especially the mutagenesis of one or both YY1 binding sites resulted in a substantial decrease in *UBC* promoter-driven luciferase expression; thus, YY1 is one of the determinants of *UBC* transcription. Conversely, mutagenesis of SP1 and SP3 binding sites did not significantly alter luciferase transcription, suggesting that, despite *in vitro* evidence, they are not necessary for *UBC* transcription *in vivo* (Bianchi M et al. 2013). However, SP1 is also capable of binding to two additional sites placed in the upstream *UBC* promoter, as proven by Marinovic et al., and may thus have a role in basal *UBC* transcriptional regulation (Marinovic C et al. 2002).

2.14 *UBC* transcriptional upregulation in stress conditions

UBC is a stress responsive gene, as its transcription can be induced by stressors such as heat shock (Finley D et al. 1987; Fornace AJ et al. 1989; Vihervaara A et al. 2013), UV irradiation (Nenoi M. 1992), oxidative stress (Fernandes R et al. 2006) and translation blockade through use of cycloheximide and canavanine (Hanna J et al. 2003). *UBB* also responds to various stressors, although to a lesser degree than *UBC*, while *UBA52* and *RPS27A* do not (Bianchi M et al. 2015). The polyubiquitin genes upregulation as a consequence of stress conditions can be explained as a method of supplying the cell with the extra ubiquitin required to face the challenge; in the case of *UBC*, its promoter houses three Heat Shock Elements (HSEs), two distal and one proximal to the Transcription Start Site (TSS). All three are bound by Heat Shock Factors (HSFs), a family of transcription factors responsible for the induction of stress-responsive genes, and in particular by HSF1; indeed, siRNA-mediated knockdown of HSF1 severely compromises stress-induced *UBC* upregulation (Bianchi M et al. 2018). Crinelli et al. discovered that while the distal HSEs upregulate *UBC* in response to proteasome inhibition, the proximal HSE suppresses stress-induced transcriptional activity, which constitutes the first report of HSE with a transcription-repressive function. Moreover, the *UBC* intron does not seem to participate in *UBC* upregulation under stressful conditions (Crinelli R et al. 2015).

2.15 *UBC* downregulation upon overexpression of exogenous ubiquitin

Given the many functions that ubiquitin has in the cell, its homeostasis is of paramount importance. A proof of the existence of this homeostatic equilibrium between ubiquitin synthesis, recycling and degradation is given by the effects of overexpressing exogenous ubiquitin in cells. HeLa cells transfected with ubiquitin-coding constructs display a significantly higher ubiquitin content, about 4-fold more than control cells, and also a decrease in the mRNA levels of *UBC* and *UBB*. Both these effects were dependent on the amount of transfected constructs, with higher amounts resulting in higher ubiquitin content and *UBC* mRNA decrease (Crinelli R et al. 2008). In turn, *UBA52* and *RPS27A* mRNA levels were not affected. Further studies showed that *UBC* and *UBB* downregulation is not due to a reduced transcriptional activity but is rather provoked by an impairment in transcript splicing (Bianchi M et al. 2019).

UBC downregulation is also dependent on the presence of conjugation-competent ubiquitin. HeLa cells were transfected with vectors expressing different ubiquitin mutants: UbG76A carries an alanine residue in place of a glycine at position 76 and interferes with the activity of DUBs, UbΔGG lacks the two C-terminal glycine residues and thus cannot be conjugated to substrates but can still generate unanchored ubiquitin chains, while UbK0 is a mutant deprived of all lysine residues and incapable of forming any kind of polyubiquitin chain. Transfection of UbG76A and UbΔGG caused an induction of *UBC* in place of a downregulation, while UbK0 yielded no alteration in *UBC* transcript levels. YY1, SP1 and HSF1 involvement in *UBC* downregulation was also tested but was excluded (Bianchi M et al. 2019).

2.16 Ubiquitin and cancer

The relation between ubiquitin and cancer has been amply established in the literature and targeting the ubiquitin system as a possible tumor therapy has been suggested.

Both *UBC* and *UBB* are overexpressed in several types of tumor, which is understandable given the increased metabolism and proliferation rates of tumor cells, and knockdown of the polyubiquitin genes has been suggested as a possible therapy. Oh et al. reported a tumor growth reduction in mice xenograft and decrease in cell proliferation of neuroblastoma, hepatocarcinoma, breast and prostatic cancer cells following siRNA-mediated *UBB* knockdown (Oh C et al. 2013). Tang et al. showed how *UBC* and *UBB* knockdown inhibits the growth of non-small cell lung cancer lines and weakens their resistance to radiations (Tang Y et al. 2015).

A number of therapeutic molecules targeting different elements of the ubiquitin cellular machinery, ranging from ubiquitin-conjugating enzymes to DUBs and the proteasome itself. However, the clinical employment of these molecules is stunted by their lack of specificity, which may lead to severe side-effects. Indeed, the most promising therapeutic targets are E3 enzymes, since they possess relatively high selectivity towards their substrates (Liu J et al. 2015).

To cite a few examples, Zeng et al. synthetized an inhibitor of the APC/C complex, TAME (Tosyl L-Arginine Methyl Ester) which binds to APC and prevents its activation by Cdc20 and

Cdh1; this results in the stabilization of cyclin B1 and subsequently in mitotic arrest (Zeng X et al. 2010; Zeng X, King RW. 2012). The same group also developed another aptly named molecule, Apcin (APC inhibitor) which preferentially binds to Cdh20 rather than to Cdh1 and inhibits ubiquitylation of substrates containing a particular Destruction-box (D-box) sequence, thus being more selective. Apcin and TAME act sinergically to block mitotic exit (Sackton KL et al. 2014).

MDM2, being the principal negative regulator of p53 stability, is the most targeted E3 ligase: among the multitude of MDM2 inhibitors, Nutlin, is the first ever produced. Nutlin binds to a specific region of p53 and blocks MDM2 access to it (Vassilev LT. 2004). Several derivatives of Nutlin, such as Idasanutlin, have since been obtained (Skalniak L et al. 2018).

AIMS OF THE THESIS

A. To characterize and compare the asset of the ubiquitin system in two gastric cancer cell lines, the primary line 23132/87 and the metastatic line MKN45, focusing on the intracellular ubiquitin content and partition between free and conjugated pools and on the differential expression of the ubiquitin genes.

B. To investigate the transcription factors and the molecular mechanisms that regulate ubiquitin gene expression in the two cell lines, in order to identify potential differences that could be relevant as biomarkers or therapy options.

C. To target ubiquitin expression in the two cell lines by siRNA-mediated knockdown of the two polyubiquitin genes *UBB* and *UBC*, in order to evaluate differences in cellular response and thus in ubiquitin dependency and its relevance to cell survival.

CHAPTER 4:

THE UBIQUITIN GENE EXPRESSION PATTERN AND SENSITIVITY TO *UBB* AND *UBC* KNOCKDOWN DIFFERENTIATE PRIMARY 23132/87 AND METASTATIC MKN45 GASTRIC CANCER CELLS

Scarpa Emanuele-Salvatore, Tasini Filippo, Crinelli Rita, Ceccarini Chiara, Magnani Mauro, Bianchi Marzia.

Department of Biomolecular Sciences, University of Urbino Carlo Bo, 61029 Urbino (PU), Italy

The Ubiquitin Gene Expression Pattern and Sensitivity to *UBB* and *UBC* Knockdown Differentiate Primary 23132/87 and Metastatic MKN45 Gastric Cancer Cells

Emanuele Salvatore Scarpa *, Filippo Tasini, Rita Crinelli, Chiara Ceccarini, Mauro Magnani † and Marzia Bianchi †

Department of Biomolecular Sciences, University of Urbino Carlo Bo, 61029 Urbino (PU), Italy;
f.tasini3@campus.uniurb.it (F.T.); rita.crinelli@uniurb.it (R.C.); chiara.ceccarini0@gmail.com (C.C.);
mauro.magnani@uniurb.it (M.M.); marzia.bianchi@uniurb.it (M.B.)

* Correspondence: emanuele.scarpa@uniurb.it; Tel.: +39-0722-305252

† Both authors contributed equally to this Manuscript.

4.1 Abstract: Gastric cancer (GC) is one of the most common and lethal cancers. Alterations in the ubiquitin (Ub) system play key roles in the carcinogenetic process and in metastasis development. Overexpression of transcription factors YY1, HSF1 and SP1, known to regulate Ub gene expression, is a predictor of poor prognosis and shorter survival in several cancers. In this study, we compared a primary (23132/87) and a metastatic (MKN45) GC cell line. We found a statistically significant higher expression of three out of four Ub coding genes, *UBC*, *UBB* and *RPS27A*, in MKN45 compared to 23132/87. However, while the total Ub protein content and the distribution of Ub between the conjugated and free pools were similar in these two GC cell lines, the proteasome activity was higher in MKN45. Ub gene expression was not affected upon *YY1*, *HSF1* or *SP1* small interfering RNA (siRNA) transfection, in both 23132/87 and MKN45 cell lines. Interestingly, the simultaneous knockdown of *UBB* and *UBC* mRNAs reduced the Ub content in both cell lines, but was more critical in the primary GC cell line 23132/87, causing a reduction in cell viability due to apoptosis induction and a decrease in the oncoprotein and metastatization marker β-catenin levels. Our results identify *UBB* and *UBC* as pro-survival genes in primary gastric adenocarcinoma 23132/87 cells.

Keywords: gastric cancer; ubiquitin; *UBB*; *UBC*; cell viability

4.2 Introduction

Ubiquitin (Ub) is a highly conserved 76 amino-acid protein that is covalently conjugated to target proteins by the consecutive actions of three enzymes (E1, E2, E3) in a process known as ubiquitylation [1].

Ub conjugation is an incredibly complex post-translational modification involved in the regulation of many cellular processes such as proteasome-mediated proteolysis, but it also has various non-degradative functions, ranging from signal transduction to transcription, from endocytosis to protein trafficking, from DNA repair to cell survival and proliferation [1,2]. In the cell, Ub is dynamically distributed among distinct pools, which mainly include free or

unconjugated Ub, and protein-conjugated Ub consisting of one or more Ub molecules that are peptide-linked to protein substrates [3]. Moreover, free unconjugated polyubiquitin chains also contribute to the total cellular Ub content [4].

In humans, Ub is encoded by four genes: *UBB, UBC, UBA52* and *RPS27A* [5–7]. *UBB* and *UBC* encode Ub linear polyproteins formed by three and nine Ub monomers, respectively [5], while *UBA52* and *RPS27A* produce a fusion product where the C-terminus of one Ub molecule is fused to a ribosomal protein [6,7]. These precursors are co- and post-translationally processed in their mature forms by deubiquitinases (DUBs), which selectively cleave Ub monomers from their fusion partners [8].

Both *UBB* and *UBC* were found to be upregulated in several cancers and their high expression levels seemed to be essential to sustain the high proliferation rate of cancer cells and to support their ability to overcome increasing cellular stresses [9–11]. Indeed, *UBB* silencing in neuroblastoma, hepatocarcinoma, breast and prostate cancer cells significantly decreased the proliferation rate of all lines tested [9]. Similar results were reported by Tang et al. in lung cancer cells, where *UBC* and *UBB* knockdown inhibits cell growth and weakens radioresistance both *in vitro* and *in vivo* [10]. Of note, an upregulation of *UBB* and *UBC* has also been detected in many human cancer specimens, when compared with paired normal adjacent tissues [12].

Despite their recognized role in cell survival and proliferation, little is known about the molecular mechanisms regulating *UBC* and *UBB* gene expression in cancer cells. The *UBC* promoter has long been in the repertoire of promoters currently used to drive exogenous gene expression [13], although its regulatory elements, under basal and stressful conditions, have been only recently characterized [14–16].

In particular, it has been demonstrated that the transcription factor (TF) Yin Yang 1 (YY1) has a pivotal role in the regulation of basal *UBC* expression, acting both as a gene-specific transactivator and as a positive regulator of intron splicing [15]. A role for Specificity Protein 1 (SP1) in the transcriptional regulation of *UBC* has also been reported [14,17,18]. By contrast, Heat Shock Factor 1 (HSF1) is the main transcription factor involved in the upregulation of *UBC* gene expression under several stress conditions [16,19–21]. In addition, several reports have demonstrated the pro-survival and pro-carcinogenetic role of YY1 [22], SP1 [23] and HSF1 [24] in gastric cancer (GC) development.

Gastric adenocarcinoma is one of the most common malignancies in the world, with a high rate of incidence in many countries [25]. The main clinical classification divides GC into two major histological subtypes: intestinal type GC has higher incidence of blood vessel invasion and liver and lung metastases, whereas diffuse type GC spreads more commonly via the lymphatic system to the pleura and peritoneum [26]. Molecular studies of alterations of single genes have provided evidence that intestinal and diffuse type GC evolve via different genetic pathways, which lead to increased resistance to apoptosis induction, uncontrolled cell proliferation and metastasis development, the latter worsening the prognosis of cancer patients [27,28].

Tian et al. [29] showed, through bioinformatics analyses of microarray data, that *UBB, UBC, UBA52* and *RPS27A* genes were overexpressed in GC human tissue samples when compared with normal stomach tissues. In addition, the authors demonstrated that *UBA52* and *RPS27A* were overexpressed in the lymph node metastases when compared with primary gastric

adenocarcinoma samples, but they did not show any results regarding the different expression levels of *UBB* and *UBC* [29]. Therefore, determining the role of the different Ub genes and of the transcription factors (YY1, HSF1 and SP1) known to be involved in Ub gene expression, both in primary and metastatic GC cells, can pave the way for future studies aimed at identifying new biomarkers involved in the carcinogenetic process that leads to the development of gastric adenocarcinoma.

Our results demonstrate the role of *UBB* and *UBC* as pro-survival genes in primary GC cell line 23132/87 and show that the combined silencing of these two Ub genes in the primary gastric adenocarcinoma cells led to a decrease in their viability, exerted through activation of the extrinsic pathway of apoptosis, and a reduction in levels of the oncoprotein β-catenin, which has a role in overproliferation, migration, invasion of various tumors and also in the epithelial to mesenchymal transition (EMT) process [30].

4.3 Results

4.3.1. Characterization of Ub Expression Profile in Primary 23132/87 and Metastatic MKN45 GC Cells

Van der Woude et al. [31] identified the pro-apoptotic protein Fas as a marker of the intestinal type of gastric adenocarcinoma. Our results show that the intestinal type 23132/87 GC cells (Figure S1A) and the hybrid intestinal/diffuse type MKN45 cells (Figure S1B) were both positive for the Fas protein (Figure S1C). Thereafter, we sought to characterize and compare the Ub expression profile in these primary (23132/87) and metastatic (MKN45) GC cell lines. To this end, we evaluated, in both cellular models, the expression levels of the four Ub coding genes, the total cellular Ub content, as well as Ub distribution among the free and conjugated pools and the proteasome activity. When the Ub transcriptome was analyzed, a statistically significant higher expression of three out of the four Ub coding genes, *UBC* (p = 0.029), *UBB* (p = 0.025) and *RPS27A* (p < 0.001), was detected in MKN45 compared to 23132/87 cells, using Beta-2-Microglobulin (*B2M*) for data normalization (Figure 1A). These results were also confirmed using glyceraldehyde 3-phosphate dehydrogenase (*GAPDH*) as a housekeeping gene (Table S1).

While *UBA52* and *RPS27A* are constitutively expressed and contribute with *UBB* and *UBC* to fulfill the ubiquitin demand in basal conditions, only *UBB* and *UBC* are induced when cells are exposed to threats such as heat shock, oxidative stress and proteotoxic stress [19–21,32]. To determine total Ub concentration, whole cell extracts from both cell lines were treated with the Usp2 deubiquitinating enzyme to convert all conjugated Ub species into monomeric Ub [33]. Usp2 is able to catalyze the hydrolysis of both Lys-48 and Lys-63 linkages of Ub, thus displaying broad specificity [34]. The total Ub protein content was accurately determined by running different amounts of Usp2-digested protein extracts and a proper range of Ub standards in the same immunoblot (Figure S2). The average of three independent assays indicates a similar (p = 0.200) Ub content in 23132/87 and MKN45 cells (1.74 ± 0.10 and 2.01 ± 0.21 ng Ub/μg protein, respectively; Figure 1B), despite the lower *UBC, UBB* and *RPS27A* transcript levels in primary GC cells (Figure 1A). Moreover, the Ub distribution between the conjugated and free pools was investigated: MKN45 and 23132/87 cells showed similar distribution of Ub between the two pools (Figure 1C). Since Ub has a pivotal role in

proteasome-mediated degradation [35] and in turn the proteasome is responsible for Ub degradation, thus affecting its cellular levels [36], we then determined the proteasome activity of these two GC cell lines by evaluating the chymotrypsin-like activity (that is, the predominant activity) of the 20S core. Our results show that MKN45 cells possess a significantly higher (p = 0.009) proteasome activity with respect to 23132/87 cells (Figure 1D).
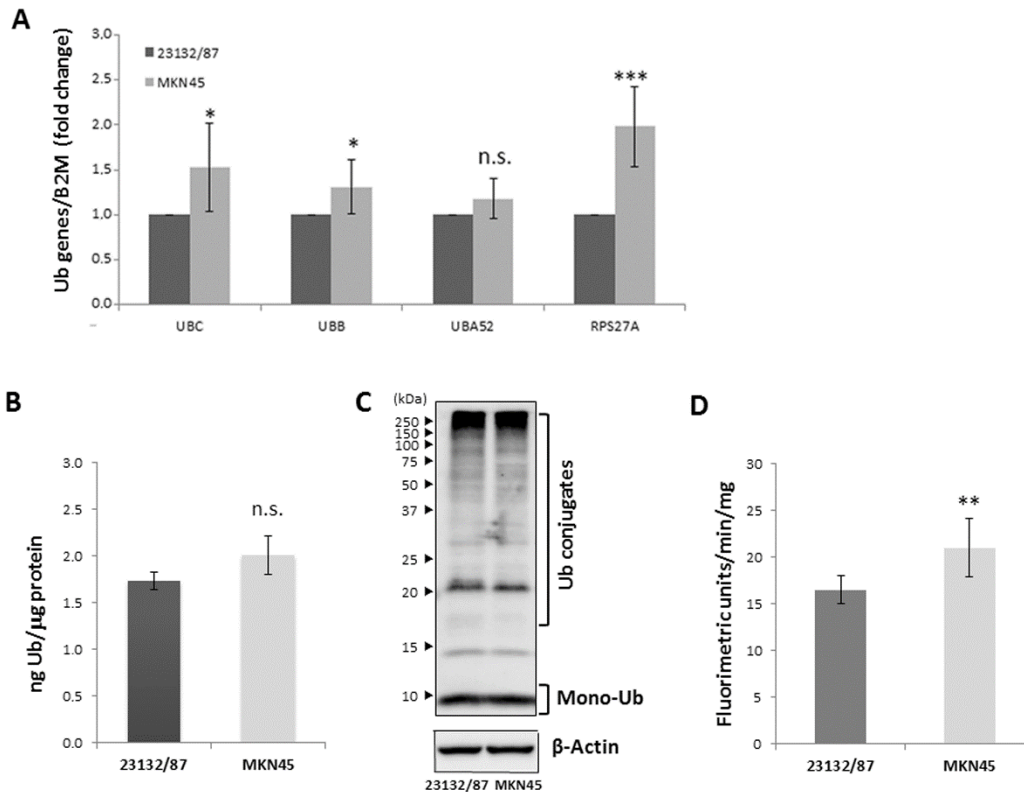
Figure 1. Evaluation of Ub gene expression, Ub protein levels and proteasome activity in 23132/87 and MKN45 cell lines. (**A**) The *UBC*, *UBB*, *UBA52* and *RPS27A* mRNAs were measured by real-time quantitative PCR; the results were normalized to *B2M* mRNA and depicted as fold change compared with the values obtained in 23132/87 cells, set to 1. Data are means ± SD (n = 6); * p < 0.05, *** p < 0.001; n.s. not significant. (**B**) Absolute quantification of total Ub (n = 3) using different amounts of Usp2-treated protein extracts and a linear range of Ub standards run in parallel (see Figure S2). Results are given as ng Ub/µg protein; n.s. not significant (p = 0.200). (**C**) Representative western immunoblots (n = 3) performed using total lysates (5 µg) of 23132/87 and MKN45 cells. The samples were loaded and probed with anti-Ub antibody to detect the poly-Ub and the mono-Ub pools; blots were reprobed with anti-β-Actin antibody, used as a loading control. Brackets indicate Ub conjugates and mono-Ub; arrowheads on the left indicate the molecular weight standards. (**D**) Proteasome activity was assayed in 23132/87 and MKN45 cell extracts using the fluorogenic peptide sLLVY-NH-Mec as a substrate (n = 3); the obtained values were expressed as fluorimetric units*min^{-1}*mg^{-1}; ** p < 0.01.

4.3.2. Cytosolic and Nuclear Distribution of YY1, HSF1 and SP1 in 23132/87 and MKN45 GC Cell Lines

Given the role of YY1 [15,22], HSF1 [16,24] and SP1 [14,17,18,23] both as transcription factors involved in Ub gene expression and as prognostic markers in GC development, the basal levels of these protein factors in whole (Figure 2A,B), cytosolic (Figure 2C,D) and nuclear extracts (Figure 2E,F) of 23132/87 and MKN45 cells were evaluated. Our results show that YY1 total levels were higher in MKN45 compared to 23132/87, while both HSF1 and SP1 levels were lower (Figure 2A,B). The same pattern was generally reflected in the cytosolic (Figure 2C,D) and nuclear content (Figure 2E,F) of these transcription factors. Even if the total and cytosolic HSF1 levels were higher ($p = 0.049$ and $p = 0.019$, respectively) in 23132/87 than in MKN45 cells (Figure 2A,D), both GC cells showed similar HSF1 levels in their nuclear extracts (Figure 2E,F). Meanwhile, the levels of YY1, which is mainly a nuclear factor, were significantly higher ($p = 0.035$) in the nuclei of MKN45 cells (Figure 2E,F). Regarding the SP1 transcription factor, the appreciable, albeit not significant, lower expression in MKN45 versus 23132/87 detected in whole cell lysates was reconfirmed in the nuclear extracts (Figure 2E,F).
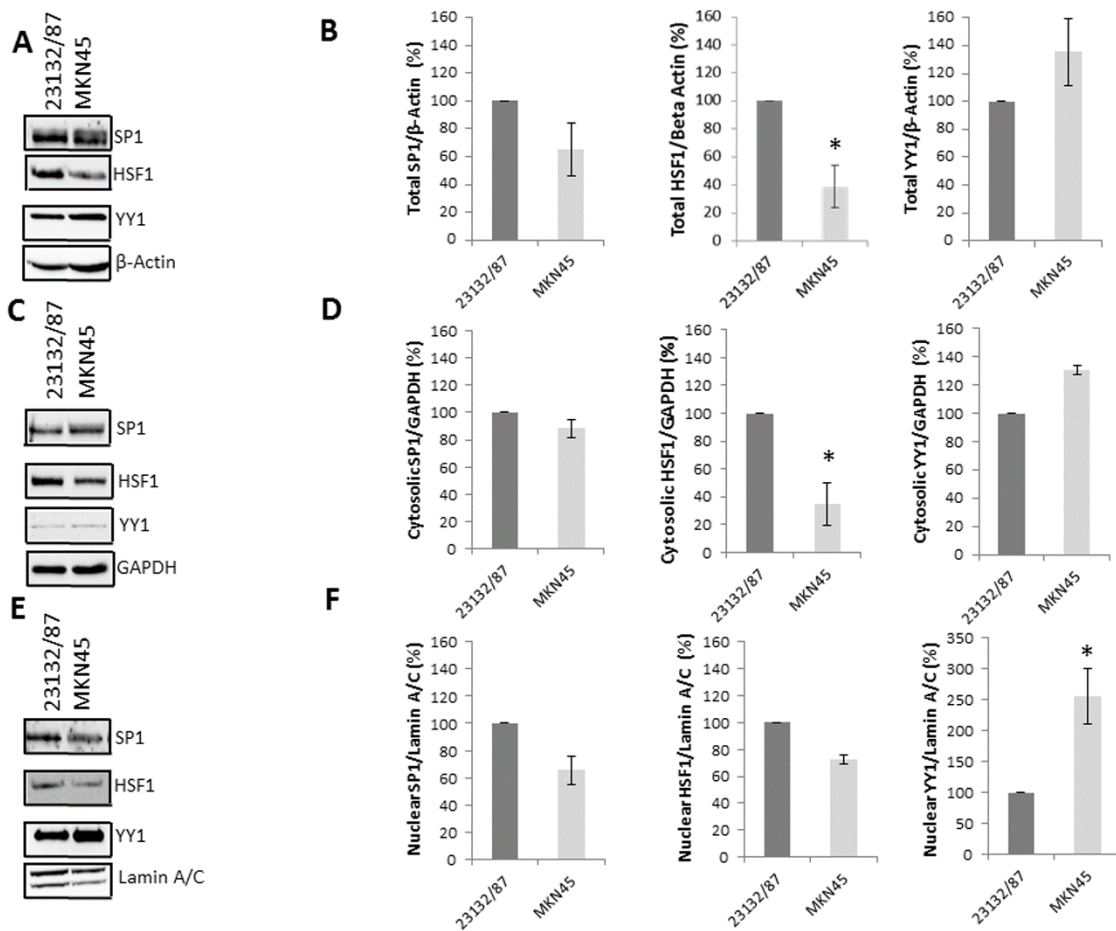

Figure 2. Analysis of total, cytosolic and nuclear levels of transcription factors SP1, HSF1 and YY1 in 23132/87 and MKN45 cell lines. Representative western immunoblots (*n* = 3) performed using total (**A**), cytosolic (**C**) and nuclear (**E**) lysates, which were obtained from 23132/87 and MKN45 cells. Quantities of

15 µg of total or cytosolic cellular proteins and 7.5 µg of nuclear proteins were loaded and probed with antibodies specific for SP1, HSF1 and YY1. Blots were reprobed with antibodies against proteins used as a loading control: anti-β-Actin for total extracts, anti-GAPDH for cytosolic extracts and anti-Lamin A/C for nuclear extracts. Quantification (**B**,**D**,**F**) of SP1, HSF1 and YY1 levels in 23132/87 and MKN45 samples was performed with Image Lab analysis software version 5.2.1. The values obtained from the ratio between SP1, HSF1 and YY1 signals and the loading control β-Actin (**B**) or GAPDH (**D**) or Lamin A/C (**F**) in MKN45 cells were calculated and compared with the values obtained in 23132/87 cells, set as 100%; * $p <$ 0.05.

4.3.3. Effect of YY1, HSF1 and SP1 Transcription Factor Silencing on Ub Gene Expression

To investigate the role of YY1, HSF1 and SP1 in determining Ub expression levels in 23132/87 and MKN45 cells, RNA interference experiments targeting these transcription factors were performed. Both cell lines were transfected with siRNAs against either *YY1*, *HSF1* or *SP1* and green fluorescent protein (*GFP*), used as a negative control. Target knockdown was effective at both the mRNA and protein levels (Figure 3A–H). RTqPCR revealed about an 80% decrease in the target mRNA for all three transcription factors in 23132/87 (Figure 3A); MKN45 displayed an average 85% reduction in *HSF1* and *YY1* mRNA levels, and a 68% reduction in the *SP1* mRNA levels (Figure 3E). A consistent reduction was also obtained at the protein level for all three transcription factors in both cell lines (Figure 3B–D and Figure 3F–H). However, TF knockdown did not affect Ub gene transcription, as detected by RTqPCR of cDNA samples derived from silenced GC cells compared to si*GFP* transfected cells (Figure 3I,J). Regarding HSF1, its activity is mainly induced in response to different stressful conditions such as heat shock, oxidative stress or proteotoxic stress [19,21]: this may account for the lack of effect on *UBC* and *UBB* gene transcription in *HSF1* silenced gastric cancer cells. Instead, the output of YY1 transcription factor silencing was further investigated by RTqPCR analysis of three known direct targets of YY1: Bcl-2-like protein 4 (*BAX*) and Avian myelocitomatosis virus oncogene cellular homolog (*c-MYC*), which are positively regulated by YY1 [37], and the survivin coding gene, which is repressed by YY1 [38]. While *BAX* and survivin transcript levels were both unchanged upon *YY1* silencing, *c-MYC* expression showed a significant reduction in both cell lines (28% and 52% reduction in 23132/87 and MKN45, respectively; Supplementary Table S2).
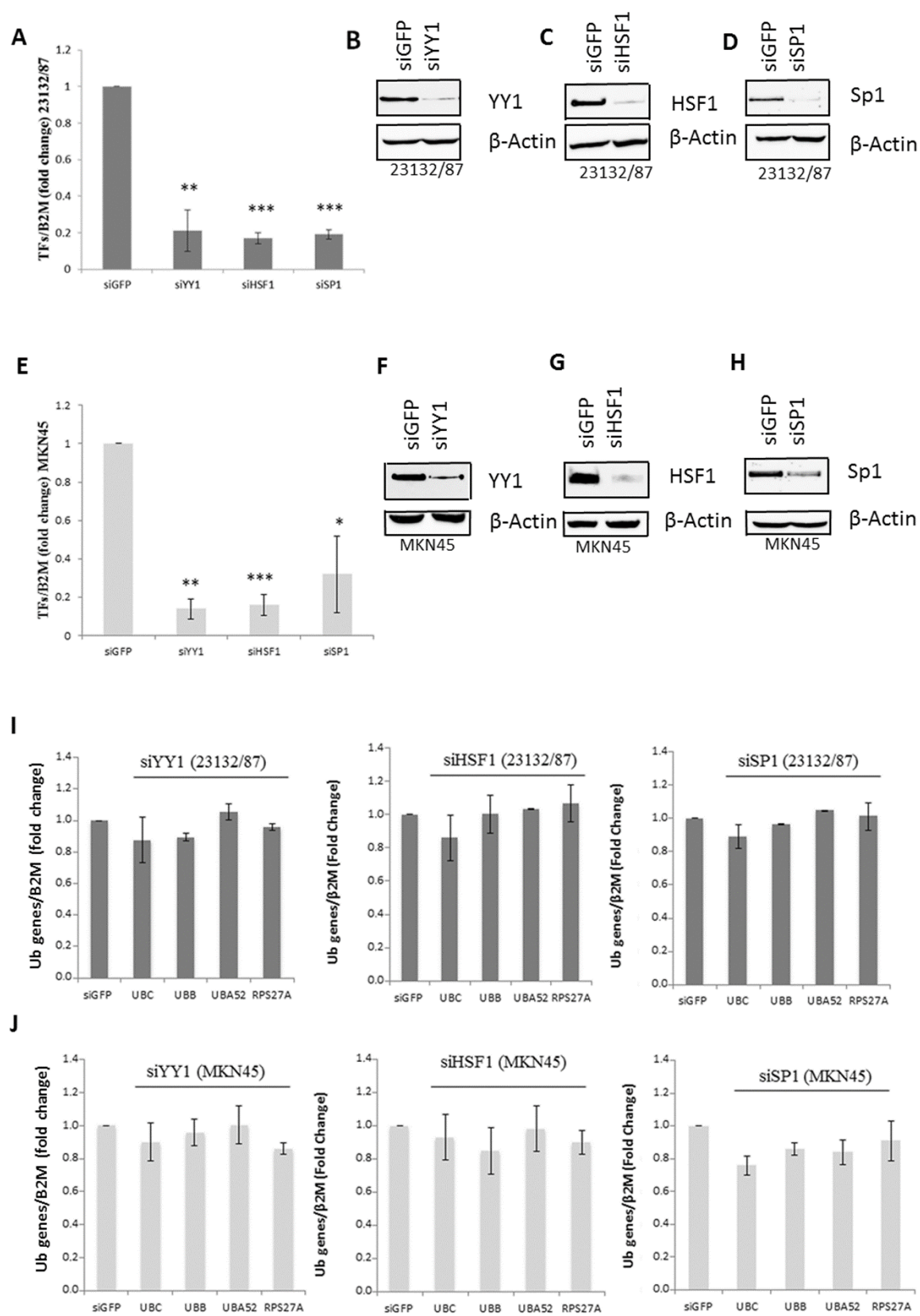
Figure 3. siRNA-mediated knockdown of YY1, HSF1 and SP1 transcription factors and Ub gene expression levels after RNA interference treatments in the 23132/87 and MKN45 cell lines. 23132/87 (**A**) and MKN45 (**E**) cells were transiently transfected with *YY1*, *HSF1*, *SP1* and control *GFP* siRNAs. At 48 h after transfection, the mRNA levels of the target genes were measured by real-time quantitative PCR, normalized to *B2M* mRNA and depicted as fold change compared with si*GFP* transfected cells. Data are means ± SD (n = 3); * $p < 0.05$, ** $p < 0.01$, *** $p < 0.001$. Representative western immunoblots of total proteins from 23132/87 (**B–D**) and MKN45 (**F–H**) cells transfected with either control (si*GFP*) or *YY1*, *HSF1* or *SP1* siRNAs, at 48 h post-transfection (n = 3). A quantity of 15 μg of total cellular proteins was loaded and probed with antibodies specific for YY1 (**B,F**), HSF1 (**C,G**) or SP1 (**D,H**); blots were reprobed with anti-β-Actin, used as a loading control. 23132/87 (**I**) and MKN45 (**J**) cells were transiently transfected with *YY1*, *HSF1*, *SP1* and control *GFP* siRNAs. After 48 h, the mRNA levels of *UBC*, *UBB*, *UBA52* and *RPS27A* genes were measured by real-time quantitative PCR, normalized to *B2M* mRNA and depicted as fold change compared with si*GFP* transfected cells, set as 1. Data are means ± SD ($n = 3$).

4.3.4. Role of UBB and UBC in Gastric Adenocarcinoma Cell Proliferation and Survival

Tang et al. demonstrated that siRNA-mediated knockdown of *UBB* and *UBC* mRNAs, targeted individually and in combination, led to a reduction in Ub levels in A549 lung cancer cells [10]. In addition, downmodulation of these "pro-survival factors" inhibited cancer cell proliferation, induced the apoptotic process and decreased the tumor size of A549-derived xenografts in vivo [10]. On these bases, we targeted *UBB* and *UBC* in 23132/87 and MKN45 GC cells. siRNA-mediated silencing of *UBB* and *UBC*, alone or in combination, led to a marked decrease in their respective mRNAs ($p < 0.001$ for *UBB* silencing with si*UBB* in both cell lines; $p = 0.002$ and $p = 0.003$ for *UBC* silencing with si*UBC* in 23132/87 and MKN45, respectively; $p = 0.007$ for *UBB* and $p = 0.029$ for *UBC* silencing with si*UBB*+si*UBC* in 23132/87; $p = 0.009$ for *UBB* and $p = 0.013$ for *UBC* silencing with si*UBB*+si*UBC* in MKN45), with *UBB* knockdown being more effective than *UBC* knockdown in both GC cell lines (Figure 4A,B). To ascertain if the downregulation of one poly-Ub gene could be compensated by the transcriptional induction of the other, we evaluated *UBC* and *UBB* transcript levels in si*UBB* and si*UBC* transfected cells, respectively. Data obtained demonstrate that an effective knockdown of *UBC* triggers *UBB* upregulation only in the 23132/87 primary cells ($p = 0.032$), while *UBB* silencing is not compensated for by *UBC* upregulation in the investigated GC cell lines (Figure 4A,B). We then sought to investigate the effects of the siRNA-mediated knockdown of *UBB* and *UBC* on the free and conjugated Ub pools in 23132/87 and MKN45 cells. Our results show that si*UBB*, si*UBC* and si*UBB*+si*UBC* transfections efficiently decreased the conjugated Ub pool in both 23132/87 and MKN45 cell lines, with the most prominent reduction detected in *UBB*+*UBC* silenced GC cells. Moreover, the knockdown of polyubiquitin genes, singularly or in combination, also caused a significant decrease in free Ub levels, with the highest effect observed in the 23132/87 primary cells, transfected with si*UBB*+si*UBC* (Figure 4C). The free Ub content upon siRNA treatments was accurately determined by running whole cell extracts along with a proper range of Ub standards in the same immunoblot (Table S3). Results of two independent experiments indicate a 50.4% reduction in free Ub content in the double knockdown 23132/87 primary cell line, while a similar lower decrease was caused by the single knockdown of *UBB* or *UBC* (Table S3). The MKN45 metastatic cell line underwent a reduction in free Ub levels following *UBB* and *UBC* silencing, with the first one being far more effective (40.5% and 22.5% reduction, respectively). Simultaneous knockdown of both *UBB* and *UBC* genes had no further impact on the free Ub

pool compared to *UBB* silencing only (Figure 4C and Table S3). Of note, a reduced level of the immunoreactive band corresponding to ubiquitinated H2A histone is appreciable in both 23132/87 and MKN45 cells treated with *UBB-* and/or *UBC-*targeting siRNAs (Figure 4C).
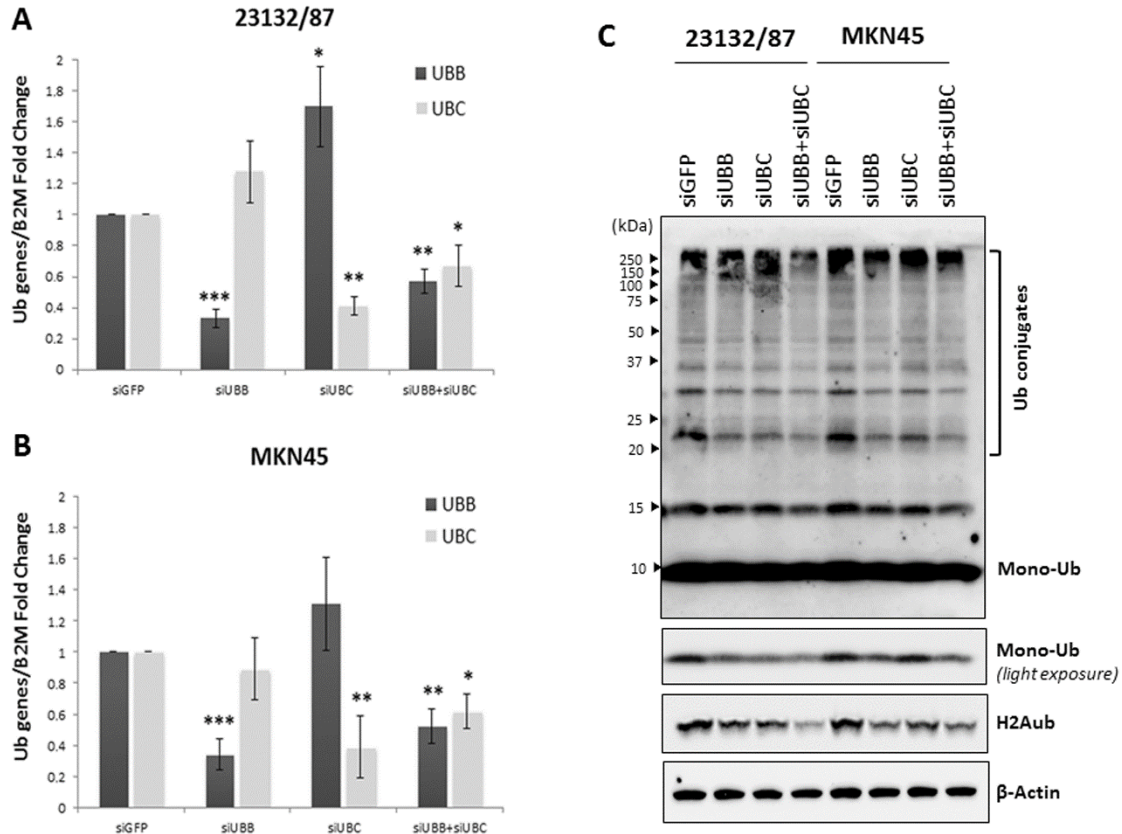

Figure 4. siRNA-mediated knockdown of *UBB* and *UBC* in 23132/87 and MKN45 cell lines. 23132/87 and MKN45 cells were transiently transfected with either control *GFP* or *UBB*, *UBC* or *UBB+UBC* siRNAs. At 48 h after transfection, the mRNA levels of *UBB* and *UBC* for 23132/87 (**A**) and MKN45 (**B**) were measured by real-time quantitative PCR, normalized to *B2M* mRNA and depicted as fold change compared with si*GFP* transfected cells, set as 1. Data are means ± SD ($n = 3$); * $p < 0.05$, ** $p < 0.01$, *** $p < 0.001$. (**C**) Representative western immunoblots ($n = 2$) of total protein lysates (5 µg) of 23132/87 and MKN45 cells obtained 48 h after transfection with si*GFP* (control), si*UBB*, si*UBC* and si*UBB*+si*UBC*. The samples were loaded and probed with anti-Ub antibody to detect the conjugated and mono-Ub pools (the latter were analyzed using the light exposure image). Blots were reprobed with anti-H2Aub and anti-β-Actin antibody, used as a loading control. Brackets indicate Ub conjugates. Arrowheads on the left indicate the molecular weight standards.

We then evaluated the pro-survival role of the poly-Ub coding genes in both primary and metastatic GC cell lines. Our results show that the combined silencing of *UBB* and *UBC* genes led to a significant decrease ($p = 0.004$) in 23132/87 cell viability (Figure 5A), detected at 48 h post-transfection, but had no effect on MKN45 cells (Figure 5B). These data indicate that 23132/87 primary GC cells are more strictly dependent on the Ub levels in order to maintain their over-proliferation rate. Finally, we looked for a molecular mechanism accounting for the

reduced cell viability observed in the 23132/87 cells after the simultaneous silencing of poly-Ub genes *UBC* and *UBB*. Considering the role of the extrinsic pathway of apoptosis in gastric adenocarcinoma [39], we evaluated if the significant decrease (p = 0.004) in 23132/87 cell viability after treatment with the combination si*UBB*+si*UBC* could be linked to an increase in Fas levels [31] and activation of caspase 3. As shown in Figure 5C, si*UBB*+si*UBC* transfection in the 23132/87 cells led to a remarkable increase in the pro-apoptotic protein Fas and to a decrease in the inactive full-length caspase 3, indicating activation of the apoptotic process [28]. Instead, the si*UBB*+si*UBC* treatment did not modify Fas and full-length caspase 3 levels in MKN45 cells (Figure 5D), which is consistent with the lack of effect on cell viability (Figure 5B).

Zhang et al. [40] showed that the transcription factor β-catenin is an oncoprotein in gastric cancer and the Kruppel-like factor 4 (KLF4)-mediated inhibition of β-catenin expression led to a reduction in the proliferation rate, migration and invasion capacities of MKN45 gastric cancer cells. In light of these results, we evaluated the β-catenin protein levels in 23132/87 and MKN45 cancer cells after si*UBB*, si*UBC* and si*UBB*+si*UBC* treatments. *UBB* and *UBC* silencing decreases the β-catenin levels in 23132/87 cells, while in MKN45 cells the β-catenin levels are not affected (Figure 5E,F).
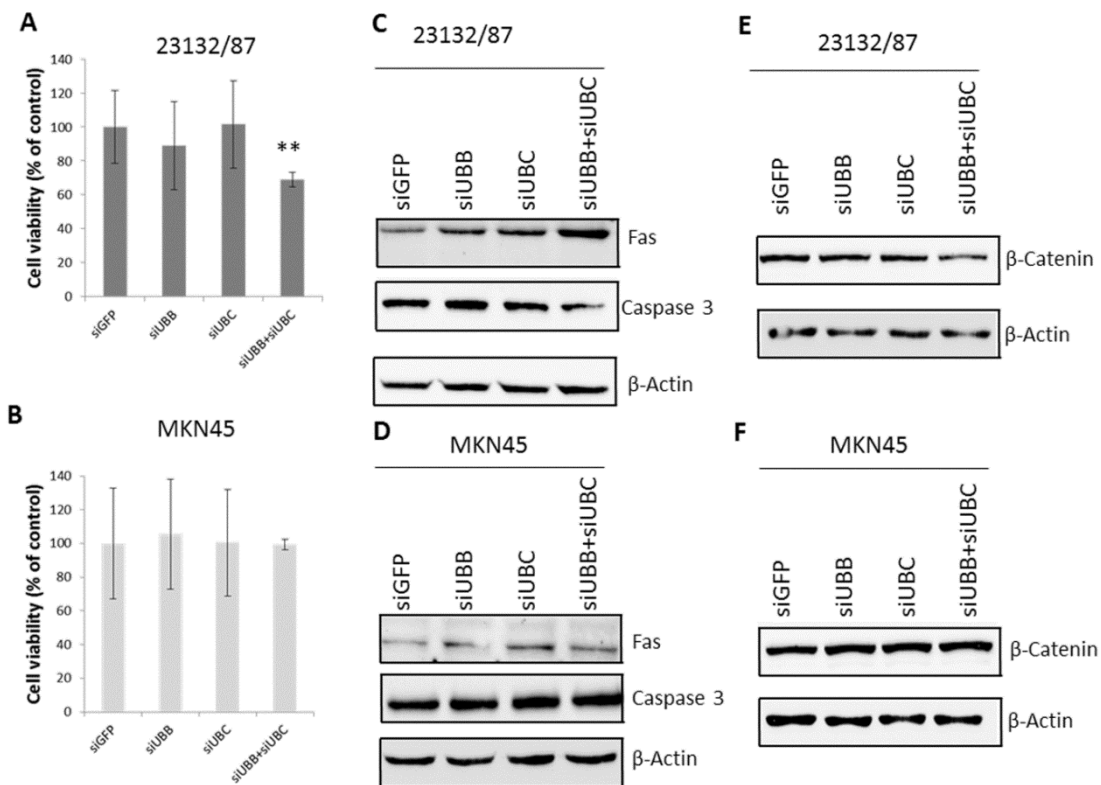
Figure 5. MTS (3-(4,5-dimethylthia-zol-2yl)-5-(3-carboxymethoxyphenyl)-2-(4-sulfophenyl)2*H*-tetrazolium) assay for 23132/87 and MKN45 cells and evaluation of apoptotic and pro-survival markers. Cell viability of 23132/87 (**A**) and MKN45 (**B**) cells transiently transfected (48 h) with either si*GFP* (control) or with *UBB, UBC* or *UBB*+*UBC* siRNAs was evaluated via MTS assay (n = 8) and shown as a percentage with respect to the si*GFP* transfected cells, set as 100%; ** p <0.01. (**C,D**) Representative western immunoblots of total proteins from 23132/87 (**C**) or MKN45 (**D**) cells transfected as in (**A**) and (**B**), respectively (n = 3). A quantity of 15 μg of total cellular proteins was loaded and probed with antibodies

specific for Fas or Caspase 3; blots were reprobed with anti-β-Actin, used as a loading control. (**E,F**) Representative western immunoblots of total proteins from 23132/87 (**E**) or MKN45 (**F**) cells transfected as in (**A**) and (**B**), respectively (n = 2). A quantity of 7.5 μg of total cellular proteins was loaded and probed with the antibody specific for β-catenin; blots were reprobed with anti-β-Actin, used as a loading control.

4.4 Discussion

Gastric adenocarcinoma is the second most common cause of cancer-related death worldwide [28]. In a recent study by Tian et al. [29], the four Ub coding genes (*UBA52*, *RPS27A*, *UBB, UBC*) were all identified as gastric-related therapeutic indicators, based on ego network analysis. In fact, their overexpression was found to be related to the progression and metastasis development of gastric cancer [29].

Our results show that Ub gene expression is significantly different in the primary and metastatic GC cell lines investigated, i.e., 23132/87 and MKN45. In particular, the metastatic MKN45 cells display higher levels of *UBB, UBC* and *RPS27A* gene transcription, in agreement with the evidence of Tian et al. [29], which links the upregulation of Ub genes to metastasis development. *UBB* and *UBC* upregulation in several cancers is widely documented [9,10]. Regarding *UBA52*, Zhou et al. [41] showed that, in colorectal cancer, the long non-coding RNA LUCAT1 controls *UBA52* by negatively affecting the Ub-RPL40 protein stability. Since LUCAT1 is also highly expressed in gastric cancer [42], it can be hypothesized that a similar post-translational control also occurs in 23132/87 and MKN45 gastric cancer cells.

In contrast to the transcript levels of the Ub genes, the two GC cell lines 23132/87 and MKN45 showed no significant differences in their total Ub levels and in the Ub distribution between the free and conjugated pools, although the MKN45 GC cell line showed a greater transcription of three out of four Ub coding genes. We hypothesize that different post-transcriptional regulatory mechanisms may account for this discrepancy. In their review, Liu et al. [43] conclude that transcription levels by themselves are not sufficient to predict protein levels in many scenarios in the cell. Multiple processes beyond transcript concentration contribute to establishing the real expression level of a protein: translation rates modulated by non-coding RNAs (such as miRNAs and long non-coding RNAs); protein synthesis delay, in which transcript changes will affect protein levels only with a certain temporal delay; and also modulation of the protein half-life through both ubiquitin-proteasome and lysosomes-autophagy pathways [43]. In addition, Schwanhausser et al. [44] finely evaluated, on a genomic scale, the correlation between mRNA and protein levels and found it to be quite low (R^2 around 0.4). Furthermore, we demonstrated that the MKN45 cell line has a higher chimotrypsin-like proteasome activity, which could be at least partially responsible for the lack of differences of total Ub levels in 23132/87 and MKN45 cells. In fact, it has been demonstrated that Ub can be degraded by the proteasome following three routes: along with its conjugated substrate, when extended with a C-terminal tail and as a monomer under different pathophysiological conditions [45].

To shed light on the molecular players supporting Ub gene expression in GC cells, we preliminarily evaluated the levels and the intracellular distribution of HSF1, YY1 and SP1 transcription factors in the MKN45 compared to the 23132/87 cell line. Several pieces of

evidence in the literature, including our previous studies, indeed reported the involvement of these transcriptional regulators in the expression of the Ub genes, either in basal or stressful conditions [14–21].

Moreover, these transcription factors have all been linked to gastric cancer development [22–24]. In particular, *HSF1* knockdown reduced the proliferation, migration and invasiveness capabilities of AGS and MKN28 gastric adenocarcinoma cell lines [24]. *YY1* overexpression enhanced GC cell proliferation, monolayer colony formation and xenograft growth, whereas *YY1* knockdown inhibited GC cell proliferation both *in vitro* and *in vivo* [22]. Arora et al. [46] showed that the cytotoxic effect of the drug triptolide in MKN45 and MKN28 GC cells is mediated by a decrease in the SP1 levels and the activation of caspases 3 and 7.

Our results show lower total and cytosolic HSF1 levels in MKN45 cells with respect to 23132/87 cells, although the nuclear levels of the transcription factor are similar in the two cell lines. HSF1 is a key player in the transcriptional programs mounted in stressed cells to maintain proteostasis, which is accomplished by HSF1-mediated expression of stress-protective genes. Interestingly, Gencer and Irmak Yazicioglu [47] demonstrated that 23132/87 cells are more prone to cellular stresses, in particular to oxidative stress accumulation, compared to MKN45 cells. In light of these findings, the higher HSF1 levels of 23132/87 cells could have a protective role in the survival of these primary gastric adenocarcinoma cells under stress challenges. Finally, it cannot be excluded that the increased proteasome activity of MKN45 is actually contributing to the reduced cytosolic levels of HSF1 in this cell line.

The other significant signature is represented by the higher nuclear levels of YY1 in the metastatic cell line, which we hypothesized could at least in part explain the higher levels of *UBC* expression in MKN45 cells compared to 23132/87 cells, but this hypothesis has been denied by the *YY1* silencing experiments (see below).

siRNA-mediated targeting of *YY1*, *HSF1* and *SP1* was effective at both mRNA and protein levels in 23132/87 and MKN45 cell lines. However, the knockdown of these transcription factors does not significantly affect the expression of the four Ub genes. The results of TF silencing herein obtained differ from those previously reported for HeLa cervical cancer cells, where YY1 regulates the basal *UBC* expression [15] and HSF1 drives the transcriptional induction of the *UBC* gene after proteotoxic and oxidative stress [16,21], while SP1 plays a role in the basal *UBC* expression [14,17], besides being involved in the glucocorticoid-mediated transcriptional induction of the *UBC* gene, in muscle and multiple myeloma cells [17,18]. This may be explained by a cancer cell-type specific role of YY1, HSF1 and SP1 in regulating basal Ub gene expression. The lack of effect on *UBC* and *UBB* gene transcription in *HSF1*-silenced gastric cancer cells may depend on the fact that HSF1 is a stress-activated TF, while for YY1 we evaluated different target genes in the si*YY1*-transfected cells and we found that they are differently affected by *YY1* knockdown. Among *BAX*, survivin and *c-MYC*, only the expression levels of the oncogene *c-MYC* were affected, showing a significant reduction after siRNA targeting *YY1*.

Several reports demonstrated the pro-survival role of *UBB* and *UBC* in cancer cells. Oh et al. [9] showed that knockdown of *UBB* in neuroblastoma, hepatocarcinoma, breast and prostate cancer cell lines led to an increase in p53 and cleaved PARP1 levels, induction of G2/M block, increase in the number of apoptotic cells and decrease in cancer cell proliferation rates. In

addition, Tang et al. [10] demonstrated that the knockdown of *UBB* and *UBC* in A549 lung cancer cells led to a reduction in cancer cell viability, activation of the intrinsic pathway of apoptosis, decrease in NF-kB and p-Akt levels (after irradiation treatment) and reduction in the volume of A549-derived xenografts. Lastly, Kedves et al. [48] showed that concurrent loss of *UBB* and *UBC* expression in several gynecological tumor cell lines led to a consistent decrease in their viability and to an increased survival of tumor-injected mice. On these bases, we targeted *UBB* and *UBC* in 23132/87 and MKN45 GC cells and found that every treatment significantly decreased the mRNA levels of the target gene. At the protein level, we found that si*UBB*, si*UBC* and si*UBB*+si*UBC* transfections were able to cause a similar reduction in conjugated Ub levels in 23132/87 and MKN45 GC cells, with the most noticeable reduction detected in the double knockdown cells. As for the levels of free Ub, they were significantly reduced by the silencing of polyubiquitin genes, with the lowest Ub levels detected in the primary 23132/87 cells treated with si*UBB*+si*UBC*, while in the same cell line, the targeting of only one gene (*UBB* or *UBC*) had a lower but similar impact on the free Ub content. While in the metastatic cell line MKN45, the *UBB* gene appears to mainly contribute to Ub homeostasis, in fact the free Ub content in *UBB* silenced cells is similar to that found in the double knockdown cells.   Moreover, the reduction in ubiquitinated H2A levels that can be appreciated after transfection of siRNAs targeting the polyubiquitin genes *UBB* and *UBC*, alone or in combination, further supports the efficacy of the silencing at the protein level. In fact, as reported by Dantuma et al. [49], a redistribution of Ub between the different pools occurs under stressful conditions and the deubiquitination of histones contributes to restoring the mono-Ub pool necessary to cope with cellular stress. We can speculate that gastric cancer cells 23132/87 and MKN45 attempted to counteract the siRNA-mediated Ub depletion in a similar way, i.e., by using the ubiquitinated histones as a "ready to use" reservoir to partially restore the free Ub pool. The use of this rescue mechanism seems more evident in the 23132/87 primary cells subjected to the double knockdown of *UBB* and *UBC* genes. Overall, H2Aub levels show the same layout as mono-Ub in both cell lines, consistent with them being a source of readily available free ubiquitin.

Of note, there was a significant upregulation of the *UBB* gene after si*UBC* treatment in 23132/87 cells, indicating that these cells try to compensate for the *UBC* downregulation through an increase in the transcription of the other poly-Ub gene, namely *UBB*.

Noteworthy, *UBB* silencing does not result in *UBC* induction to restore cellular Ub levels, suggesting that *UBC* knockdown is more detrimental for 23132/87 cell survival given its higher coding potential compared to *UBB*. In this light, targeting both poly-Ub genes could prevent primary GC cells from activating those survival mechanisms able to restore their Ub levels. Interestingly, while MKN45 viability was not affected by *UBB* and *UBC* knockdown, 23132/87 suffered a cell viability reduction after treatment with a combination of si*UBB* and si*UBC*, which caused an increase in the tumor suppressor protein Fas and activation of the apoptotic process. In agreement with the lack of cell viability reduction in the metastatic MKN45 cells, neither Fas nor caspase 3 levels were modified by the si*UBB*+si*UBC* treatment. The role of extrinsic apoptosis in the reduction in cell viability of GC cells has been investigated by Hsu et al. [39]. The authors showed that the activation of the apoptotic process reduced the proliferation rate of AGS and SNU-16 GC cells, particularly after Fas ligand (FasL) treatment and activation of Fas [39]. The interaction of FasL with the transmembrane protein Fas indeed

leads to the activation of caspase 8 and caspase 3, inducing the extrinsic apoptotic pathway [28,50]. Apoptosis is a tightly controlled process, characterized by three pathways, namely, the mitochondrial [28], endoplasmic reticulum [51] and death receptor signaling pathways [28]. Interestingly, Zhang et al. have demonstrated, in several cancer cell lines, that the oncoprotein Cysteine-rich intestinal protein 1 (CRIP1) can interact with Fas, enhancing its ubiquitination and degradation and leading to inhibition of caspases 8 and 3, thus underlining the tumor suppressor role of this transmembrane protein [52].

Interestingly, the role of the oncoprotein β-catenin in overproliferation, migration and invasion of several tumors, including gastric adenocarcinoma, has been reported [40]. We found that the siRNA-mediated knockdown of both *UBB* and *UBC* mRNAs decreases the β-catenin levels in 23132/87 cells, but not in MKN45 cells. The reduction in β-catenin levels correlates with the cell viability decrease after si*UBB*+si*UBC* treatment detected only in the primary 23132/87 gastric cancer cells. These data complement the evidence by Zhang et al. [40] and further consolidate the role of β-catenin as an important factor in the "survivability fitness" of these cell lines, in particular for MKN45 cells, which are able to preserve steady levels of this metastatic marker.

Results herein obtained show that the combined silencing of *UBB* and *UBC* genes triggers the molecular pathways of extrinsic apoptosis only in 23132/87 cells, suggesting that Ub downmodulation may counteract the pro-survival role of poly-Ub genes in primary but not in metastatic gastric adenocarcinoma. This different sensitivity to reduction in Ub levels of the primary and metastatic GC cell lines cannot be explained by a different intracellular Ub content/distribution between pools but rather by a different dependence on Ub levels for survival and proliferation.

Up- and downregulation of Ub content has been demonstrated to affect the levels/activity of many regulatory proteins in a cell- and context-specific manner [53,54]. Furthermore, little is known about the trans-acting factors controlling Ub gene transcription in cancer cells.

Our data allow us to exclude the involvement of YY1, HSF1 and Sp1 in driving Ub expression in 23132/87 and MKN45 GC cell lines. Thus, further studies on the molecular players involved in the control of Ub gene expression as well as on signaling cascades affected by altered Ub levels will be of value for the characterization of the molecular patterns associated with GC development.

Meanwhile, the role of Ub in the regulation of intracellular levels of various tumor suppressor proteins should be addressed in GC, as already reported for BAX [55] and p53 [56] in other cancers. In a very recent paper, Peng et al. [55] showed that mutation of the two ubiquitin-binding sites in the pro-apoptotic protein BAX increased its half-life and its ability to activate the intrinsic pathway of apoptosis in HCT116 tumor cells. Zhou et al. [56] demonstrated that the oncoprotein MNAT1 binds to p53 leading to its ubiquitin-mediated degradation through Mouse double minute 2 homolog (MDM2), decreasing apoptosis and increasing cell growth in human colorectal cancers. On these bases, it would be important to investigate if decreasing the Ub levels in GC through the targeting of the poly-Ub coding genes affects the levels of such apoptotic markers. Our preliminary evidence shows that combined targeting of poly-Ub genes *UBB* and *UBC* significantly affects the cellular Ub protein content in the two GC cell lines, being more detrimental for the viability of primary gastric adenocarcinoma 23132/87

cells. Further *in vitro* experiments (i.e., using other GC cell lines such as AGS and SNU-16 [39]) and *in vivo* studies are needed to warrant *UBB* and *UBC* as potential therapeutic targets and Ub protein levels as a new biomarker in gastric adenocarcinoma.

4.5 Materials and Methods

4.5.1. Cell Cultures and Chemicals

23132/87 and MKN45 GC cell lines were purchased from DMSZ (German Collection of Microorganisms and Cell Cultures GmbH; Braunschweig, Germany). 23132/87 cells have been identified as primary gastric adenocarcinoma of the intestinal type [57], while MKN45 have been identified as a metastatic GC cell line displaying the characteristics of both diffuse and intestinal types [58]. The web reference "https://cansarblack.icr.ac.uk/cell-line/MKN-45/copy-number" [59] reports average copy numbers of 1.132, 1.091 and 1.104 for *HSF1*, *YY1* and *SP1* in MKN-45, respectively, and 1.100, 1.094, 1.061 and 1.127 for *UBC*, *UBB*, *UBA52* and *RPS27A*, respectively. MKN45 cells are also reported by the DSMZ site as a hypertryploid cell line, with 8% of polyploidy; the percentage seems to roughly correspond with the average copy numbers reported above. 23132/87 cells were grown at 5% CO_2 at 37 °C in Roswell Park Memorial Institute (RPMI) 1640 medium supplemented with 20% heat-inactivated fetal bovine serum (Sigma-Aldrich, St. Louis, MO, USA), 2 mM glutamine and 1x antibiotics (100 μg/mL streptomycin and 100 U/mL penicillin), both from Sigma-Aldrich. MKN45 cells were grown at 5% CO_2 at 37 °C in the same medium, but 20% heat-inactivated fetal bovine serum (10270-106) from Gibco (ThermoFisher Scientific, Waltham, MA, USA) was used instead. All cell lines were sub-cultivated at a 1:3 ratio, 3 times per week. The 23132/87 and MKN45 GC cell lines were proved to be mycoplasma-free (every 6 months) using the EZ-PCR Mycoplasma Test Kit (BI, Biological Industries). The most recent Mycoplasma Test assay was performed on January 17th, 2020 (Figure S1D). All chemicals were purchased from Sigma-Aldrich, unless otherwise specified.

4.5.2. Small Interfering RNA Transfection in 23132/87 and MKN45 Cells

Small interfering RNA (siRNA)-mediated gene silencing in 23132/87 and MKN45 cells was achieved by transfecting siRNA duplexes with RNAiMAX (Invitrogen, Thermo Fisher Scientific), according to the standard transfection protocol. Briefly, 3×10^5 and 6×10^5 cells for 23132/87 and MKN45, respectively, were seeded in 6-well plates, while 5×10^3 cells were seeded in 96-well plates for both cell lines. After 24 h, siRNAs targeting *UBB*, *UBC* (or their combination at 10 nM si*UBB* and 10 nM si*UBC*), *YY1*, *HSF1* or *SP1* mRNA and the *GFP*-targeting control siRNA were transfected at a final concentration of 20 nM in the presence of 9 μL and 1.5 μL of RNAiMAX transfection reagent for 6-well plates and 96-well plates, respectively. The samples were collected after 48 h. *HSF1* siRNA was purchased from Qiagen (Hilden, Germany); *SP1*, *UBB* and *UBC* siRNAs were purchased from Sigma-Aldrich, while the *YY1* siRNA and *GFP* control siRNA were from Biomers (Ulm, Germany). The oligonucleotide targeting sequences are reported below:

Hs_*YY1*: ATGCCTCTCCTTTGTATATTA
Hs_*HSF1*: CAGGTTGTTCATAGTCAGAAT
Hs_*SP1*: TTGGGTAAGTGTGTTGTTTAA
Hs_*UBB*: CCAAGATCCAAGATAAAGA
Hs_*UBC*: GATCAGCAGAGGTTGATCT
GFP: CGGCAAGCTGACCCTGAAGTTCAT

4.5.3. Real-Time Quantitative Polymerase Chain Reaction (RT-qPCR)

For gene-specific expression analysis, total RNA was isolated using the RNeasy Plus Mini kit (Qiagen, Hilden, Germany). A quantity of 0.5 µg of total RNA was reverse-transcribed using Primescript RT Master Mix (Perfect Real Time; Takara Bio Europe SAS, Saint-Germain-en-Laye, France) with oligo-dT and random hexamer primers, following the manufacturer's instructions. qPCR detection and expression analysis of genes was performed with Synergy Brands (SYBR) green quantitative real-time PCR, using the Hot-Rescue Real Time PCR Kit (Diatheva s.r.l., Cartoceto PU, Italy), according to the manufacturer's instructions. Briefly, the reaction was set up in a 25 µL final volume, using 5 ng cDNA as the template and 200 nM of each specific primer. For RT-qPCR amplifications, 40 PCR cycles were run with the following thermal profile: 15 s at 95 °C melting temperature, 15 s at 60 °C annealing and 1 min at 72 °C extension temperature per cycle; before cycling, 10 min at 95 °C were allowed for Hot-Rescue Taq DNA polymerase activation. Fluorescence intensity of each amplified sample was measured with an ABI PRISM 7700 Sequence detection system (Applied Biosystems, Foster City, CA, USA). All measurements were performed at least in triplicate and reported as the average values ± standard deviation of the mean (mean ± SD). Target gene values were normalized with *B2M* mRNA measurements, and expression data were calculated according to the $2^{-\Delta\Delta Ct}$ method [60]. Primers were designed using Primer 3 Plus, and their sequences are reported in Table 1.

Table 1. Oligonucleotides used for quantitative real-time PCR.

Forward Primer	Sequence (5′ to 3′)	Reverse Primer	Sequence (5′ to 3′)
UBC-f	GTGTCTAAGTTTCCCCTTTTAAGG	UBC-r	TTGGGAATGCAACAACTTTATTG
UBB-f	CTTTGTTGGGTGAGCTTGTTTGT	UBB-r	GACCTGTTAGCGGATACCAGGAT
UBA52-f	CTGCGAGGTGGCATTATTGAG	UBA52-r	GTTGACAGCACGAGGGTGAAG
RPS27A-f	TCGTGGTGGTGCTAAGAAAAGG	RPS27A-r	TTCAGGACAGCCAGCTTAACCT
B2M-f	GCCTGCCGTGTGAACCAT	B2M-r	CATCTTCAAACCTCCATGATGCT
HSF1-f	CTGACGGACGTGCAGCTGAT	HSF1-r	CCCGCCACAGAGCCTCAT
YY1-f	GAAGCCCTTTCAGTGCACGTT	YY1-r	ACATAGGGCCTGTCTCCGGTAT
SP1-f	GCCTCTCAACTGCCCTAAGTCCT	SP1-r	ACCTGCCCTTGTCCACAATGTT
C-MYC-f	CTGAAGAGGACTTGTTGCGGAAAC	C-MYC-r	TCTCAAGACTCAGCCAAGGTTGTG

39

4.5.4. Cell Extracts

To obtain whole protein extracts, cells were scraped from plates with a buffer containing 50 mM Tris/HCl pH 7.8, 0.25 M sucrose, 2% (*w/v*) sodium dodecyl sulfate (SDS), 10 mM N-ethylmaleimide (NEM), 1 mM NaF and 1 mM Na_3VO_4, supplemented with a cocktail of protease inhibitors (Roche Diagnostics, Mannheim, Germany). Lysates were boiled, sonicated twice at 100 Watts for 10 sec and cleared by centrifugation at 12,000× *g* for 10 min, then the supernatant was recovered. To obtain cytosolic and nuclear extracts, after washing with phosphate buffered saline (PBS), cells were scraped from the dishes with cold buffer A (10 mM HEPES/KOH pH 7.9, 1.5 mM $MgCl_2$, 1 mM NEM, 1 mM ethylenediaminetetraacetic acid (EDTA), 10 mM KCl, 0.1% (*v/v*) Nonidet-P40, 0.5 mM dithiotreitol (DTT), 1 mM NaF and 1 mM Na_3VO_4, supplemented with protease inhibitors (Roche Diagnostics). The samples were then incubated on ice for 10 min before centrifugation at 12,000 × *g* for 10 min at 4 °C. Supernatants (containing cytosolic proteins) were recovered, while the nuclear pellets were lysed in the same buffer used to obtain whole protein extracts, then boiled, sonicated and cleared by centrifugation at 12,000× *g* for 10 min to obtain nuclear fractions. The protein content in whole cell extracts and nuclear fractions was determined by the method of Lowry, while the Bradford assay (Bio-Rad, Hercules, CA, USA) was used for the cytosolic fractions.

4.5.5. Western Blot Analysis

Proteins were resolved by SDS polyacrylamide gel electrophoresis (SDS-PAGE) and electroblotted onto a nitrocellulose membrane (0.2 μm pore size) (Bio-Rad). The blots were probed with the following primary antibodies: anti-HSF1 (#4356, polyclonal), anti-Fas (#4233, monoclonal: C18C12), anti-Lamin A/C (#4777, monoclonal: 4C11; for nuclear extracts), anti-Caspase 3 (#9668, monoclonal: 3G2) and anti-H2AUb (Lys 119) (#8240, monoclonal: D27C4) from Cell Signaling Technology (Danvers, MA, USA); anti-YY1 (#sc-7341, monoclonal: H-10), anti-SP1 (#sc-420, monoclonal: 1C6), anti-Ub (rabbit polyclonal, kindly provided by Prof. A. L. Haas, Louisiana State University, Health Sciences Center, New Orleans), anti-β-Actin (#sc-47778, monoclonal: C4; for whole extracts) and anti-β-catenin (#sc-7963, monoclonal: E-5) from Santa Cruz Biotechnology (Dallas, TX, USA); anti-GAPDH (#A300-641A-T, polyclonal; for cytosolic extracts) from Bethyl Laboratories (Montgomery, TX, USA). Immunoreactive bands were detected by horseradish peroxidase (HRP)-conjugated secondary antibodies (Bio-Rad). Peroxidase activity was detected with the enhanced chemiluminescence detection method (WesternBright ECL, Advasta, Menlo Park, CA, USA) using the ChemiDoc MP Imaging System (Bio-Rad). Quantification of the protein bands was performed using Image Lab analysis software version 5.2.1 (Bio-Rad).

4.5.6. Cell Viability Assay

The effect of siRNA transfections (performed in 96-well plates as detailed above) on cell viability was evaluated by using the CellTiter 96 AQueous One Solution Cell Proliferation Assay (Promega s.r.l., Milan, Italy). This assay is based on the reduction of the MTS reagent [3-(4,5-dimethylthia-zol-2yl)-5-(3-carboxymethoxyphenyl)-2-(4-sulfophenyl)2*H*-tetrazolium, inner salt] into a colored formazan product that is soluble in culture medium. This conversion is

accomplished by NADPH or NADH produced by dehydrogenase enzymes in metabolically active cells. The quantity of formazan product, measured by absorbance at 490 nm, is directly proportional to the number of living cells in the culture. The results were expressed as a percentage of residual cell viability compared to control cells treated with 20 nM si*GFP* (set at 100% cell viability) for both 23132/87 and MKN45 cell lines.

4.5.7. Proteasome Activity Assay

The chymotrypsin-like activity of the 20S proteasome was measured in 23132/87 and MKN45 GC cell lysates using the fluorogenic substrate *N*-succinyl-Leu-Leu-Val-Tyr-7-amido-4-methylcoumarin (sLLVY-NH-Mec, from Sigma-Aldrich, St. Louis, MO, USA) as previously described [21]. Briefly, untreated 23132/87 and MKN45 cells were homogenized on ice in a buffer consisting of 50 mM HEPES/KOH pH 7.8, 1 mM DTT and 0.25 M sucrose. Then, 25, 50 and 75 µg of cleared extracts were incubated at 37 °C in 100 mM HEPES/KOH buffer, pH 7.8, 5 mM $MgCl_2$ and 10 mM KCl and the reaction was initiated by addition of 0.2 mM fluorogenic substrate. The breakdown of the peptide was monitored using a fluorescence microplate reader (FLUOstar OPTIMA, BMG Labtech GmbH, Offenburg, Germany) with an excitation wavelength of 355 nm and an emission wavelength of 460 nm. Proteasome activity in each sample, expressed as fluorimetric units/min/mg, was calculated by submitting data to linear regression analysis ($R^2 > 0.99$).

4.5.8. Ubiquitin Carboxyl-Terminal Hydrolase 2 (Usp2) Digestion and Mono-Ubiquitin Quantification

23132/87 and MKN45 cells were washed with ice cold PBS and lysed in a buffer consisting of 20 mM Hepes/KOH pH 7.9, 25% glycerol, 0.42 M NaCl, 1.5 mM $MgCl_2$ and 1% Nonidet P40, supplemented with a cocktail of protease inhibitors. After 20 min incubation on ice, cell extracts were cleared by centrifugation and protein content was determined by the Bradford assay. Twenty micrograms of extract were incubated at 37 °C for 90 min in a water bath with 0.5 µg of recombinant Usp2 protein or without Usp2 addition (for the undigested control), in a final volume of 40 µL. The digestions were stopped by adding an equal volume of SDS-PAGE sample buffer and boiling. The effective deconjugation of Ub after Usp2 treatment was always verified by running undigested and digested extracts in parallel. To quantify total Ub protein levels, different amounts of Usp2-treated extracts were run on the same gel, in parallel with different amounts of purified ubiquitin (Sigma-Aldrich) used as the reference standard, and submitted to western immunoblotting analysis with an antibody against Ub [53]. The adjusted volume intensity of the ubiquitin immunoreactive bands, in both Ub standard and sample cell lines, was determined using Image Lab analysis software version 5.2.1. Calibration curves were generated, for each immunoblot, by plotting band intensities (adjusted volumes) against Ub standard concentrations. A regression line equation was then generated and used to calculate the Ub concentration in the cell protein samples. The coefficient of determination (R^2) for ubiquitin standard curves was always in the range 0.98–0.99.

4.5.9. Statistical Analysis

The data were expressed as mean ± SD from at least three independent experiments. Student's *t*-test performed with GraphPad Prism Software version 3.06 (La Jolla, CA, USA) was

used for statistical analysis of the data; differences between groups were considered statistically significant when $p < 0.05$. The actual p-values have been reported in the text.

Abbreviations

|	
B2M	Beta-2-Microglobulin
BAX	Bcl-2-like protein 4
C-MYC	Avian myelocitomatosis virus oncogene cellular homolog
CRIP1	Cysteine-rich intestinal protein 1
DTT	Dithiotreitol
DUB	Deubiquitinase
EDTA	Ethylenediaminetetraacetic acid
EMT	Epithelial to mesenchymal transition
FasL	Fas ligand
GAPDH	Glyceraldehyde 3-phosphate dehydrogenase

GC	Gastric cancer
GFP	Green fluorescent protein
HRP	Horseradish peroxidase
HSF1	Heat shock factor 1
KLF4	Kruppel-like factor 4
LUCAT1	Lung cancer-associated transcript 1
MDM2	Mouse double minute 2 homolog
MTS	3-(4,5-dimethylthia-zol-2yl)-5-(3-carboxymethoxyphenyl)-2-(4-sulfophenyl)2H-tetrazolium
NEM	N-ethylmaleimide
PARP1	Poly(ADP-ribose) polymerase 1
PBS	Phosphate buffered saline
RPS27A	Ribosomal protein s27a
RT-qPCR	Real-time quantitative polymerase chain reaction
SDS	Sodium dodecyl sulfate
SDS-PAGE	SDS polyacrylamide gel electrophoresis
siRNA	Small interfering RNA
SP1	Specificity protein 1
SYBR	Synergy Brands
TF	Transcription factor
Ub	Ubiquitin
UBB	Ubiquitin B
UBA52	Ubiquitin a-52 residue ribosomal protein fusion product 1
UBC	Ubiquitin C
Usp2	Ubiquitin carboxyl-terminal hydrolase 2
YY1	Yin yang 1

4.6 Supplementary data
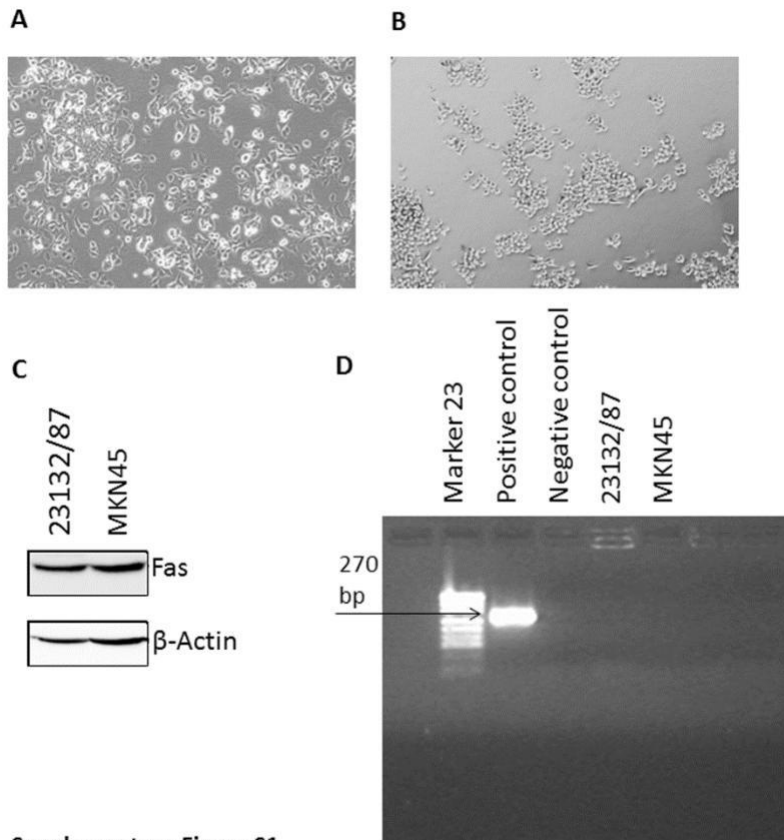
Supplementary Figure S1

Figure S1. Characterization of 23132/87 and MKN45 gastric adenocarcinoma cells. Representative images of 23132/87 (A) and MKN45 (B)were acquired using Olympus IX51 microscope at 20x magnification. (C) Representative western immunoblots (n=3) performed with anti-Fas antibody using 15 µg of total lysates extracted from 23132/87 and MKN45 cell lines; blots were reprobed with anti ß-Actin antibody, used as loading control. (D) Mycoplasma detection assay performed in 23132/87 and MKN45 GC cells; Marker 23 stands for pUC19 DNA/MspI (HpaII) (Thermo Fisher Scientific, Waltham, MA, USA).

A

	Ubiquitin (ng)				23132/87 (µg)				MKN45 (µg)			
11.4	5.7	2.85	1.425	0.7125	0.625	1.25	2.5	3.75	0.625	1.25	2.5	3.75

B

$$y = 1{,}026{,}424.28x - 1{,}338{,}752.61$$
$$R^2 = 0.98$$

Ubiquitin (ng)	Adj. Vol. (Int)
11.4000	10,722,923
5.7000	4,090,443
2.8500	689,118
1.4250	359,600
0.7125	115,299
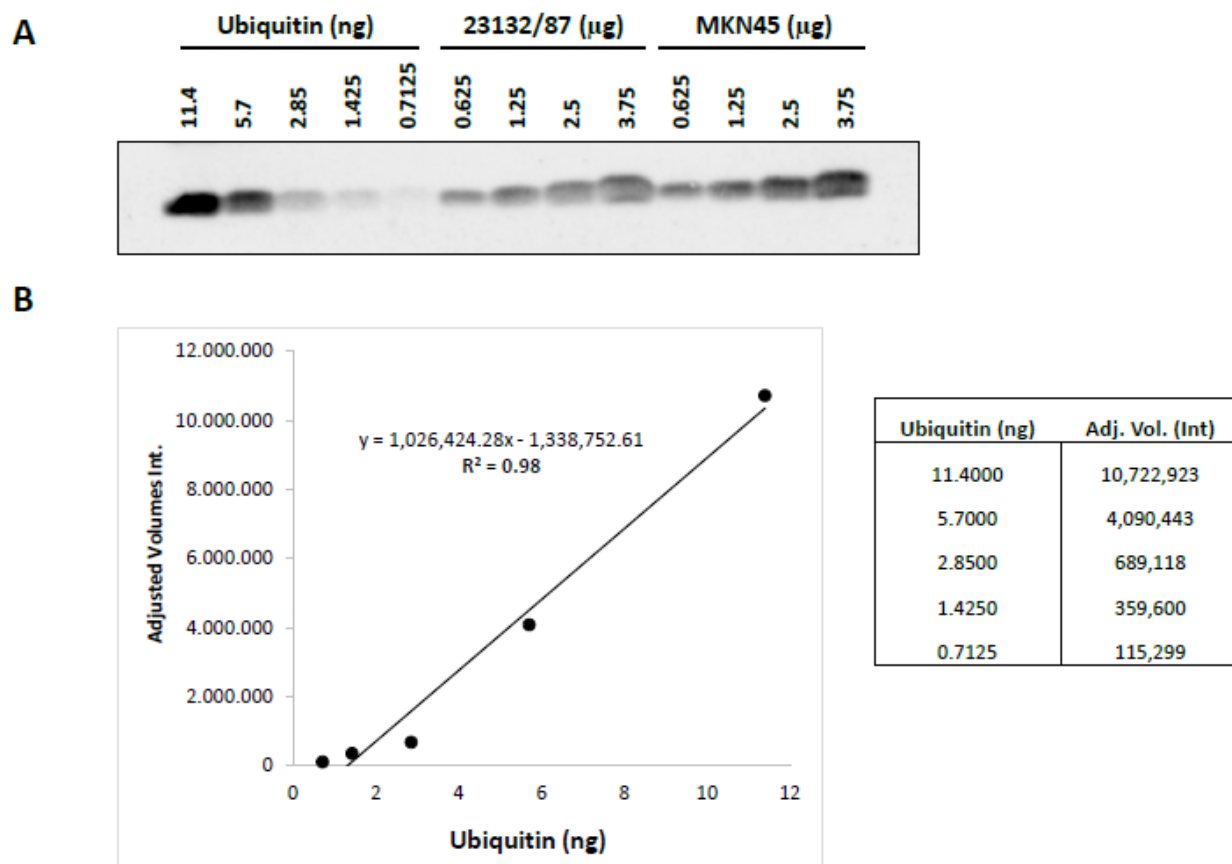
Figure S2. Quantification of total ubiquitin content in 23132/87 and MKN45 gastric cancer cells. (A) A representative immunoblot used for the absolute quantification of total Ub. Whole protein extracts were obtained as described in the Materials and Methods section 4.8. Different amounts of Usp2-treated protein samples were loaded for both 23132/87 and MKN45 cells; Ub standards were provided in the same immunoblot, as indicated. (B) Standard curve derived from the Ub standards of the immunoblot by plotting band intensities (adjusted volumes) against Ub concentrations (the values used are shown in the table on the right). The equation generated by linear regression and the coefficient of determination (R2) are shown.

Figure S3. Full length immunoblots for results shown in Figure 1 and Figure 2.
Lanes highligthed by a star represent samples unrelated to this study.
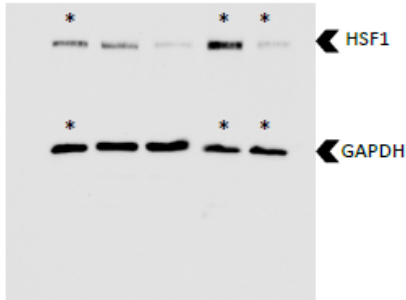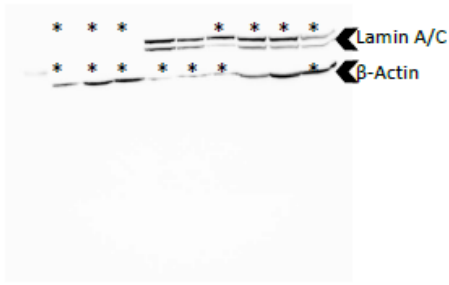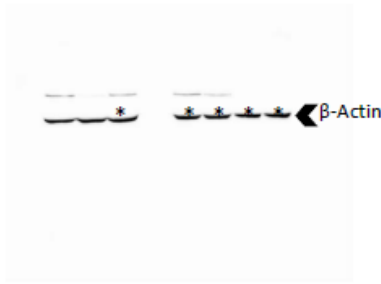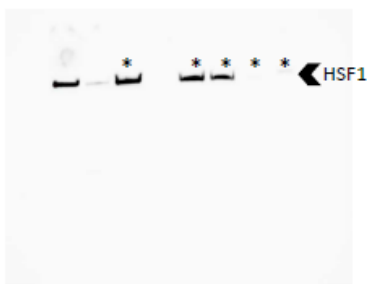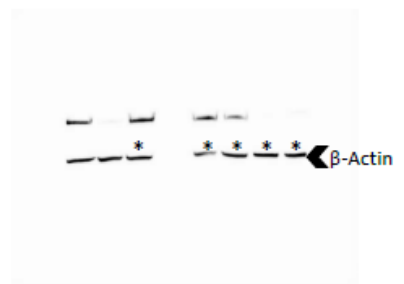
Figure S4. Full length immunoblots for results shown in Figure 2 and Figure 3.
Lanes highligthed by a star represent samples unrelated to this study.
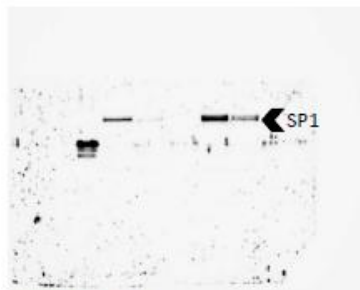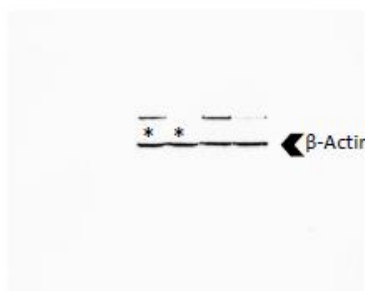
Figure S5. Full length immunoblots for results shown in Figure 3.
Lanes highligthed by a star represent samples unrelated to this study.

High exposure

Ub conjugates

Fig 4C

Light exposure

◄ Mono-Ub

Fig 4C

◄ H2Aub

Fig 4C

◄ β-Actin
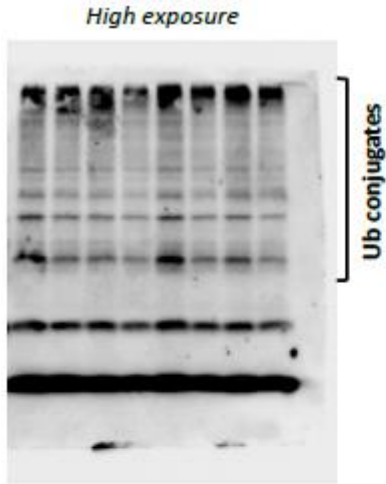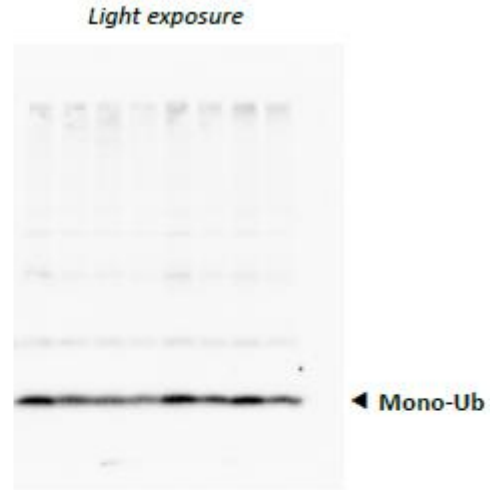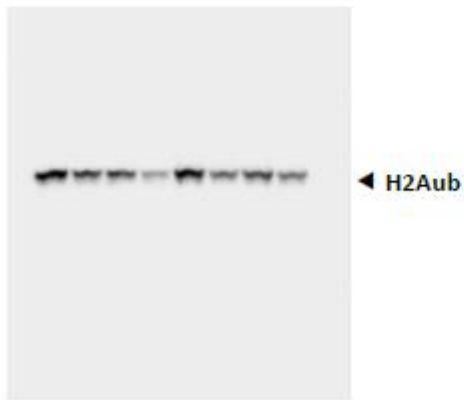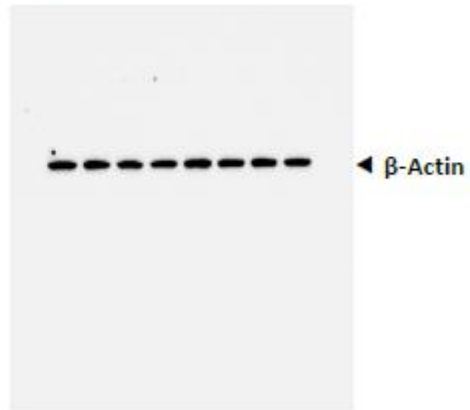
Fig 4C

Figure S6. Full length immunoblots for results shown in Figure 4.

49
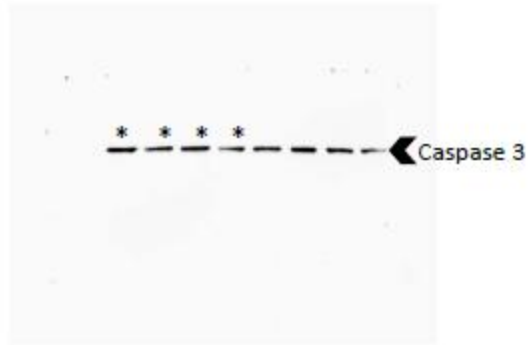
Fig 5C

Fig 5C

Fig 5C
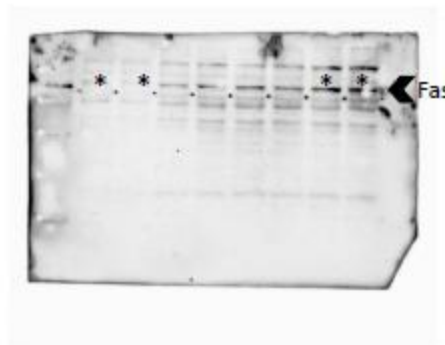
Fig 5D

Figure S7. Full length immunoblots for results shown in Figure 5.
Lanes highligthed by a star represent samples unrelated to this study.
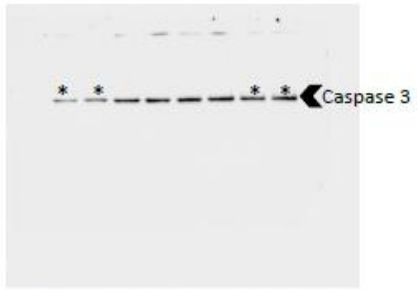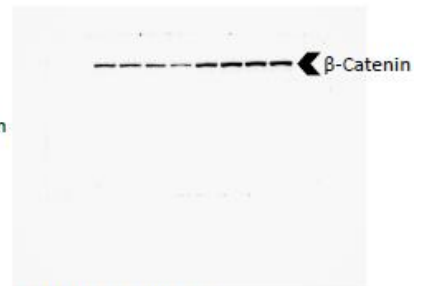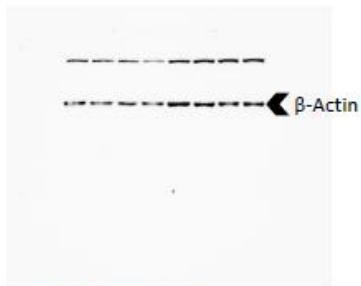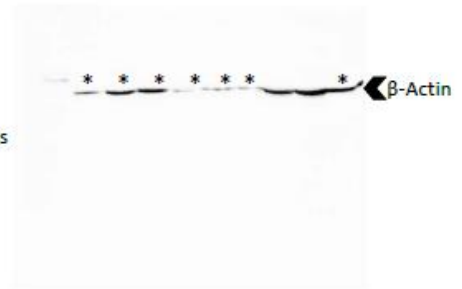
Figure S8. Full length immunoblots for results shown in Figure 5 and Supplementary Figure S1. Lanes highligthed by a star represent samples unrelated to this study.

**FOLD-CHANGES CALCULATED WITH GAPDH AS HOUSEKEEPING GENE**

	UBC		UBB		UBA52		RPS27A	
	UBC 2^-ddCt		UBB 2^-ddCt		UBA52 2^-ddCt		RPS27A 2^-ddCt	
	mean	SD	mean	SD	mean	SD	mean	SD
23132/87	1,00	0,00	1,00	0,00	1,00	0,00	1,00	0,00
MKN45	1,66	0,54	1,16	0,11	1,02	0,19	1,69	0,26

Table S1. Fold changes of UBC, UBB, UBA52 and RPS27A expression levels in 23132/87 and MKN45 gastric cancer cells, after normalization with GAPDH mRNA levels.

	23132/87			MKN45	
	Mean	SD		Mean	SD
siGFP	1.00	0.00	siGFP	1.00	0.00
siYY1	0.72	0.01	siYY1	0.48	0.05
	**			**	

Table S2. Fold changes of C-MYC expression levels in 23132/87 and MKN45 gastric cancer cells, after YY1 silencing. C-MYC mRNA was measured by RT-qPCR, in both 23132/87 and MKN45 cells transfected with siYY1 and siGFP as a control. The mRNA levels of c-MYC were normalized to B2M levels and expressed as fold change relative to siGFP transfected cells set as 1. Data shown are the means ± SD of three independent experiments. Asterisks denote statistical significance; **p< 0.01.

	23132/87 (ng free Ub/µg protein)			MKN45 (ng free Ub/µg protein)		
	Mean	SD	P		Mean	SD	P value
siGFP	1.29	0.309		siGFP	1.11	0.169	
siUBB	0.77	0.130	**	siUBB	0.66	0.091	**
siUBC	0.79	0.125	**	siUBC	0.86	0.068	ns
siUBB+siUBC	0.64	0.107	**	siUBB+siUBC	0.62	0.142	**

Table S3. Quantification of free Ub content in 23132/87 and MKN45 gastric cancer cells, after UBB, UBC and UBB+UBC silencing. Absolute quantification of free Ub (n=2) using 5 µg of protein extracts of GC cells, transfected with siRNAs as indicated, and a linear range of Ub standards run in parallel (for details see Figure S2). Results are given as ng free Ub/µg protein. Asterisks denote statistical significance versus the siGFP control; **P < 0.01; ns, not significant.

4.7 References

1. Hershko, A.; Ciechanover, A. The ubiquitin system. *Annu. Rev. Biochem*. **1998**, *67*, 425-479.
2. Komander, D.; Rape, M. The ubiquitin code. *Annu. Rev. Biochem*. **2012**, *81*, 203-229.
3. Park, C.W.; Ryu, K.Y. Cellular ubiquitin pool dynamics and homeostasis. *BMB Rep*. 2014, *47*, 475-482.
4. Kaiser, S.E.; Riley, B.E.; Shaler, T.A.; Trevino, R.S.; Becker, C.H.; Schulman, H.; Kopito, R.R. Protein standard absolute quantification (PSAQ) method for the measurement of cellular ubiquitin pools. *Nat. Methods* 2011, *8*, 691-696.
5. Wiborg, O.; Pedersen, M.S.; Wind, A.; Berglund, L.E.; Marcker, K.A.; Vuust, J. The human ubiquitin multigene family: some genes contain multiple directly repeated ubiquitin coding sequences. *EMBO J.* 1985, *4*, 755-759.
6. Finley, D.; Bartel, B.; Varshavsky, A. The tails of ubiquitin precursors are ribosomal proteins whose fusion to ubiquitin facilitates ribosome biogenesis. *Nature* 1989, *338*, 394-401.
7. Baker, R.T.; Board, P.G. The human ubiquitin-52 amino acid fusion protein gene shares several structural features with mammalian ribosomal protein genes. *Nucleic Acids Res.* 1991, *19*, 1035-1040.
8. Reyes-Turcu, F.E.; Ventii, K.H.; Wilkinson, K.D. Regulation and cellular roles of ubiquitin-specific deubiquitinating enzymes. *Annu. Rev. Biochem.* 2009, *78*, 363-397.
9. Oh, C.; Park, S.; Lee, E.K.; Yoo, Y.J. Downregulation of ubiquitin level via knockdown of polyubiquitin gene Ubb as potential cancer therapeutic intervention. *Sci. Rep.* 2013, *3*, 2623-2631.
10. Tang, Y.; Geng, Y.; Luo, J.; Shen, W.; Zhu, W.; Meng, C.; Li, M.; Zhou, X.; Zhang, S.; Cao, J.; et al. Downregulation of ubiquitin inhibits the proliferation and radioresistance of non-small cell lung cancer cells in vitro and in vivo. *Sci. Rep.* 2015, *5*, 9476-9487.
11. Deshaies, R.J. Proteotoxic crisis, the ubiquitin-proteasome system, and cancer therapy. *BMC Biol.* **2014**, *12*, 94-107.
12. Wan, Q.; Dingerdissen, H.; Fan, Y.; Gulzar, N.; Pan, Y.; Wu, T.J.; Yan, C.; Zhang, H.; Mazumder, R. BioXpress: an integrated RNA-seq-derived gene expression database for pan-cancer analysis. *Database* (Oxford). **2015**; 2015. pii: bav019.
13. Cooper, A.R.; Lill, G.R.; Gschweng, E.H.; Kohn, D.B. Rescue of splicing-mediated intron loss maximizes expression in lentiviral vectors containing the human ubiquitin C promoter. *Nucleic Acids Res.* **2015**, *43*, 682-690.
14. Bianchi, M.; Crinelli, R.; Giacomini, E.; Carloni, E.; Magnani, M. A potent enhancer element in the 5'-UTR intron is crucial for transcriptional regulation of the human ubiquitin C gene. *Gene* **2009**, *448*, 88-101.
15. Bianchi, M.; Crinelli, R.; Giacomini, E.; Carloni, E.; Radici, L.; Magnani, M. Yin Yang 1 intronic binding sequences and splicing elicit intron-mediated enhancement of ubiquitin C gene expression. *PLoS One* **2013**, 8:e65932.
16. Crinelli, R.; Bianchi, M.; Radici, L.; Carloni, E.; Giacomini, E.; Magnani, M. Molecular Dissection of the Human Ubiquitin C Promoter Reveals Heat Shock Element Architectures with Activating and Repressive Functions. *PLoS One* **2015**, 10:e0136882.
17. Marinovic, A.C.; Zheng, B.; Mitch, W.E.; Price, S.R. Ubiquitin (UbC) expression in muscle cells is increased by glucocorticoids through a mechanism involving Sp1 and MEK1. *J. Biol. Chem.* **2002**, *277*, 16673-16681.
18. Mao, X.; Zhu, X.; Hurren, R.; Ezzat, S.; Schimmer, A.D. Dexamethasone increases ubiquitin transcription through an SP-1 dependent mechanism in multiple myeloma cells. *Leukemia Res.* **2008**, *32*, 1480-1482.
19. Vihervaara, A.; Sergelius, C.; Vasara, J.; Blom, M.A.; Elsing, A.N.; Roos-Mattjus, P.; Sistonen, L. Transcriptional response to stress in the dynamic chromatin environment of cycling and mitotic cells. *P. Natl. Acad. Sci. U. S. A.* **2013,** *110*, E3388-97.

20. Bianchi, M.; Giacomini, E.; Crinelli, R.; Radici, L.; Carloni, E.; Magnani, M. Dynamic transcription of ubiquitin genes under basal and stressful conditions and new insights into the multiple UBC transcript variants. *Gene* **2015,** *573*, 100-109.

21. Bianchi, M.; Crinelli, R.; Arbore, V.; Magnani, M. Induction of ubiquitin C (UBC) gene transcription is mediated by HSF1: role of proteotoxic and oxidative stress. *FEBS Open Bio* **2018**, *8*, 1471-1485.

22. Kang, W.; Tong, J.H.; Chan, A.W.; Zhao, J.; Dong, Y.; Wang, S.; Yang, W.; Sin, F.M.; Ng, S.S.; Yu, J.; et al. Yin Yang 1 contributes to gastric carcinogenesis and its nuclear expression correlates with shorter survival in patients with early stage gastric adenocarcinoma. *J. Transl. Med.* **2014**, *12*, 80-90.

23. Yao, J.C.; Wang, L.; Wei, D.; Gong, W.; Hassan, M.; Wu, T.T.; Mansfield, P.; Ajani, J.; Xie, K. Association between expression of transcription factor Sp1 and increased vascular endothelial growth factor expression, advanced stage, and poor survival in patients with resected gastric cancer. *Clin. Cancer Res.* **2004**, *10*, 4109-4117.

24. Kim, S.J.; Lee, S.C.; Kang, H.G.; Gim, J.; Lee, K.H.; Lee, S.H.; Chun, K.H. Heat Shock Factor 1 Predicts Poor Prognosis of Gastric Cancer. *Yonsei Med. J.* **2018**, *59*, 1041-1048.

25. Torre, L.A.; Bray, F.; Siegel, R.L.; Ferlay, J.; Lortet-Tieulent, J.; Jemal, A. Global cancer statistics, 2012. *CA Cancer J. Clin.* **2015**, *65*, 87-108.

26. Hu, B.; El Hajj, N.; Sittler, S.; Lammert, N.; Barnes, R.; Meloni-Ehrig, A. Gastric cancer: Classification, histology and application of molecular pathology. *J. Gastrointest. Oncol.* **2012**, *3*, 251-261.

27. Grabsch, H.I.; Tan, P. Gastric cancer pathology and underlying molecular mechanisms. *Digest. Surg.* **2013**, *30*, 150-158.

28. Hanahan, D.; Weinberg, R.A. Hallmarks of cancer: the next generation. *Cell* **2011**, *144*, 646-674.

29. Tian, X.; Ju, H.; Yang, W. An ego network analysis approach identified important biomarkers with an association to progression and metastasis of gastric cancer. *J. Cell. Biochem.* 2019, *120*, 15963-15970.

30. Kolligs, F.T.; Bommer, G.; Goke, B. Wnt/Beta-Catenin/Tcf Signaling: A Critical Pathway in Gastrointestinal Tumorigenesis. *Digestion* **2002**, *66*, 131-144.

31. van der Woude, C.J.; Kleibeuker, J.H.; Tiebosch, A.T.; Homan, M.; Beuving, A.; Jansen, P.L.; Moshage, H. Diffuse and intestinal type gastric carcinomas differ in their expression of apoptosis related proteins. *J. Clin. Pathol.* **2003**, *56*, 699-702.

32. Fornace, A.J. Jr; Alamo, I. Jr.; Hollander, M.C.; Lamoreaux, E. Ubiquitin mRNA is a major stress-induced transcript in mammalian cells. *Nucleic Acids Res.* **1989,** *17*, 1215-1230.

33. Ryu, K.Y.; Baker, R.T.; Kopito, R.R. Ubiquitin-specific protease 2 as a tool for quantification of total ubiquitin levels in biological specimens. *Anal. Biochem.* **2006**, *353*, 153-155.

34. Davis, M.I.; Pragani, R.; Fox, J.T.; Shen, M.; Parmar, K.; Gaudiano, E.F.; Liu, L.; Tanega, C.; McGee, L.; Hall, M.D.; et al. Small Molecule Inhibition of the Ubiquitin-specific Protease USP2 Accelerates cyclin D1 Degradation and Leads to Cell Cycle Arrest in Colorectal Cancer and Mantle Cell Lymphoma Models. *J. Biol. Chem.* **2016**, *291*, 24628-24640.

35. Zhang, N.Y.; Jacobson, A.D.; Macfadden, A.; Liu, C.W. Ubiquitin chain trimming recycles the substrate binding sites of the 26 S proteasome and promotes degradation of lysine 48-linked polyubiquitin conjugates. *J. Biol. Chem.* **2011**, *286*, 25540-25546.

36. Shabek, N.; Herman-Bachinsky, Y.; Ciechanover, A. Ubiquitin degradation with its substrate, or as a monomer in a ubiquitination-independent mode, provides clues to proteasome regulation. *Proc. Natl. Acad. Sci. U.S.A.* **2009,** *106*, 11907-11912.

37. Sarvagalla, S.; Kolapalli, S.P.; Vallabhapurapu, S. The Two Sides of YY1 in Cancer: A Friend and a Foe. *Front. Oncol.* **2019**, *9*, 1230-1249.

38. Galloway, N.R., Ball, K.F., Stiff, T. and Wall, N.R. Yin Yang 1 (YY1): Regulation of Survivin and Its Role In Invasion and Metastasis. *Crit Rev Oncog.* **2017**, 22, 23–36.

39. Hsu, T.S.; Mo, S.T.; Hsu, P.N.; Lai, M.Z. c-FLIP is a target of the E3 ligase deltex1 in gastric cancer. *Cell Death Dis.* **2018,** *9*, 135-146.

40. Zhang, N.; Zhang, J.; Shuai, L.; Zha, L.; He, M.; Huang, Z.; Wang, Z. Kruppel-like factor 4 negatively regulates β-catenin expression and inhibits the proliferation, invasion and metastasis of gastric cancer. *Int. J. Oncol.* **2012**, *40*, 2038-2048.

41. Zhou, Q.; Hou, Z.; Zuo, S.; Zhou, X.; Feng, Y.; Sun, Y.; Yuan, X. LUCAT1 promotes colorectal cancer tumorigenesis by targeting the ribosomal protein L40-MDM2-p53 pathway through binding with UBA52. *Cancer Sci.* **2019**, *110*, 1194-1207.

42. Chi, J.; Liu, T.; Shi, C.; Luo, H.; Wu, Z.; Xiong, B.; Liu, S.; Zeng, Y. Long non-coding RNA LUCAT1 promotes proliferation and invasion in gastric cancer by regulating miR-134-5p/YWHAZ axis. *Biomed. Pharmacother.* **2019**, *118*:109201.

43. Liu, Y.; Beyer, A.; Aebersold, R. On the Dependency of Cellular Protein Levels on mRNA Abundance. *Cell* **2016**, *165*, 535-550.

44. Schwanhausser, B.; Busse, D.; Li, N.; Dittmar, G.; Schuchhardt, J.; Wolf, J.; Chen W.; Selbach, M. Global quantification of mammalian gene expression control. *Nature* **2011**, *473*, 337-342.

45. Shabek, N.; Ciechanover, A. Degradation of ubiquitin: the fate of the cellular reaper. *Cell Cycle* **2010,** *9*, 523-530.

46. Arora, N.; Alsaied, O.; Dauer, P.; Majumder, K.; Modi, S.; Giri, B.; Dudeja, V.; Banerjee, S.; Von Hoff, D.; Saluja, A. Downregulation of Sp1 by Minnelide leads to decrease in HSP70 and decrease in tumor burden of gastric cancer. *PLoS One* **2017**, *12*, e0171827.

47. Gencer, S.; Irmak Yazicioglu, M.B. Differential response of gastric carcinoma MKN-45 and 23132/87 cells to H2O2 exposure. *Turk. J. Gastroenterol.* **2011**, *22*, 145-151.

48. Kedves, A.T.; Gleim, S.; Liang, X.; Bonal, D.M.; Sigoillot, F.; Harbinski, F.; Sanghavi, S.; Benader, C.; George, E.; Gokhale, P.C.; et al. Recurrent ubiquitin B silencing in gynecological cancers establishes dependence on ubiquitin C. *J. Clin. Invest.* **2017**, *127*, 4554-4568.

49. Dantuma, N.P.; Groothuis, T.A.M.; Salomons, F.A.; Neefjes, J. A dynamic ubiquitin equilibrium couples proteasomal activity to chromatin remodeling. *J. Cell Biol.* **2006**, *173*, 19-26.

50. Holdenrieder, S.; Stieber, P. Apoptotic markers in cancer. *Clin. Biochem.* **2004**, *37*, 605-617.

51. Di Girolamo, M.; Fabrizio, G.; Scarpa, E.S.; Di Paola, S. NAD+-dependent enzymes at the endoplasmic reticulum. *Curr. Top. Med. Chem.* **2013**, *13*, 3001-3010.

52. Zhang, L.; Zhou, R.; Zhang, W.; Yao, X.; Li, W.; Xu, L.; Sun, X.; Zhao, L. Cysteine-rich intestinal protein 1 suppresses apoptosis and chemosensitivity to 5-fluorouracil in colorectal cancer through ubiquitin-mediated Fas degradation. *J. Exp. Clin. Canc. Res.* **2019**, *38*, 120-133.

53. Crinelli, R.; Bianchi, M.; Menotta, M.; Carloni, E.; Giacomini, E.; Pennati, M.; Magnani, M. Ubiquitin over-expression promotes E6AP autodegradation and reactivation of the p53/MDM2 pathway in HeLa cells. *Mol. Cell. Biochem.* **2008**, *318*, 129-145.

54. Hanna, J.; Meides, A.; Zhang, D.P.; Finley, D. A ubiquitin stress response induces altered proteasome composition. *Cell* **2007**, *129*, 747-759.

55. Peng, R.; Zhu, J.; Deng, S.; Shi, H., Xu, S.; Wu, H.; Zou, F. Targeting BAX ubiquitin-binding sites reveals that BAX activation is essential for its ubiquitin-dependent degradation. J. *Cell Biochem.* **2020**, *121*, 2802-2810.

56. Zhou, S.; Lu, J.; Li, Y.; Chen, C.; Cai, Y.; Tan, G.; Peng, Z.; Zhang, Z.; Dong, Z.; Kang, T.; Tang, F. MNAT1 is overexpressed in colorectal cancer and mediated p53 ubiquitin-degradation to promote colorectal cancer malignance. *J. Exp. Clin. Cancer Res.* **2018**, *37*, 284-300.

57. Geyer, P.E.; Maak, M.; Nitsche, U.; Perl, M.; Novotny, A.; Slotta-Huspenina, J.; Dransart, E.; Holtorf, A.; Johannes, L.; Janssen, K.P. Gastric Adenocarcinomas Express the Glycosphingolipid Gb3/CD77: Targeting of gastric Cancer Cells with Shiga Toxin B-Subunit. *Mol. Cancer Ther.* **2016**, *15*, 1008-1017.

58. Rocha, S.; Teles, S.P.; Azevedo, M.; Oliveira, P.; Carvalho, J.; Oliveira, C. Gastric Cancer Extracellular Vesicles Tune the Migration and Invasion of Epithelial and Mesenchymal Cells in a Histotype-Dependent Manner. *Int. J. Mol. Sci.* **2019**, *20*, 2608-2624.

59. CanSAR Black - Cancer Drug Discovery Platform. Available online: https://cansarblack.icr.ac.uk/cell-line/MKN-45/copy-number (accessed on 21/05/20).
60. Livak, K.J.; Schmittgen, T.D. Analysis of relative gene expression data using real-time quantitative PCR and the 2(-Delta Delta C(T)) Method. *Methods* **2001**, *25*, 402-408.

CHAPTER 5:

A NEGATIVE FEEDBACK MECHANISM LINKS *UBC* GENE EXPRESSION TO UBIQUITIN LEVELS BY AFFECTING RNA SPLICING RATHER THAN TRANSCRIPTION

Bianchi Marzia, Crinelli Rita, Giacomini Elisa, Carloni Elisa, Radici Lucia, Scarpa Emanuele-Salvatore, Tasini Filippo, Magnani Mauro.

Department of Biomolecular Sciences, University of Urbino Carlo Bo, 61029 Urbino (PU), Italy

A negative feedback mechanism links *UBC* gene expression to ubiquitin levels by affecting RNA splicing rather than transcription

Marzia Bianchi*, Rita Crinelli, Elisa Giacomini, Elisa Carloni, Lucia Radici, Emanuele-Salvatore Scarpa, Filippo Tasini & Mauro Magnani

Department of Biomolecular Sciences, University of Urbino Carlo Bo, 61029 Urbino (PU), Italy
*e-mail: marzia.bianchi@uniurb.it

5.1 Abstract: *UBC* gene plays a critical role in maintaining ubiquitin (Ub) homeostasis. it is upregulated under stress conditions, and herein we report that it is downregulated upon Ub overexpression. Downregulation occurs in a dose-dependent manner, suggesting the existence of a fine-tuned Ub sensing mechanism. this "sensor" requires a conjugation competent ubiquitin to detect Ub levels. Searching the sensor among the transcription factors involved in basal and stress-induced *UBC* gene expression was unsuccessful. Neither HSF1 and HSF2, nor Sp1 and YY1 are affected by the increased Ub levels.

Moreover, mutagenesis of their binding sites in the *UBC* promoter-driven reporter constructs does not impair the downmodulation effect. Epigenetic studies show that H2A and H2B ubiquitination within the *UBC* promoter region is unchanged upon ubiquitin overexpression. Noteworthy, quantification of nascent RNA molecules excludes that the downmodulation arises in the transcription initiation step, rather pointing towards a post-transcriptional mechanism. Indeed, a significantly higher fraction of unspliced *UBC* mRNA is detected in ubiquitin overexpressing cells, compared to empty vector transfected cells. Our findings suggest how increasing cellular ubiquitin levels may control the expression of *UBC* gene by negatively affecting the splicing of its pre-mRNA, providing a straightforward feedback strategy for the homeostatic control of ubiquitin pools.

5.2 Introduction: The protein ubiquitin (Ub) is probably the most important post-translational modifier of the proteome in eukaryotic cells, regulating the stability, function, localization of its target substrates and as such, it controls an array of cellular processes and affects many signaling pathways[1,2].

Ubiquitin has many peculiar features: (1) Ub is not encoded as a single polypeptide, but rather is translated as a fusion product either to ribosomal proteins or with multiple Ub moieties in tandem[3,4]; the precursor is processed by specific enzymes (DUBs) to give as final product Ub monomers[5]; (2) Ub is encoded by four different genes[6–8] which ultimately yield the same product (monomeric Ub), but are not redundant in their functions, as demonstrated by the effects of selective knockout of the *UBB* or *UBC* locus[9–12]; (3) Ub exists inside the cell mainly partitioned into free and conjugated pools which are not static, but in dynamic equilibrium that changes to meet the changing cellular needs[13,14]; (4) Ub is one of the most abundant proteins, but surprisingly it is not produced in excess, as demonstrated by the upregulation of polyubiquitin coding genes *UBC* and *UBB*, under stressful conditions[9,15,16]. When the demand of Ub increases,

e.g. during proteotoxic stress, besides the *de novo* synthesis of the protein and an improved Ub sparing from proteasomal degradation[17,18], a redistribution of ubiquitin from histones to unfolded protein conjugates has been observed[19]. This "competition" between different Ub demanding processes reflects the limited pool of free Ub. This is also demonstrated by the evidence that, in yeast, Ub depletion may represent the main cause of toxicity induced by translational inhibitors[20]. Given the involvement of Ub in many different cellular functions (in both normal and stressful conditions), maintaining Ub homeostasis is of paramount importance for every cell type and requires a highly dynamic but stringent regulation. In fact, it has been demonstrated that any alteration in Ub homeostasis, resulting in either an excess or a deficiency of free Ub, causes a "ubiquitin stress response"[21]. In particular, elevated Ub levels are intrinsic features of a variety of pathophysiological conditions, that upregulate Ub[22–25], but may also derive from exogenous manipulation of cellular Ub levels, leading to ectopic Ub overexpression[9,20]. In a very recent paper, Han and coworkers[26] developed a new system to increase the cellular Ub levels in a more physiological fashion; they used the CRISPR-Cas9 technology to induce upregulation of the endogenous *UBC* gene under normal conditions.

The authors claim that this system may be useful to study the cellular response to an excess of Ub under normal conditions and to highlight if this prior upregulation of *UBC* may have a protective role towards incoming stress insults. Ubiquitin overexpression has been proved to be protective in the rescue from toxicity provoked by inhibitors of translation, which deplete free Ub by reducing its *de novo* synthesis[20]. On the other side, alteration of Ub homeostasis in mice, by overexpression of Ub in the neuronal compartment, impaired the synaptic function[27].

Moreover, when the authors investigated the potential effects of the higher Ub levels on the main components of the ubiquitin-proteasome system, they found a significant decrease in the expression of the endogenous polyubiquitin genes *UBC* and *UBB*, arguing that this is consistent with the need for a tightly regulated Ub homeostasis in neurons[25,27]. However, they did not further investigate the molecular mechanisms for this transcriptional downregulation.

The need for a Ub sensor able to detect ubiquitin levels within the cell has been envisaged by different authors[9,18], but the cellular component(s) able to fulfill this role have not been identified yet. In the present work we aimed to investigate the molecular mechanisms underlining *UBC* downregulation in Ub overexpressing cells. Indeed, we found that overexpression of wild-type ubiquitin in different human cell lines (both normal and tumor derived) resulted in lowered levels of *UBC* and *UBB* mRNAs; moreover, the *UBC* fold-decrease was directly related to the amount of ubiquitin overexpressed, suggesting that a proper negative feedback regulatory mechanism, able to sense the Ub levels, could act to maintain Ub within a defined concentration range under unstressed conditions. Another challenging issue is to highlight the *cis*-acting elements in the promoter region of *UBC* and *UBB*, which make these two genes the main targets and effectors of the ubiquitin sensing mechanism. The harvested data point towards a post-transcriptional ubiquitin-mediated modulation of *UBC* gene expression.

5.3 Results

5.3.1 Overexpression of ubiquitin downregulates the endogenous *UBC* gene expression.

Wild-type ubiquitin (Ubwt) was overexpressed in HeLa cells as a fusion product with a C-terminal Myc-tag, a strategy that reproduces the endogenous expression mechanisms[28]. Previous work has shown that Ub-transfected cells displayed a significantly higher Ub content (about 4-fold) compared to cells receiving the empty vector pCMV-Myc or left untreated, equally distributed between the free and conjugated pools[28]. To determine if ubiquitin overexpression had effects on its endogenous expression, we first examined the mRNA levels of the four Ub coding genes by RTqPCR. No significant changes in the *UBA52* and *RPS27A* transcripts were detected (Fig. 1A). In contrast, ubiquitin overexpression caused a significant decrease (around 50%) in the mRNA levels of the endogenous *UBC* and *UBB* genes (Fig. 1A). Transfection of different amounts of Ub construct resulted in an increase of total ubiquitin content which was strictly correlated to the quantity of transgene delivered[28] (Fig. 1B). Downregulation of the *UBC* gene by exogenous Ub occurred in a dose dependent manner (Fig. 1C), starting from cells transfected with 50 ng of Ub plasmid, where the concentration of ubiquitin was ~2.4-fold compared to the one detected in pCMV-Myc transfected cells, indicating that this regulatory loop may have a physiological relevance. To investigate whether *UBC* downregulation upon Ub overexpression was a general "buffer" mechanism to maintain Ub homeostasis, we transfected other cell lines with the Ubwt expression vector, namely NCTC-2544 and HEK293, which are normal cells and U2OS, which are tumor cells, but of different origin than HeLa. Immunoblotting analysis with anti-Ub specific antibody, at 48 h post-transfection, confirmed Ub overexpression in all treated samples (Fig. 1D). When the *UBC* gene transcript was detected by qPCR, an expression profile similar to HeLa was found for all the cell lines investigated (Fig. 1E–G).

5.3.2 A conjugation competent ubiquitin is required for *UBC* downregulation.

To explore how raising the intracellular ubiquitin levels caused a significant decrease of *UBC* mRNA, we hypothesized the presence of a cellular "ubiquitin sensor" capable of detecting the ubiquitin pool dynamics and affecting the expression of two out of the four Ub coding genes. Ubiquitin signals in many different ways: substrate modifications range from a single ubiquitin molecule to complex polymeric chains, with different types of ubiquitylation often eliciting distinct outcomes[29]. While Lys48-linked polyUb acts notoriously as proteasomal degradation signal, Lys63-linked Ub chains have various non-proteolytic roles[30,31]. To test whether *UBC* downregulation relies on a ubiquitin and proteasomal dependent degradation event or on a non-proteolytic Ub-mediated mechanism, HeLa cells were transfected with two ubiquitin mutants containing single lysine to arginine mutations, respectively at position 48 (UbK48R) and 63 (UbK63R), in parallel with the Ubwt expression plasmid and the empty vector pCMV-Myc. To further address if ubiquitin conjugation to the target "sensor(s)" was required to elicit *UBC* downmodulation or if, alternatively, non-covalent Ub binding was involved, we developed three new ubiquitin mutants: UbG76A, carrying an alanine residue instead of glycine at position 76 (this mutant has been reported to interfere with the activity of deubiquitylating enzymes)[32,33]; UbΔGG, a mutant ubiquitin lacking the two C-terminal glycine residues (which cannot be conjugated to other proteins but can be ubiquitinated to generate unanchored

ubiquitin chains in the cell)[34]; UbI44A, carrying a mutation in the hydrophobic patch (L8, I44 and V70) that is critical forUb interaction with many partner proteins and the proteasome[35].

All ubiquitin mutants were expressed at high levels, as demonstrated by the increase in the immunoreactive signal compared to that detected in Myc-transfected cells (Fig. 2A,B). Moreover, some differences in the Ub distribution between the free and conjugated pools were appreciable consistently with the expected mechanism of action of the analogues (Fig. 2A,B). Specificity of interference with the ubiquitin pathway was demonstrated by the accumulation of HSF2 protein in cells overexpressing the Ub analogues compared to cells transfected withthe Ubwt construct or the empty vector pCMV-Myc, with the only exception represented by UbK63R transfected cells (Fig. 2C). This is in agreement with several reported observations that K63-linked polyubiquitination of proteins does not affect their degradation kinetics[36,37]. Of note, no significant differences in the HSF2 content were found between Ubwt and Myc transfected cells (1.05 ± 0.05 versus Myc set as 1; n = 3) (Supplementary Fig. S1).

RTqPCR analysis of *UBC* mRNA revealed a statistically significant repression of gene transcription by UbK48R and UbK63R ($p < 0.001$ versus Myc), indicating that the K48- and K63-assembled Ub chains were not involved (Fig. 2D). In contrast, the downregulation effect was lost in cells transfected with UbK0, a lysine-lessubiquitin mutant, theoretically incapable of forming any polyubiquitin chain (Fig. 2D). On the whole these results suggest that a Ub poly-chain based on lysines other than K48 and K63 may be involved. Transfection of UbI44A resulted in *UBC* downregulation, as occurred with wild-type Ub (Fig. 2E). By contrast in cells overexpressing UbG76A or UbΔGG we found, instead of downregulation, an induction (about 1.8-fold versus Myc) of *UBC* expression (Fig. 2E). It is known that UbG76A is conjugated less efficiently than wild-type Ub and once incorporated cannot be deconjugated[32,33]. A strong accumulation of Ub-conjugated proteins was indeed detected in UbG76A expressing cells compared to Ubwt and UbI44A transfected cells (Fig. 2B). Conversely, UbΔGG cannot be conjugated[34], but it can be the substrate for the building of free polyUb chains which are evident in the blot of Fig. 2B as immunoreactive bands with an electrophoretic mobility consistent with the molecular weight of di- (about 17 kDa), tri- (about 26 kDa) and tetra-Ub (about 34 kDa) polymers. Although these two mutants have different mechanisms of interference with the ubiquitination machinery, they share the ability to sequester the endogenous wild-type Ub into the conjugated fraction, thus they are expected to cause depletion of the free Ub pool which could in turn be responsible for *UBC* induction (Fig. 2E). Unfortunately, the depletion effect cannot be appreciated from the blot by comparing the ubiquitin pattern of UbG76A and UbΔGG expressing cells with Myc-transfected cells, since the mutants have been deliberately expressed as untagged proteins to avoid tag interference, thus they are indistinguishable from endogenous Ub.
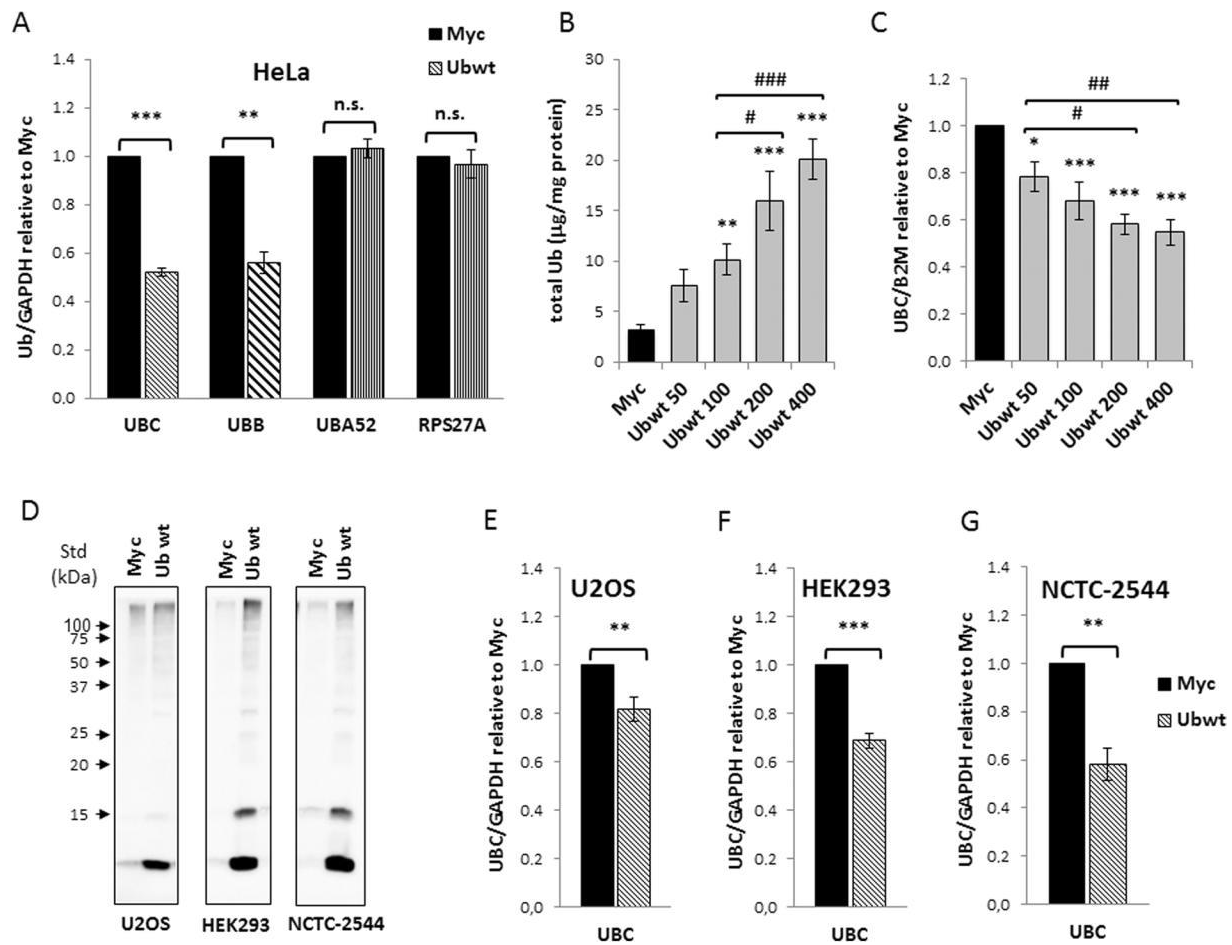
Figure 1. Overexpression of wild-type ubiquitin leads to *UBC* downregulation in different cell lines. (**A**) HeLa cells were transiently transfected with Ub wild-type expression vector (Ubwt) or the control empty vector pCMV-Myc (Myc). At 48 h post-transfection, the mRNA levels of the four Ub coding genes were determined by RT-qPCR (n = 12 each), normalized to *GAPDH*, and expressed as the fold change relative to the control Myc. (**B**) Quantification of total Ub content in whole cell lysates obtained from HeLa cells transfected with increasing amounts of Ubwt expression vector (n = 3). Total ubiquitin content was quantified after Usp2 digestion by solid phase immunoassay using purified bovine ubiquitin as standard. (**C**) Ub induces *UBC* downmodulation in a dose-dependent manner. RTqPCR (n = 6) of *UBC* mRNA in HeLa samples transfected as in (B); *UBC* was normalized to *B2M* and expressed as the fold change relative to the control Myc. (**D**) Western immunoblot analysis of U2OS, HEK293 and NCTC-2544 cells transfected with Ubwt or control vector pCMVMyc, harvested 2 days post-transfection. Cell lysates, resolved by sodium dodecyl sulfate polyacrylamide gel electrophoresis (SDS-PAGE), were probed with anti-ubiquitin antibody. Arrowheads indicate molecular weight standards. (**E,F,G**) RTqPCR of *UBC* mRNA, respectively in U2OS (n = 14), HEK293 (n = 3) and NCTC-2544 (n = 3) cells harvested 48 h post-transfection with pCMV-Myc and Ubwt expression vectors. *UBC* mRNA levels were normalized to *GAPDH* and expressed as fold change versus the control Myc. Data are presented as means ± SEM from the indicated number of samples. *,#p < 0.05; **,##p < 0.01; ***/###p < 0.001 vs. control (Myc) or between two samples as indicated by horizontal bars. n.s., not significant.
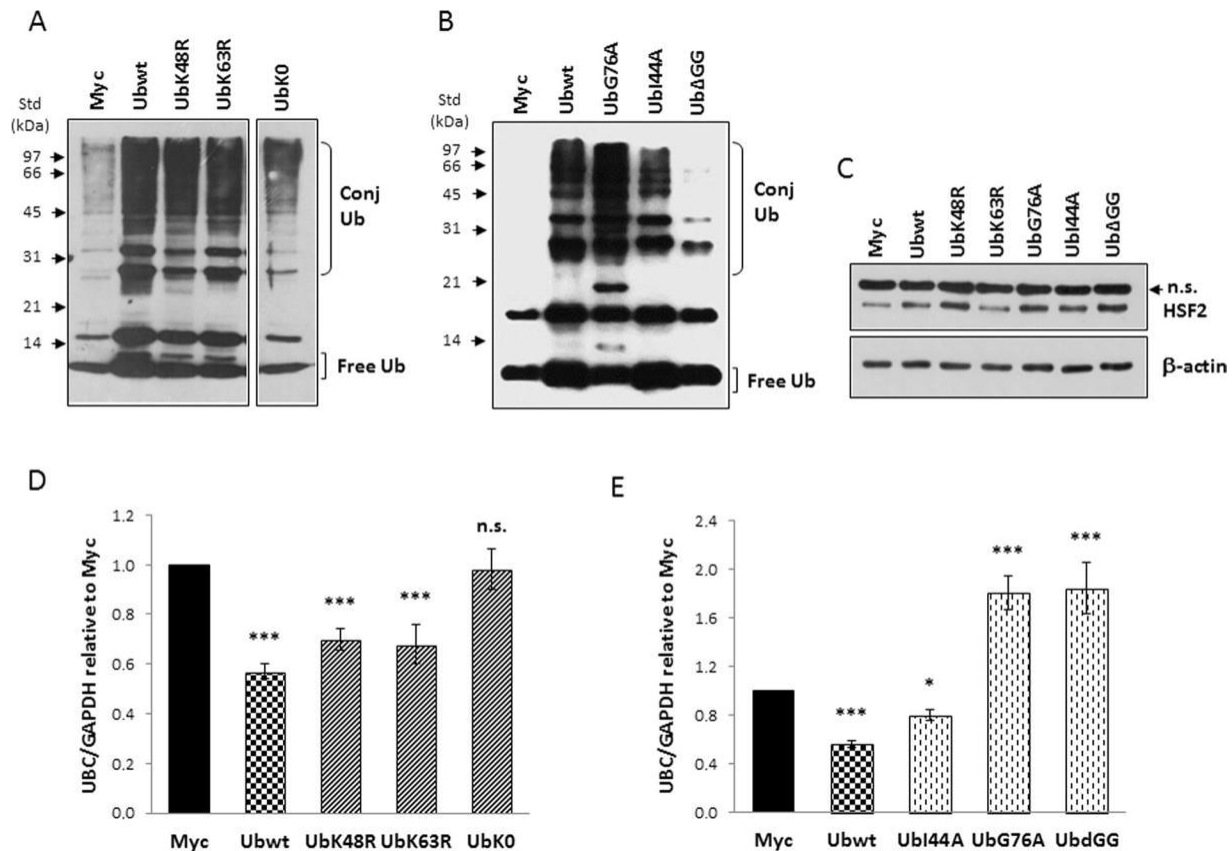
Figure 2. A conjugation competent ubiquitin is required for *UBC* downregulation. (**A,B**) Western blot analysis of HeLa cells transiently transfected with wild-type Ub or the different Ub mutants, in parallel with the control empty vector pCMV-Myc, harvested 48 h post-transfection. Cell lysates, resolved by SDS-PAGE, were probed with anti-ubiquitin antibody. Arrowheads indicate the molecular weight standards. (**C**) HSF2 levels in whole extracts obtained from HeLa cells transfected with the indicated constructs. Actin was detected as loading control and is shown in the lower panel. (**D,E**) *UBC* mRNA levels were determined, in HeLa cells transfected with the indicated constructs, by RTqPCR (n = 6 each), normalized to *GAPDH* and expressed as the fold change versus the control Myc. Data presented in (**D,E**) are means ± SEM from the indicated number of samples. *p < 0.05; ***p < 0.001 vs. control (Myc); n.s., not significant. The images shown in (**A,B,C**) are representative of three independent experiments. Vertical spaces inserted between lanes in panel A indicate removal of intervening, irrelevant samples. Full-length immunoblots are presented in Supplementary Fig. S5.

5.3.3 Promoter analysis by transfection of reporter constructs reveals the importance of the *UBC* intron for the downmodulation effect.

To narrow down the promoter region responsible for the *UBC* gene responsiveness to the increase in cellular ubiquitin levels, we cotransfected different 5′ and 3′ serially deleted promoter constructs, with the Ubwt expression vector or the pCMV-Myc empty vector. Most of the luciferase reporter constructs have been previously described[38,39] while others (P254, P195, P123 and P84) were developed during this study (Fig. 3A). They differ for the length of the upstream promoter region (5′ deletions) and the presence or not of the *UBC* intron (3′ deletions). The luciferase activity was given for each reporter vector with respect to the value obtained for
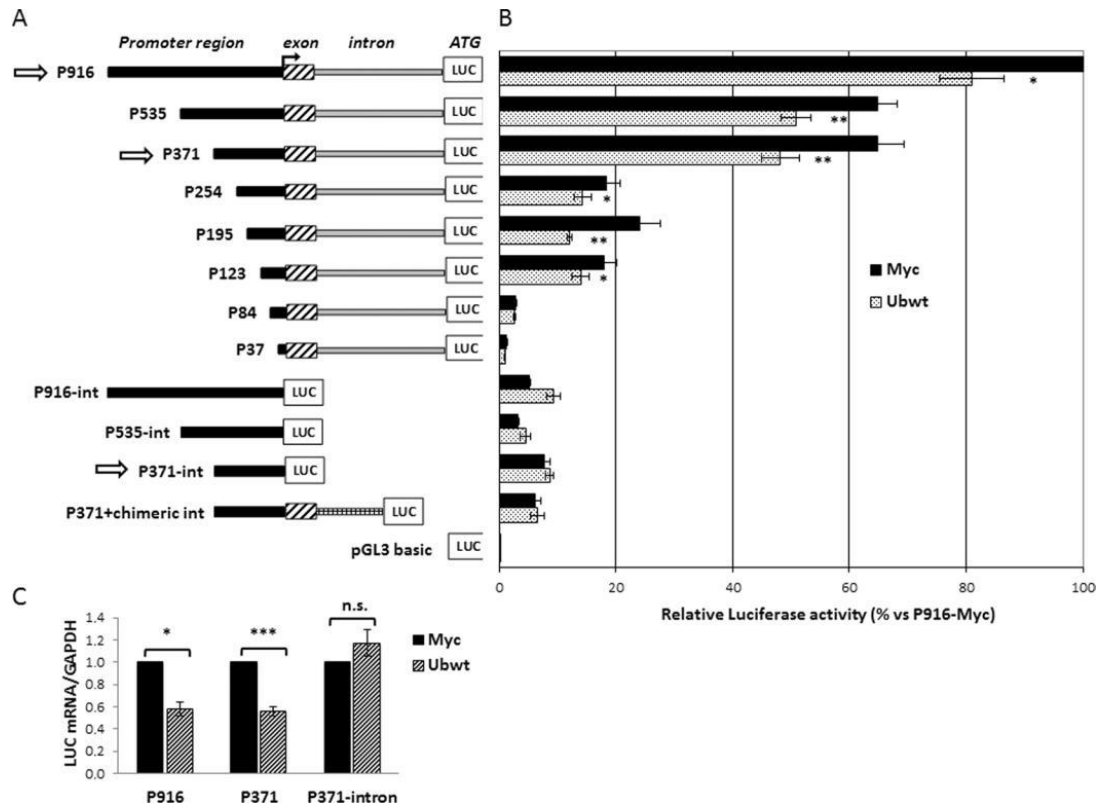
Figure 3. Effect of ubiquitin transfection on *UBC* promoter-driven luciferase expression. (**A**) Diagram of the 5'- and 3'-nested deletions of *UBC* promoter constructs. At the top there is the longer construct (P916) bearing 916 bp of the promoter region upstream of the TSS, the first non coding exon and the unique *UBC* intron, before the luciferase coding sequence (LUC). The name of the reporter vectors indicates the length of the upstream promoter region included (from −916 to −37). The contructs "–int" are devoid of the intron sequence, while in the P371+ chimeric int construct, a heterologous chimeric intron replaces the endogenous *UBC* intron.pGL3-basic is the promoter-less luciferase vector, used as control. (**B**) HeLa cells were transiently cotransfected with the reporter constructs shown in (A) and the Ubwt expression vector or the empty vector pCMV-Myc. Forty-eight hours post-transfection cells were harvested and luciferase activity was determined and normalized against total protein concentration. All values were referred to the sample cotransfected with P916/pCMVMyc, set arbitrarily to 100 (n = 3). (**C**) Luciferase mRNA expression of the intron-bearing (P916 and P371) and intron-less (P371-int) constructs after overexpression of ubiquitin in HeLa cells. LUC mRNA was detected by RTqPCR and normalized to *GAPDH*. The value obtained in Ub overexpressing cells was expressed relative to the Myc transfected sample, set to 1 (n = 8). Data presented in (B,C) are means ± SEM from the indicated number of experiments. *p < 0.05; **p < 0.01; ***p < 0.001 vs. control (Myc); n.s., not significant.

the largest construct cotransfected with the empty vector (P916 + Myc), set as 100%. This preliminary screening highlighted that promoter downmodulation was detectable for all the intron bearing constructs, with the exception of the constructs with longer 5' deletions (P84 and P37) which exhibited a very low promoter activity (Fig. 3B). It is remarkable that intron elimination not only drastically weakened the *UBC* promoter activity, but also resulted in the lack of ubiquitin-driven downregulation. Significantly, replacement of the endogenous *UBC* intron with a chimeric intron (P371 + chimeric int), PCR-amplified from the phRL-CMV vector

(Promega) as previously described[38], did not restore the downregulation effect upon Ub overexpression. The promoter activities of P916 and P371 vectors, which possess similar activity under basal conditions[38], and of the intron-less version of P371 were determined, after Ub overexpression, by measuring the luciferase mRNA levels, besides luciferase enzymatic activity. In fact, due to its robustness and high sensitivity, RTqPCR is certainlya more appropriate and direct method to measure promoter-driven transcription and also allows to exclude any possible interference of ubiquitin with post-transcriptional mechanisms controlling luciferase protein levels[40,41]. As shown in Fig. 3C, luciferase mRNA expression of constructs P916 and P371 lowered when ubiquitin levels raised, while there was no significant change in the intron-less construct driven luciferase expression, suggesting that the downregulation event requires the presence of the intron.

Previous studies by our team[38,39,42] and others[43] have identified the *cis-trans* elements which mediate *UBC* promoter activity under basal and stressful conditions. Briefly, YY1 binding sites have been found in the intron and the upstream promoter sequence[39]. Likewise, Sp1 binding motifs are positioned both upstream of the transcription start site (TSS)[43] and within the intron sequence[38,39], while three Heat Shock Elements (HSEs) were characterized in the proximal and distal promoter region[16,42]. Both YY1 and Sp1 transcription factors (TFs) were found to sustain basal *UBC* gene expression, while HSF1 and HSF2 mediate *UBC* induction upon different stresses. These findings, which represent the starting background for the present study, are summarized in the schematic diagram of Supplementary Fig. S2A.

5.3.4 Role of HSF1 and HSF2 in *UBC* downregulation.

Both HSF1 and HSF2 undergo ubiquitin and proteasome dependent degradation[44–46]. In light of the above, we wondered if the downregulatory effect on *UBC* gene activity, in ubiquitin overexpressing cells, could be mediated by these two members of the Heat Shock Factor family. We measured HSF1 and HSF2 total levels in pCMV-Myc and ubiquitin transfected cells by western immunoblotting and found no difference (Fig. 4A). To further investigate the possible role of these HSFs in the *UBC* downregulation, we took advantage of available reporter vectors where luciferase expression is driven by a *UBC* promoter sequence with intact HSEs (P916 wt) or with these sites mutagenized, one at a time or in combination[42] (see Supplementary Fig. S2B). Cotransfection of these reporter constructs with the empty or Ub expression vector revealed that mutagenesis of HSF binding sites did not affect the downmodulation effect (Fig. 4B). These data were also confirmed by ChIP experiments showing that HSF1 and HSF2 *in vivo* occupancy of the *UBC* promoter did not change upon ubiquitin overexpression (Fig. 4C). Moreover, having demonstrated that HSF1 and HSF2 drive *UBC* induction under proteotoxic stress triggered by transient proteasome inhibition[42], we challenged ubiquitin overexpressing cells with MG132 to check what happened to *UBC* expression. As shown in Fig. 4D, *UBC* transcription was induced upon MG132 treatment both in Myc and Ubwt transfected cells, with a similar fold change versus the corresponding DMSO treatment, used as control. The same behavior was found for *HSP70* mRNA, detected as representative HSF1 target gene (Fig. 4E). On the whole, these results show that cells respond to MG132 treatment by inducing *UBC*, despite the high intracellular Ub levels, meaning that the Heat Shock Response (HSR) and the downregulation

effect, both impacting on *UBC* gene expression, are distinct (not intersecting) regulatory mechanisms. HSF1 and HSF2 are not the Ub sensor we were looking for.
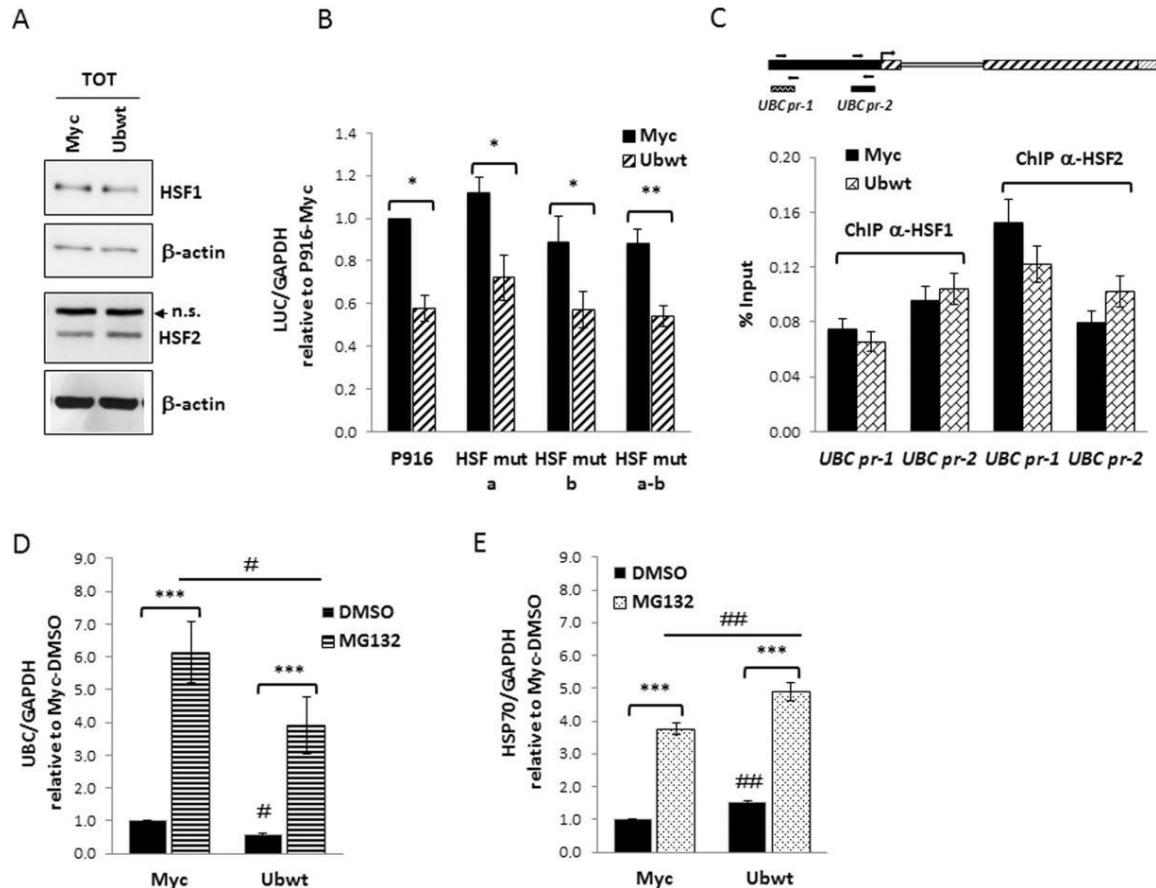
Figure 4. Investigating the role of HSF1 and HSF2 transcription factors in *UBC* downregulation. (**A**) Immunoblot analysis of HSF1 and HSF2 protein factors in whole extracts obtained from HeLa cells transiently transfected with the Ub expression vector (Ubwt) or the empty control vector (Myc). β-actin was used as loading control (lower panels). (**B**) The wild-type reporter construct P916 and the HSF mutant counterparts(HSF mut a, b, a-b) were cotransfected in HeLa cells with the Ub expression construct or the empty vector pCMV-Myc. Forty-eight hours post-transfection, luciferase mRNA levels were determined by RTqPCR, normalized to *GAPDH* and expressed as fold change versus the P916/Myc cotransfected sample, set to 1 (n = 4). (**C**) ChIP analysis of Myc and Ubwt transfected cells, using antibodies specific for HSF1 and HSF2; for the internal IP control, no Ab was added. RealTime PCR was carried out on chromatin before (Input) and after immunoprecipitation (ChIPed DNA) using selected primer pairs which amplify the *UBC* promoter regions (outlined above the graph) containing the previously identified HSEs (*UBC* pr-1 and *UBC* pr-2, respectively). Data are expressed as % of chromatin input controls, calculated using the formula $2-\Delta Ct \times 100$. Results shown in the histogram represent the mean ± SEM of two independent experiments, assayed in duplicate. (**D,E**) Myc and Ubwt transfected cells were treated with 20 μM MG132 or the vehicle DMSO as control for 4 h. *UBC* (**D**) and *HSP70* (**E**) mRNA levels were determined by RTqPCR (n = 4), normalized to *GAPDH* and expressed as the fold change relative to the control (Myc/DMSO). Data presented in (**B-E**) are means ± SEM from the indicated number of experiments. *,#$p < 0.05$; **,##$p < 0.01$; ***$p < 0.001$ vs. control (Myc) or between two samples as indicated by horizontal bars. n.s., not significant. The images shown in (**A**) are representative of three independent experiments. Full-length immunoblots are presented in Supplementary Fig. S6.
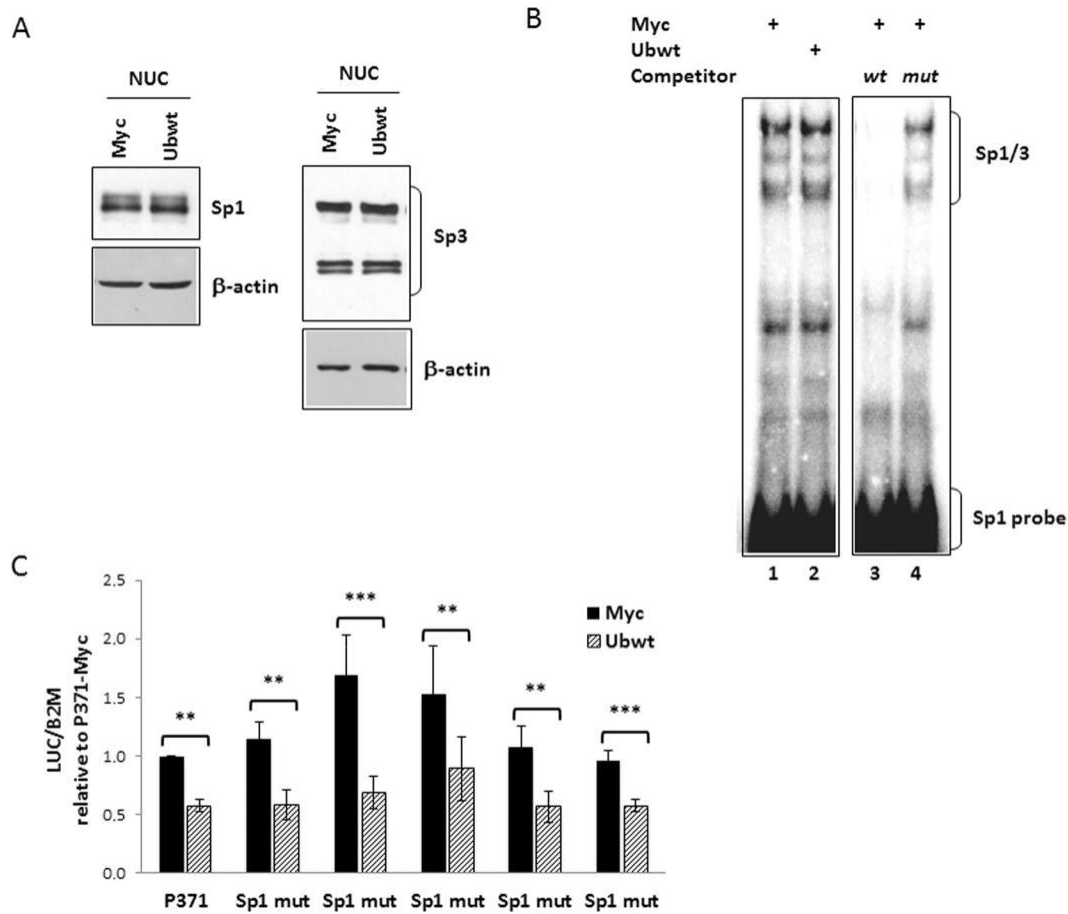
Figure 5. Investigating the role of Sp1 and Sp3 transcription factors in *UBC* downregulation. (**A**) Immunoblot analysis of Sp1 and Sp3 protein factors in nuclear extracts obtained from HeLa cells transiently transfected with the Ub expression vector (Ubwt) or the empty control vector (Myc). β-actin was used as loading control. (**B**) EMSA using, as probe, a 32P-labeled oligonucleotide containing the tandem binding sites for Sp1 identified in the −319/−280 region of *UBC* promoter[43]. Protein/DNA complexes were detected upon incubation of probe with nuclear extracts (5 μg) from cells transfected as in (**A**) (lanes 1–2). Specificity of retarded bands was assessed by competition experiments where nuclear extracts from Myc-transfected cells were preincubated with a 50-fold excess of cold wild-type or mutant h*UBC* Sp1 competitor (lanes 3–4). (**C**) The wild-type reporter construct P371 and the Sp1 mutant counterparts (Sp1 mut a, b, c, d, a-d) were cotransfected in HeLa cells with the Ub expression construct or the empty vector Myc. Forty-eight hours post-transfection, luciferase mRNA levels were determined, normalized to *B2M* and expressed as fold change versus the P371/Myc cotransfected sample, set to 1 (n = 4). Data presented in (**C**) are means ± SEM from the indicated number of experiments. **p < 0.01; ***p < 0.001 vs. control (Myc). The images shown in (**A**,**B**) are representative of three independent experiments. Vertical spaces inserted between lanes in panel B indicate removal of intervening, irrelevant samples. Full-length immunoblots and EMSA are presented in Supplementary Fig. S7.

5.3.5 Role of Sp1 in *UBC* downregulation.

To explore the potential role of Sp1 in the *UBC* downregulation, we determined the Sp1 levels in the nuclear fractions of pCMV-Myc and Ubwt transfected cells by Western blot analysis and found no significant difference (Fig. 5A). The same occurred for Sp3 (Fig. 5A), another member of the Sp family of transcription factors, with similar DNA binding properties as Sp1, as supported by our evidences that Sp3 occupies, at least *in vitro*, the same binding sites as Sp1 in the *UBC* promoter[38]. To assess if the higher cellular ubiquitin levels affected the ability of Sp1 to bind to its target sites in the *UBC* promoter, rather than modulating its protein levels, we performed a bandshift assay using an oligonucleotide containing the tandem binding sites for Sp1 identified in the *UBC* promoter (−319/−280 region)[43]. Incubation of the 32P-labeled DNA duplex with nuclear extracts derived from both pCMV-Myc and Ubwt transfected cells resulted in the appearance of several protein/DNA complexes, with a typical Sp1/Sp3 pattern[39] (Fig. 5B). Protein binding specificity was assessed by competition experiments where nuclear extracts from Myc transfected cells were pre-incubated with an excess of unlabeled ODN containing the wild-type Sp1 consensus sequence which was able to prevent protein complex formation while a mutagenized competitor sequence was not (Fig. 5B). But most importantly, no difference in the pattern and/or intensity of retarded bands could be appreciated between ubiquitin-overexpressing and control cells. These results are in agreement with those obtained by cotransfection of luciferase reporter constructs with the Ub expression vector: both P371 and P254 reporter vectors (carrying and lacking, respectively, the upstream Sp1 binding sites) were downregulated by ubiquitin overexpression (Fig. 3B). Concerning the Sp1 binding sitespreviously identified within the intron sequence[39], when either the single site Sp1 mutants (Sp1 mut a, b, c, d) or the reporter vector with mutations in all Sp1 binding motifs (Sp1 mut a-d), were cotransfected with the Ub expression plasmid, they exhibited a reduction of luciferase mRNA expression similar to the wild-type construct P371 (Fig. 5C). Taken together, the evidences obtained indicate Sp1 as not involved in the ubiquitin-driven downmodulation of *UBC*.

5.3.6 Role of YY1 in *UBC* downregulation.

We previously demonstrated that YY1 positively regulates *UBC* gene expression in basal conditions, by interacting with two intronic binding sites[39]. Based on this finding andon the evidence that ubiquitin-proteasome mediated degradation of YY1 represents a post-translational regulatory mechanism for this protein factor[47], we examined the possible effects of ubiquitin overexpression on YY1 protein levels and/or intracellular distribution. Western blot analysis of whole cell lysates, as well as of nuclear and cytosolic extracts obtained from pCMV-Myc and Ubwt transfected cells showed that total YY1 content did not change upon Ub transfection and there was no difference in the amount of YY1 in either the cytosolic and nuclear fractions (Fig. 6A). Next, we examined whether increasing Ub pools affected the DNA binding activity of YY1; however, the EMSA performed with a probe containing the most upstream intronic YY1 binding site, revealed a comparable pattern of retarded bands of similar intensities, in control and ubiquitin overexpressing cells (Fig. 6B). Next, we investigated the effects of Ub overexpression on the transcriptional activity of different reporter constructs (depicted in Supplementary Fig. S2B) where luciferase expression is driven by the *UBC*

promoter fragment, referred to as P371, harboring wild-type or mutagenized YY1 binding sites. The results shown in Fig. 6C demonstrated that the mutant constructs behaved the same as the wild-type construct, that is luciferase mRNA significantly decreased after ubiquitin transfection, suggesting that YY1 may not be involved in the downregulation effect. Further confirmation has been obtained by the *in vivo* ChIP assay showing that YY1 occupancy of the *UBC* promoter region did not change upon ubiquitin overexpression (Fig. 6D). A similar percent input was indeed detected for pCMV-Myc and Ub transfected cells when ChIPed DNA was amplified with primers encompassing the main YY1 binding site in the intron (*UBC* intron), the YY1 motif detected in the proximal promoter region and previously proved to be not functional (*UBC* pr-2) and a negative control sequence (*UBC* 3'-UTR).

5.3.7 H2A and H2B histone ubiquitination signatures of *UBC* promoter do not change upon ubiquitin overexpression.

Ubiquitination of histone proteins (mainly of H2A and H2B) has been characterized as an important epigenetic mechanism regulating gene transcription. In particular, H2AK119ub functions as a transcriptional repressor[48,49], while H2BK120ub in general promotes gene transcription, by different mechanisms, like favoring H3K4 methylation[50,51]. Therefore, we sought to investigate if ubiquitin overexpression could alter the ubiquitination status of the *UBC* promoter region, thus accounting for the lowered *UBC* mRNA levels detected upon Ub transfection. We performed chromatin immunoprecipitation on cells transfected with Ub or the control empty vector, using antibodies specific for monoubiquitinated histones H2A and H2B, followed by amplification of different promoter regions. No significant differences were detected in the percent input obtained for control (Myc) and ubiquitin overexpressing (Ubwt) cells (Fig. 7A). Likewise, chromatin immunoprecipitation with anti-H3K4me3 and anti-H3ac (both marks of transcriptionally active chromatin) did not show significant differences between Myc and Ub samples (Fig. 7B).

5.3.8 Ubiquitin overexpression does not impact the transcriptional activity of the *UBC* promoter, but rather the splicing of nascent *UBC* transcripts.

Having not found the *cis-trans* elements involved in the *UBC* downregulation during Ub overexpression, we measured the *UBC* transcriptional activity using the run-on assay. This approach relies on the quantification of biochemically labeled nascent RNA molecules by RTqPCR. Transfected cells were pulsed with 0.2 mM and 0.5 mM 5-ethynyl Uridine, respectively for 14 h and 0.5 h. RTqPCR analysis of nascent *UBC* transcripts showed a ubiquitin-dependent downmodulation of *UBC* (similar to the one detected by RTqPCR of "steady-state" RNA samples) when pulse labeling was left overnight, but no difference in the transcription rate was found after 0.5 h pulse labeling (Fig. 8A). The same layout has been observed for *UBB*, the other ubiquitin coding gene repressed by ubiquitin overexpression (Fig. 8B), while the absence of downregulation was reconfirmed for the Ub-ribosomal fusion genes *UBA52* and *RPS27A*, in both pulse labeling conditions (Fig. 8C,D). These results prompted us to investigate a post-transcriptional mechanism accounting for ubiquitin overexpression-dependent *UBC* downregulation. Thus, we focused on the splicing process to see if ubiquitin overexpression could in some way affect the splicing efficiency of the unique intron of the *UBC* gene. The first

stage was the preparation of intact nuclei from Myc and Ub-transfected cells to measure the amount of unspliced transcripts within the pool enriched of nascent RNAs. Different assays were performed to check the fidelity of nuclei harvesting and proper separation of the cytosolic fraction: intact nuclei were visualized by light microscopy and compared with whole cells (Supplementary Fig. S3A); western blot analysis of protein expression in the purified nuclei revealed the presence of lamin A/C (as expected) but the absence of GAPDH, which is a typical cytoplasmic marker (Supplementary Fig. S3B). RNA samples purified from the nuclear and cytosolic fractions were analyzed by denaturing agarose gel electrophoresis, in parallel with a total RNA sample extracted from whole cells. As shown in the Supplementary Fig. S3C, the ribosomal RNAs (18 S and 28 S) were predominant in the cytosol compared to the nuclear fraction, in agreement with their shuttling to the cytosol upon maturation and assembly with the ribosomal proteins. The nuclear total RNA samples were subjected to retrotranscription followed by RTqPCR, performed both with primers expressly designed to detect the unspliced transcripts, and with standard primers used to measure total mRNAs (Supplementary Table S1). In the ubiquitin overexpressing cells, the fraction of unspliced *UBC* mRNA was about 2.4-fold higher compared to pCMV-Myc transfected cells (Fig. 9A); the same occurred for the *UBB* RNA (2.5-fold more unspliced transcript in Ubwt vs Myc; Fig. 9B); while the percentage of immature nascent RNAs, in Myc and Ub samples, was not statistically different for the housekeeping genes *GAPDH* (Fig. 9C) and *B2M* (Fig. 9D) (~1.2-fold in Ubwt vs. Myc sample for both targets). The same analysis performed on cytoplasmatic RNAs did not detect any difference in the residual unspliced transcripts between Myc and Ub receiving cells, for all the targets investigated.

Finally, we sought to investigate the stability of *UBC* mRNA in a steady state, after inhibition of *the novo* transcription by Actinomycin D, which blocks RNA polymerases. HeLa cells transfected with Myc and Ubwt expression vectors were treated with ActD, harvested at 5 time points (0, 1, 2, 3 and 4 h) after ActD treatment, and then analyzed by RTqPCR. The estimated half-lives of *UBC* mRNA were not statistically different in Myc and Ubwt samples (1.28 and 1.21 h, respectively) (Supplementary Fig. S4).
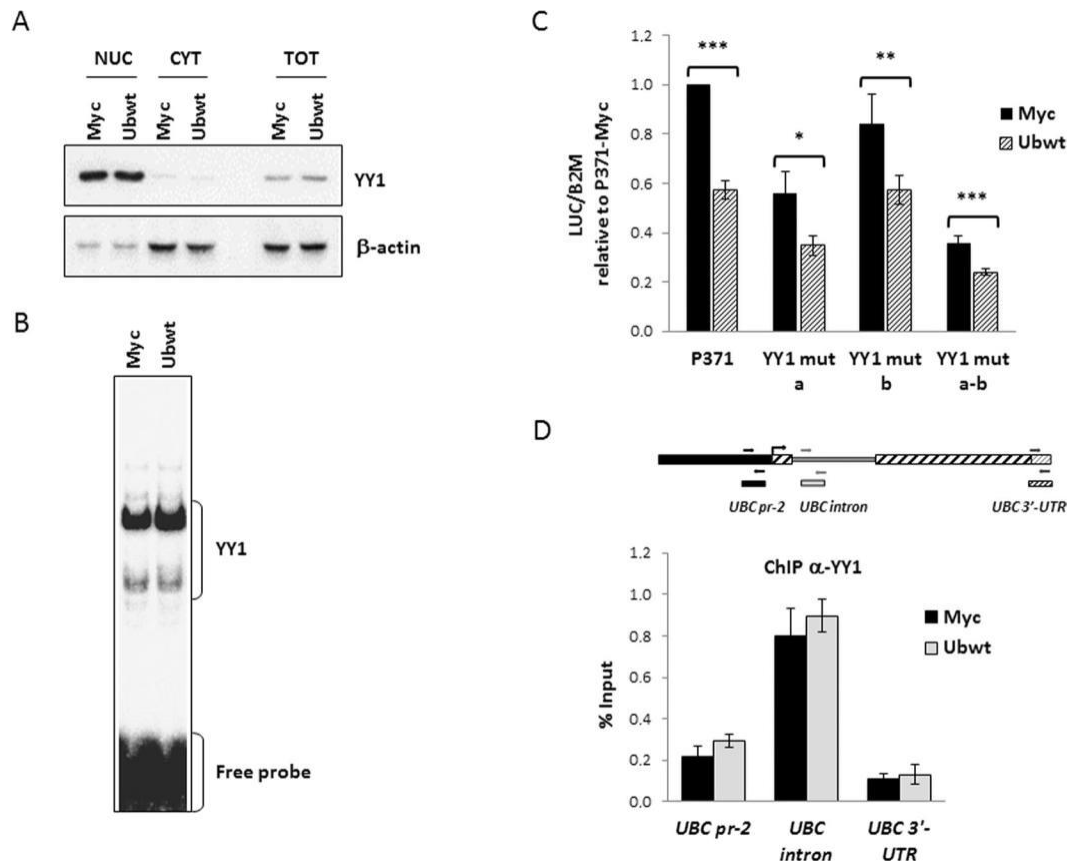
Figure 6. Investigating the role of YY1 transcription factor in *UBC* downregulation. (**A**) Immunoblot analysis of YY1 protein factor in nuclear, cytosolic and whole extracts obtained from HeLa cells transiently transfected with the Ub expression vector (Ubwt) or the empty control vector (Myc). β-actin was used as loading control. (**B**) EMSA analysis was performed using a 32P-labeled oligonucleotide containing the most upstream YY1 binding site previously identified in the *UBC* intron region[39], as probe. Protein/DNA complexes were detected upon incubation of probe with nuclear extracts (5 µg) from cells transfected as in (**A**). (**C**) The wild-type reporter construct P371 and the YY1 mutant counterparts (YY1 mut a, b, a-b) were cotransfected in HeLa cells with the Ub expression construct or the empty vector pCMV-Myc. Forty-eight hours post-transfection, luciferase mRNA levels were determined, normalized to *B2M* and expressed as fold change versus the P371/Myc cotransfected sample, set to 1 (n = 6). (**D**) ChIP analysis of Myc and Ubwt transfected cells, using an antibody specific for YY1; for the internal IP control, no Ab was added. Detection of ChIPed DNA and data analysis were as described in the legend of Fig. 4C (n = 2, assayed in duplicate). Positions of the primers used are depicted in the scheme above the histogram. Data presented are means ± SEM from the indicated number of experiments. Asterisks indicate statistical significance: *p < 0.05; **p < 0.01; ***p < 0.001 vs. control (Myc). The images shown in (**A,B**) are representative of three independent experiments. Full-length immunoblots and EMSA are presented in Supplementary Fig. S8.
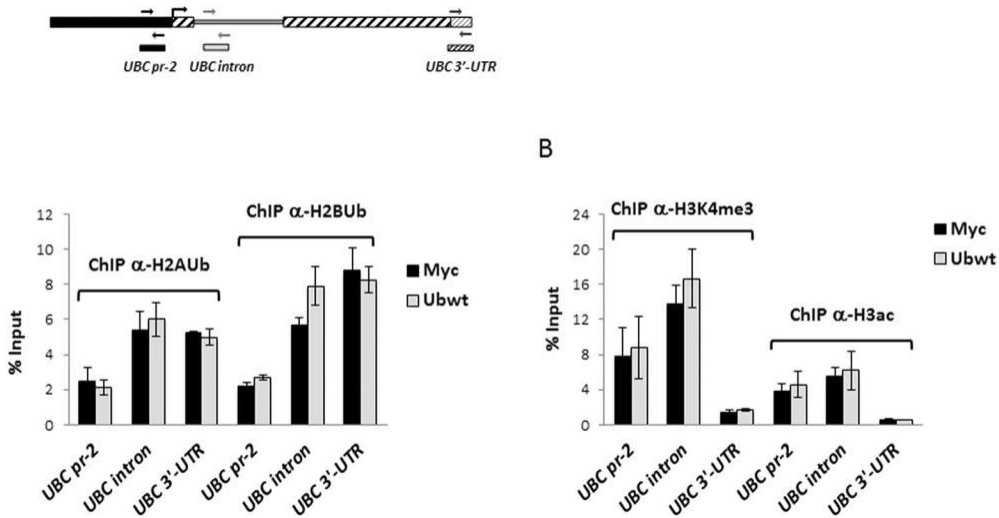
Figure 7. Investigating the role of histone modifications in *UBC* downregulation. (**A**,**B**) Chromatin immunoprecipitation experiments on HeLa cells transfected with the Ub expression vector (Ubwt) or the empty control vector (Myc). Cells were harvested 48 h post transfection and ChIP was performed, as detailed in Materials and Methods, using antibodies specific for H2AUb and H2BUb (**A**) or for H3K4me3 and H3ac (**B**). The scheme on top shows the location of the primers used in RealTime PCR. Results are expressed as % of chromatin input controls. The histograms show the mean ± SEM of two independent experiments, analyzed in duplicate. No statistical significance was detected in Ubwt versus Myc control sample.

5.4 Discussion

Ubiquitin coding genes serve housekeeping functions providing cells with adequate levels of free ubiquitin required to sustain homeostasis. We previously reported that the polyubiquitin gene *UBC* mainly contributes to the intracellular ubiquitin content under basal conditions[52]; moreover, it is at the frontline to supply the extra-ubiquitin needed upon cell exposure to a variety of stresses[9,16,42,52,53]. The ability to buffer different cellular needs requires a highly dynamic but strict regulation of the *UBC* gene[54]. The molecular bases of *UBC* induction, when cells demand more Ub, have been extensively investigated; less known are the consequences of raising the intracellular Ub levels on *UBC* gene expression. In this study, we generated Ub overexpressing cells, in which both the free and conjugated Ub pools proportionally increased[28], demonstrating that the exogenous ubiquitin is properly processed and channeled into the pathways to be used as a signaling tag. Furthermore, Ub overexpression led to a significant decrease in the Ub expression from the two polyubiquitin genes *UBB* and *UBC*. To the best of our knowledge, a similar evidence has only been described by the S. M. Wilson team in transgenic mice that expressed a HA-poly-Ub, under the control of a neuronal promoter[25,27]. The authors highlighted the selective sensitivity of neurons towards minimal changes in the Ub pool, which hence requires a strict controlof Ub homeostasis in the neuronal system, but did not investigate the molecular mechanisms underlining this behavior. These latter became the focus of this study. Firstly, the evidence that downregulation of *UBC* occurred in different cell lines, both normal and tumor-derived, suggested that it might constitute a widespread regulatory response to Ub overexpression. Secondly, transfection of different amounts of Ub expression
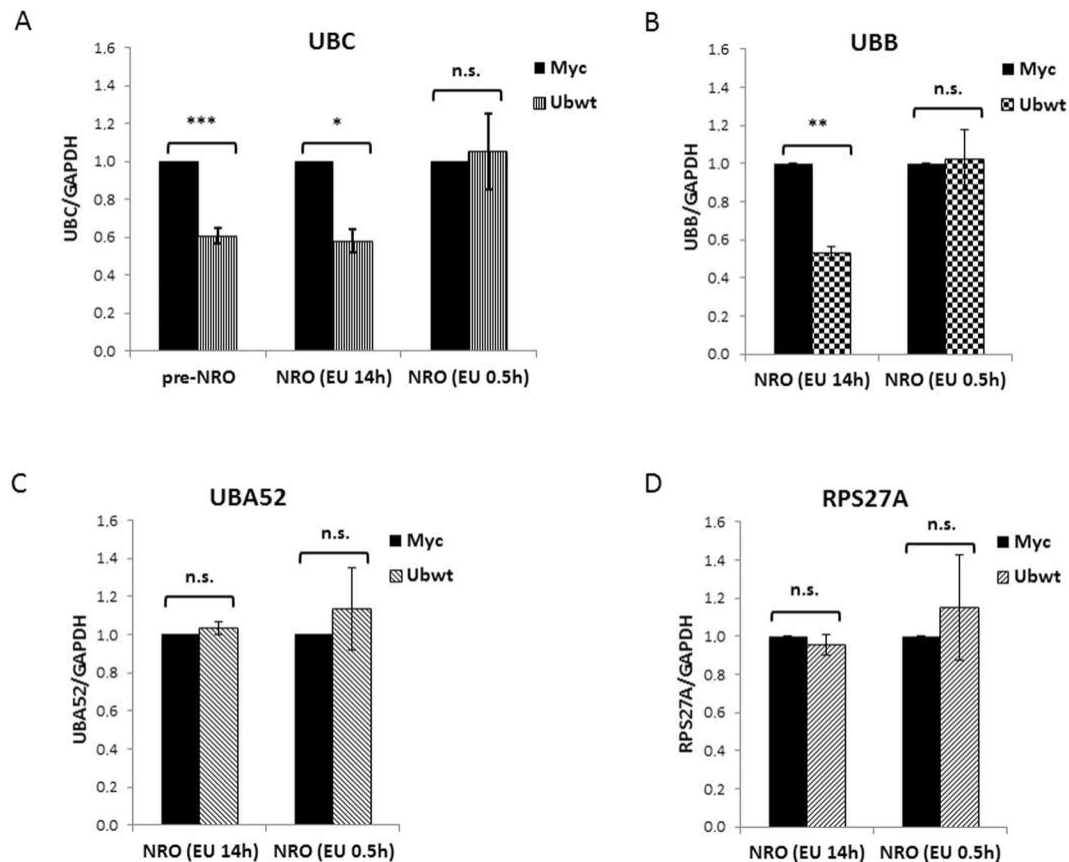
Figure 8. Metabolic labeling of nascent transcripts. HeLa cells transfected with the Ubwt expression construct or the empty vector pCMV-Myc were pulsed (48 h post-transfection) either with 0.5 mM 5-ethynyl Uridine for 0.5 hours (NRO, EU 0.5 h) or with 0.2 mM 5-ethynyl Uridine overnight (NRO, EU 14 h). Cells were then collected and processed essentially following the protocol provided with the Click-iT Nascent RNA Capture kit (Thermo Fisher Scientific). (**A**) RTqPCR analysis of nascent *UBC* transcripts in transfected HeLa cells, pulsed as described above. For comparison, the RTqPCR performed on total RNA extracted from unpulsed Myc and Ub transfected cells is shown in the histogram (pre-NRO). (**B**–**D**) RTqPCR analysis of *UBB* (**B**), *UBA52* (**C**) and *RPS27A* (**D**) nascent transcripts in transfected HeLa cells, pulsed as above. The values of RT-qPCR shown are mean ± SEM of five independent experiments assayed in duplicate. Statistical significance: *p < 0.05; **p < 0.01; ***p < 0.001 vs. control (Myc); n.s., not significant.

plasmid allowed to raise the ubiquitin levels without dramatically overexpressing it, thus enhancing the chance of identifying regulatory pathways that operate in a physiological fluctuation range of Ub and not in the context of a ubiquitin stress response[21]. Doubling the total Ub pool is sufficient to significantly downregulate *UBC* in HeLa cells. Thus, the downmodulation of *UBC* may be part of an (auto)regulatory feedback loop through which ubiquitin attempts to maintain its cellular homeostasis. This entails the existence of a sensing mechanism capable to detect the ubiquitin levels and consequently modulate the transcriptional programs of the polyubiquitin gene *UBC*. This study aimed to identify this putative Ub sensor, as well as the relevant *cis*-elements in the *UBC* promoter engaged in downmodulation. Actually, the Ub sensor could act by binding non-covalently to Ub or by direct conjugation to Ub itself.

To dissect the "language" of ubiquitin sensing, we took advantage of several Ub analogues. The data obtained suggest that Ub sensing requires ubiquitin conjugation, since transfection of Ub mutants devoid of a wild-type C-terminus (UbG76A and particularly UbΔGG) does not cause *UBC* downregulation. Among the lysine mutants, only UbK0, an engineered form of ubiquitin in which all seven lysine residues are replaced with arginine[55], failed to induce the downmodulation of *UBC* gene, when overexpressed in HeLa cells, suggesting that the assembly of a poly-Ub chain not linked via K48 or K63 (excluded by the K48R and K63R Ub mutants) might be necessary for downregulation to occur. Although the use of Ub analogues, mainly of those highly mutagenized, has been debated, Huang *et al*.[56] demonstrated that K0-Ub adopts the same backbone structure as wild-type ubiquitin and, what is more important, it is readily managed by the enzymes E1 and E2.

On the whole, Ub analogues indicated that the "cellular component" in charge of Ub sensing relies on a direct Ub conjugation event, feeding the attractive hypothesis that the "excess" of ubiquitin could promote the destruction or inactivation of protein(s) involved in *UBC* gene transcription, thus providing a straightforward negative feedback loop responsive to intracellular ubiquitin levels. Previous studies by our group[38,39] and others[43,53] have partially dissected the transcriptional regulation of *UBC* promoter defining the relevant *trans*-acting factors responsible for basal and stress-inducible gene expression.

When the luciferase reporter vector P916 (containing the *UBC* promoter region spanning from 916 nt upstream of the TSS to the end of the intron) was cotransfected in HeLa cells with the Ub expression construct, a decreased luciferase transcription was detected, suggesting that the regulatory button might be contained within this sequence. *UBC* has long been labeled as "stress-responsive gene" and HSF1 and HSF2 transcription factors have been demonstrated to be the key regulators of *UBC* induction under different stressful conditions. Although the mechanism of their activation is different[57], both HSFs undergo ubiquitin and proteasome dependent degradation[44–46]. Therefore, we sought to investigate if overexpression of ubiquitin affected their levels and/or DNA binding activity: we didn't find any difference in Ub overexpressing cells compared to pCMV-Myc transfected cells. But, when cells transfected with the Ubwt expression vector were treated with the proteasome inhibitor (MG132), they activated the HSR, as demonstrated by the HSF1-dependent expression of *HSP70*. Strangely enough, in these conditions, they also induced *UBC* gene transcription, despite the abundant cellular Ub content. This may be explained by the activation mechanism of HSF1, requiring its dissociation from the inhibitory partners, namely chaperones, which are displaced by misfolded proteins accumulating under proteotoxic stress environment[44,58]. Free HSF1 acquires competence to bind the HSEs in the promoter of target genes, inducing their transcription. For *UBC*, this occurs independently of the high cellular Ub content, since HSF1 does not sense the ubiquitin levels, but the presence of unfolded proteins[58,59]. It is intriguing that the *UBC* promoter can be modulated by and respond to opposing mechanisms at the same time: the downmodulation driven by the high Ub levels on one side, and the HSF-mediated upregulation triggered by the induced proteotoxic stress on the other side. The molecular bases of this regulatory crossroad and the seemingly contradictory behavior of the *UBC* gene certainly deserve further investigations.
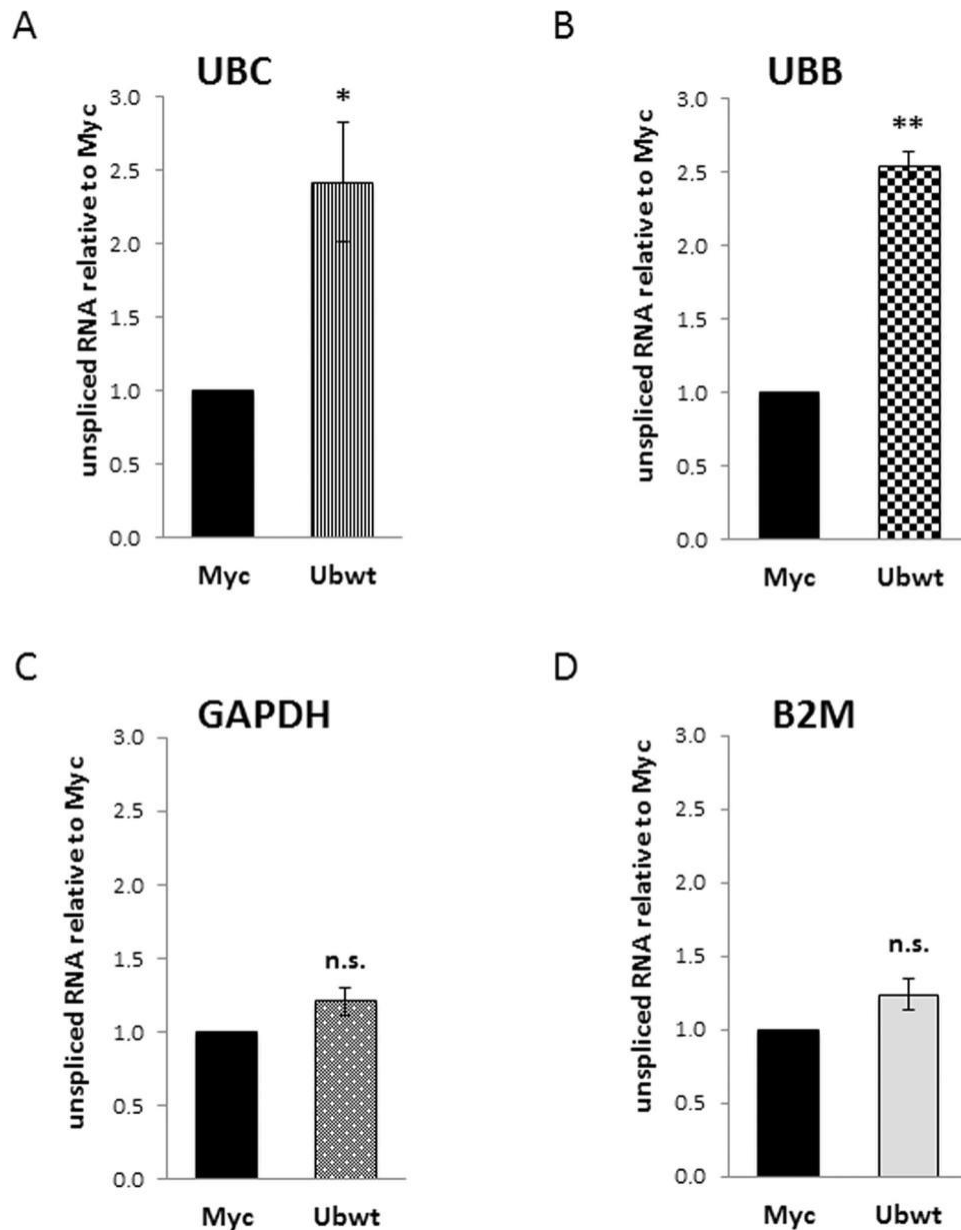
Figure 9. Analysis of unspliced transcripts in the nuclear fractions. (**A–D**) RTqPCR analysis of unspliced transcripts in the nuclear RNA samples extracted from Myc and Ub-transfected cells. Each target gene was analyzed with both primers amplifying total mRNA and primers detecting only the unspliced transcript. The fraction of unspliced transcripts in Myc and Ub samples was calculated with the $2^{-\Delta Ct}$ formula (where ΔCt means $Ct_{unspliced}$ mRNA-Ct_{total} mRNA). Graphs show the fold change of unspliced mRNA in Ubwt versus Myc, set to 1. The values of RTqPCR data shown in (**A–D**) are the average ± SEM of four independent experiments analyzed in duplicate. Statistical significance: *$p < 0.05$; **$p < 0.01$ vs. control (Myc); n.s., not significant.

Data obtained by cotransfection of reporter constructs with the Ub expression vector provided compelling *in vivo* evidence that the *UBC* promoter region warranting the downregulation effect requires the presence of the intron and of an upstream promoter sequence of at least 123 nt, although the essential *cis*-elements for a strong basal expression are comprised within the

−371/+876 spanning sequence[38,43]. This region harbors different binding sites for the ubiquitous TF specificity protein 1 (Sp1), which has been proved to be important for the basal expression of *UBC* gene[38,43]. Moreover, it is known that Sp1 undergoes ubiquitination-dependent proteasomal degradation[60,61]. However, its participation to *UBC* downregulation has been ruled out by different *in vitro* and *in vivo* experiments.

Intron removal from the luciferase reporter constructs abolished the downregulation effect, so we turned our attention towards YY1, the main TF previously found to sustain basal *UBC* gene expression by interacting with multiple binding sites in the intron sequence[39]. Using various *in vitro* experimental approaches, we demonstrated that Ub overexpression did not alter either YY1 protein levels and intracellular distribution or its DNA binding activity. Moreover, *in vivo* studies confirmed that YY1 occupancy of the *UBC* promoter was unchanged in Ub transfected cells and, according to this evidence, mutagenesis of the intronic YY1 binding motifs in the reporter construct did not impair the downregulation mechanism.

The hitherto reported evidences point towards a different kind of contribution of the intron to the downregulation effect, beyond the interaction with transcriptional regulators: it might for example undergo conformational changes, upon Ub transfection, that negatively affect the assembly and/or activity of the transcriptional machinery. Histone ubiquitination is an important epigenetic mechanism for regulating chromatin structure and ultimately gene transcription. Mono-ubiquitination of histone H2A (H2AUb) is a reversible transcriptionally repressive mark[49], while H2B ubiquitylation (H2BUb), interferes with chromatin compaction and leads to an open and more accessible conformation, thus favoring transcription[50]. In addition, depletion of ubiquitylated histone H2A has been detected during proteotoxic stress, to support the accumulation of Ub conjugates, meaning that a redistribution of ubiquitin between different "Ub demanding substrates" indeed exists[19,62,63]. Remarkably, we found no changes in the ubiquitination of histones H2A and H2B within the *UBC* promoter region uponubiquitin overexpression, meaning that likely it is not a change in histone ubiquitylation responsible for the *UBC* downregulation.

Taken together, the evidences so far described show that the main protein factors related to gene transcription do not seem to be involved in the downregulation and the chromatin landscape around the *UBC* promoter region doesn't exhibit noteworthy signatures upon Ub overexpression. Therefore, we wondered whether the higher Ub levels actually dampened *UBC* gene expression, by acting at transcriptional level. To investigate the transcription initiation step, we detected the nascent *UBC* transcripts using the Click-iT technology, which facilitates the partitioning of the newly synthesized RNA transcripts from the already existing RNAs, without the need to isolate the nuclei, as in the classical run-on assay. Of note, results of RT-qPCR analysis of nascent transcripts, upon short pulse labeling with 5-ethynyl uridine, showed that Ub overexpression did not produce significant changes in *UBC* transcription. On the contrary, when labeling with EU was maintained for longer time, a downregulation similar to that found for "steady-state" RNA samples was detected. While the first condition allowed the determination of the actual frequency of generation of nascent transcripts (i.e., the transcription initiation rate), the longer time pulse measured the steady state levels of mRNAs which, besides the "real" promoter activity, depend on several post-transcriptional events. Analysis of nascent transcripts from the *UBB* gene, which was found downregulated upon exogenous Ub

expression like *UBC*, produced the same output as *UBC*. Information gained by nascent transcript analysis excludes a transcription rate control, while results from reporter constructs highlight the requirement of the endogenous intron for the *UBC* gene response: on the whole, these evidences put forward the idea that the downregulation effect might arise in the co- or post-transcriptional phase. This was assessed by determining the levels of unspliced mRNAs in the pool of transcripts purified from the nuclear fractions. For *UBC*, the unspliced pre-mRNAs were significantly increased in Ub overexpressing cells relative to cells transfected with the empty vector. Of note *UBB* showed an increase of the unspliced fraction like *UBC*, while the housekeeping genes *GAPDH* and *B2M* were unaffected by the higher ubiquitin levels, suggesting that the effect is specific. Notably, from studies on reporter constructs we found out that the replacement of the endogenous *UBC* intron with a "splicing-competent" heterologous intron sequence did not support the downregulation following Ub overexpression, indicating that, in addition to splicing sites, other *cis-trans* acting elements specific to the *UBC* intron are strictly required for downregulation to occur. Regarding the *UBB* gene, which exhibited a comparable change on splicing efficiency like *UBC*, in silico analyses showed that human *UBB* and *UBC* introns do not share much similarity (around 47%). Moreover, searching for transcription factor binding sites, using two bioinformatic tools, ALGGEN (http://alggen.lsi.upc.es/cgi-bin/promo_v3/promo/promoinit.cgi?dirDB=TF_8.3) and TFBIND (http://tfbind.hgc.jp/) found different putative YY1 binding sites within *UBB* intron. This is quite intriguing and certainly deserves further investigation, although YY1 seems to not participate to the ubiquitin mediated *UBC* downmodulation.

The finding that increased Ub levels impaired splicing of the *UBC* transcript may represent one of the mechanisms leading to *UBC* downmodulation. The involvement of ubiquitination/deubiquitination cycles in the regulation of co-transcriptional splicing has recently been documented[64–66]. Milligan *et al*. reported that reversible ubiquitination of the catalytic subunit of RNA polymerase II is required to induce a slowed elongation rate (transcriptional pausing), thus favoring co-transcriptional splicing, and is then removed by a protease complex associated with the nascent transcript[64]. Moreover, cells make a large use of ubiquitin and ubiquitin-like proteins (UBLs) to modify (either covalently or non covalently) different spliceosomal components, in order to modulate spliceosome assembly, to control splicing fidelity and to fine-tune the process of pre-mRNA splicing (reviewed in[65]). Of particular interest is the role of the UBL Sde2, a ubiquitin-fold containing splicing regulator that confers intron specificity to the spliceosome[65,66]. The Sde2 precursor undergoes a ubiquitin-like processing, mediated by DUBs, to be activated and then incorporated into the spliceosome, to promote splicing of selected introns from a subset of pre-mRNAs. Moreover, the N-terminal lysine residue of processed Sde2 makes it a short-lived protein being a good substrate of the N-end rule pathway of proteasomal degradation[66]. Based on these evidence, it would be exciting to investigate if the elevated ubiquitin levels affect the post-translational modifications of spliceosomal components and/or the abundance of intron-specific splicing regulators, similar to Sde2. To summarize results herein presented, under Ub overexpression background, the mature *UBC* mRNA levels significantly decrease, while the fraction of unspliced *UBC* pre-mRNA increases. Having excluded a transcriptional control, we speculate that the inefficient *UBC* intron splicing generates a higher amount of intron-retaining transcripts, which are quickly

degraded by the cell to prevent the expression from these nonfunctional RNAs[67–69] and this results in lower *UBC* gene expression. We previously demonstrated and investigated at molecular level the role of the intron in basal *UBC* expression; herein we found evidence that efficient intron splicing may be affected by the cellular ubiquitin levels, thus providing an additional layer of regulation of the *UBC* gene, and a cellular strategy to control Ub pool homeostasis. Additional work is needed to dissect how ubiquitin and/or its sensor(s) participate to modulate this activity.

5.5 Materials and Methods

5.5.1 Cell lines and treatments. Mammalian cell lines used in this study were the cervical carcinoma HeLa cells, the osteosarcoma U2OS cells, the human embryonic kidney 293 (HEK293) cells, all obtained from American Type Culture Collection (ATCC, Manassas, VA, USA) and the normal human keratinocytes NCTC-2544, obtained from Interlab Cell Line Collection (ICLC, Genova, Italy). HeLa cells were maintained in Roswell Park Memorial Institute (RPMI) 1640 medium containing 10% fetal bovine serum, 100 U/mL penicillin and 100 μg/ mL streptomycin, while the other cell lines were maintained in Dulbecco's Modified Eagle Medium (DMEM) supplemented as above, with the addition of 0.1 mM nonessential amino acids for HEK293. All the cell lines were grown at 37 °C and proved to be mycoplasma-free using EZ-PCR Mycoplasma Test Kit (BI, Biological Industries). Two days post-transfection, cells were treated with 20 μM proteasome inhibitor MG132 (Selleckchem, Munich, Germany) or the vehicle DMSO as a control, for 4 h at 37 °C, and then harvested for gene expression analyses. To measure mRNA half-life, at day 2 post-transfection of HeLa cells with the ubiquitin expression construct, 2.5 μg/
mL Actinomycin D (ActD; Sigma, St. Louis, MO, USA) was added to cells to inhibit transcription. Cells receiving the vehicle DMSO were set up as control. After 0, 1, 2, 3 and 4 h of ActD treatment, cells were collected, RNA was extracted, and qPCR was carried out with primers used to measure total mRNAs.

5.5.2 Plasmid constructs and transfections. The preparation of the expression constructs for wild-type ubiquitin and for the lysine mutants K48R and K63R has been described elsewhere[28], while the ubiquitin mutant UbG76A has been obtained as detailed in[33]. The wild-type and mutant Ub-Myc coding sequences were released from the resident plasmid by Pst I/Klenow and Kpn I treatment and cloned into the pCMV-Myc vector between the Apa I/Klenow and Kpn I sites. The plasmid encoding for the I44A ubiquitin has been obtained using the Quick-Change Site-Directed Mutagenesis kit (Stratagene Inc., La Jolla, CA), with the wild-type construct as template, and the degenerate primers designed to introduce the selected amino acid substitution, shown in the Supplementary Table S1. To generate the recombinant vector for the expression of an ubiquitin molecule lacking the two carboxy-terminal glycines (UbΔGG), the construct bearing the wild-type Ub coding sequence was used as a template in a PCR reaction, performed with the Platinum Pfx DNA polymerase (Invitrogen, Carlsbad, CA, USA), according to the manufacturing instructions, and the degenerate primers shown in the Supplementary Table S1. The forward primer was engineered to be cut with Apa I restriction enzyme, while the

reverse primer, bearing a Kpn I cutting site, was designed to allow the deletion of the glycine codons at positions 75 and 76, and to provide a translation stop codon to the insert. The PCR product, Apa I/Kpn I digested, was then inserted into the pCMV-Myc vector (Clontech, Mountain View, CA), cut with the same restriction enzymes. DNA encoding for a Lys-less mutant ubiquitin (UbK0), an engineered form of ubiquitin in which all seven lysine residues are replaced with arginine, has been obtained from the pRK5-HA-Ubiquitin-K0, which was a gift from Ted Dawson (Addgene plasmid # 17603; http://n2t.net/addgene:17603; RRID:Addgene_17603)[70]. Forward primer containing an Apa I restriction site and reverse primer with a Kpn I restriction site were used to amplify the UbK0 coding sequence, which was cloned into the pCMV-Myc. The UbK0 expression vector underwent a mutagenesis reaction to put a Kozak sequence just upstream of the translation initiation codon, using the primer reported in the Supplementary Table S1.

Most of the 5'- and 3'-serially deleted reporter constructs for the *UBC* promoter study have been previously developed[38,39]. New reporter constructs were generated during the present study with four different forward primers (named, respectively, −254, −195, −123 and −84 according to their upstream position relative to the TSS, set to +1), all bearing a Sac I cutting site and a common reverse primer, carrying a Hind III cutting site, positioned 876 nt downstream of the transcription start site, at the end of the *UBC* intron (see Supplementary Table S1). The single-site and multi-site mutations of Sp1 and YY1 transcription factor binding motifs lying in the intron sequence, were all performed using the reporter construct carrying the −371/+876 *UBC* promoter region (P371, previously referred to as P3), as template[39]. The mutagenesis of the HSEs in the untranscribed region of the longer promoter construct (P916, previously named P1) to obtain the HSF mutants has been already described[42]. All DNA sequences were validated and confirmed through DNA sequencing using a PE310 Perkin Elmer capillary sequencer. The plasmid constructs used in this study are listed in the Supplementary Table S2. Plasmid DNA for mammalian cell transfection was propagated in XL1-Blue or NovaBlue bacterial strains and purified by EndoFree Plasmid Maxi Kit (Qiagen Inc., Valencia, CA, USA). HeLa and U2OS cells were transiently transfected using Effectene Transfection Reagent (Qiagen), while HEK293 and NCTC-2544 were transfected using the GeneCellin reagent (BioCellChallenge SAS, France), following the protocols' instructions. Healthy cells were seeded the day before transfection in 6-well plates in order to reach ~60–70% confluence at the time of transfection with 0.4 μg (Effectene) or 2 μg (GeneCellin) plasmid DNA/well, respectively. When HeLa cells were transfected with increasing amounts of Ubwt expression plasmid, the total amount of transfected DNA was kept constant at 0.4 μg by compensating with the pCMV-Myc vector. In cotransfection experiments, 0.2 μg of luciferase reporter plasmid and 0.4 μg of Ub expression vector or empty vector pCMV-Myc, were added to each well. Cells were harvested 2 days after transfection for luciferase assay, RNA and protein analyses.

5.5.3 Luciferase reporter assay. Forty-eight hours post-transfection cells were treated with lysing buffer and luciferase activity was determined by the Luciferase Assay Reagent (Promega s.r.l., Milano, Italia) according to the manufacturer's protocol, on a FLUOstar OPTIMA multifunction microplate reader (BMG-LABTECH GmbH). The firefly luciferase activity was normalized against total protein concentration, as previously reported[38].

5.5.4 RNA preparation and quantitative real-time RT-PC R (RTqPC R). RNA was extracted from transfected cells by using the RNeasy Plus Mini kit (Qiagen) according to the manufacturer´s instructions, followed by DNase treatment (with the TURBO DNA-free™ Kit from Ambion, Austin, TX) to remove any traces of plasmid DNA, when cells received luciferase constructs. RNA concentration was measured by Nanodrop ND-1000 System (NanoDrop Technologies, Wilmington, DE). cDNA for all samples was prepared from 500 ng of total RNA using PrimeScriptTM RT Master Mix (Perfect Real Time; Takara Bio Europe SAS, Saint-Germain-en-Laye, France). SYBR green based Real-Time PCR was performed with Hot-Rescue Real Time PCR Kit (Diatheva s.r.l., Cartoceto PU, Italy), essentially according to the manufacturer's instructions, using an ABI PRISM 7700 Sequence detection system (Applied Biosystems, Foster City, CA, USA)[16]. Thermal cycling was performed as follows: 10 min at 95 °C; 40 cycles of denaturation at 95 °C for 15 s, annealing at 60 °C for 15 s, and extension at 72 °C for 30 s. At the end of PCR cycles, a melting curve was generated to verify the specificity of PCR products. All measurements were performed in triplicate and reported as the average values ± standard error of the mean (mean ± SEM). Target gene values were normalized with the housekeeping genes glyceraldehyde 3-phosphate dehydrogenase (*GAPDH*) or beta 2-microglobulin (*B2M*), as specified. Expression data were calculated according to the 2−ΔΔCt method[71]. Sequences of primers used for RTqPCR are reported in the Supplementary Table S1.

5.5.5 Cell extracts. For protein expression analysis, cells harvested 48 h post-transfection were washed in PBS and lysed by sonication in sodium dodecyl sulfate (SDS) buffer containing 50 mM Tris/HCl pH 8.0, 2% (w/v) SDS, 10 mM N-ethylmaleimide supplemented with a cocktail of protease inhibitors (Roche Diagnostics, Mannheim, Germany). Lysates were boiled and then cleared by centrifugation at 12,000 × *g*. Protein concentration was determined according to Lowry, using bovine serum albumin as standard. Nuclear extracts were obtained by low salt/ detergent cell lysis followed by high salt extraction of nuclei as previously described and protein concentration was determined by the Bradford assay.

5.5.6 Western blotting. For Western blot analysis, protein samples were separated by SDS-PAGE, transferred to a nitrocellulose membrane (0.2 mm pore size; Bio-Rad, Hercules, CA, USA). The blots were probed with the primary antibodies listed below and bands were detected by horseradish peroxidase (HRP)-conjugated secondary antibody (Bio-Rad). Peroxidase activity was detected with the enhanced chemiluminescence detection method (WesternBright ECL, Advasta, Menlo Park, CA, USA). Primary antibodies used in this study were: rabbit polyclonal anti-ubiquitin antibody (kindly provided by Prof. A. L. Haas, Dept. of Biochemistry and Molecular Biology, Louisiana State University Health Sciences Center, New Orleans); anti-HSF2 (sc-13056), anti-YY1 (sc-281), anti-specificity protein 1 (Sp1) (sc-420) and anti-specificity protein 3 (Sp3) (sc-644) from Santa Cruz Biotechnology (Dallas, TX, USA); anti-Lamin A/C (4C11) and anti-HSF1 (4356) from Cell Signaling Technology (Danvers, MA, USA); anti-GAPDH (A300-641A) from Bethyl Laboratories, Inc.; anti-actin (A 2066) from Sigma-Aldrich (Steinheim, Germany).

5.5.7 USP2 digestion and solid phase immunoassay. For quantification of total Ub levels, cells were washed with ice-cold PBS and lysed by sonication (4 cycles of 15 sec at 25 Watt) in 50 mM Na_2HPO_4/NaH_2PO_4 pH 7.4, 140 mM NaCl, 2 mM β-mercaptoethanol supplemented with protease inhibitors. Cell extracts were cleared by centrifugation and protein content was determined by the method of Bradford. Twenty μg of extract were incubated at 37 °C for 60 min with 0.5 μg of human recombinant Usp2 protein in a final volume of 40 μL. The digestions were stopped by adding an equal volume of SDS-PAGE sample buffer and boiling. Conversion of polymeric Ub to Ub monomers was checked by western immunoblotting of undigested and digested extracts with an anti-Ub antibody. Quantification of ubiquitin content was performed by submitting Usp2-digested extracts to solid phase immunoassay as previously reported[28]. Briefly, protein samples were serially diluted with 140 mM NaCl so that the signal obtained after staining was linear with the amount applied and within the linear range of purified ubiquitin (from 10 to 0.6 ng) used as the reference standard. Samples and standard ubiquitin dilutions were loaded onto a nitrocellulose filter (0.2 μm pore size, BioRad) with the aid of a 96-well Dot Blot apparatus (BioRad) and processed as described[28]. Fixed blots were immunochemically stained for ubiquitin. Detection and densitometric quantification were performed in a Chemidoc apparatus (BioRad) equipped with the Quantity One software.

5.5.8 Electrophoretic mobility shift assay (EMSA). Nuclear extracts were prepared as described above. Synthetic ODNs (HPLC-purified) were purchased from Thermo Fisher Scientific GmbH (Ulm, Germany) and their sequences (both wild-type and mutated) are depicted in the Supplementary Table S1. Double stranded oligonucleotides were 5' end-labeled with [γ-32P] ATP (Perkin Elmer Life Sciences, Boston, USA) and T4 polynucleotide kinase (T4 PNK, Roche Diagnostics, Mannheim, Germany). For direct binding experiments, nuclear extracts (5 μg) were preincubated with 3 μg of double-stranded non-specific DNA competitor poly(dI-dC) (Amersham Pharmacia Biotech) for 10 min on ice in binding buffer[42]. After this time, a 32P-end-labeled DNA probe was added to the mixtures at a final concentration of 4 nM and the incubation was continued for an additional 30 min. Reaction mixtures were then submitted to electrophoretic separation on 5% native polyacrylamide gels. DNA/protein complexes were detected by exposing the dried gel in a Molecular Imager (Bio-Rad). For competition experiments, nuclear extracts were incubated with a 50-fold excess of double stranded competitor ODN for 10 min before adding the 32P-labeled probe.

5.5.9 Chromatin immunoprecipitation (ChIP). ChIP assay was performed using the EZ-ChIPTM Assay kit (Upstate Biotechnology Inc., New York, NY, USA), essentially according to the manufacturer's instructions, as described[39]. Briefly, HeLa cells were transfected with the Ubwt expression vector or the empty vector pCMV-Myc (also shortened as Myc). Two days after, cells were cross-linked with 1% formaldehyde and cross-linked DNA underwent twelve 15 s sonication pulses at 45 watts by using a Labsonic 1510 Sonicator (Braun, Melsungen, Germany), to obtain sheared chromatin with an average size of 200/500 bp. For each immunoprecipitation, $2×10^6$ cell equivalents of sheared chromatin were incubated overnight at 4 °C with 10 μg of specific antibodies (listed below), or with no antibody (negative control). Immunoprecipitated chromatin (bound fractions) and an aliquot of input chromatin (1%) were

subjected to de-crosslinking and DNA purification. ChIPed DNA was then analyzed using the SYBR green Real-Time master mix described above and the primer sets reported in the Supplementary Table S1. Cycling conditions were as described above for gene expression studies. Raw data (threshold cycle, Ct) of promoter-specific amplifications from ChIPed DNA (IP sample) were expressed as % of chromatin input controls, calculated using the formula $2-\Delta Ct \times 100$, where $\Delta Ct = CtIP$ sample - Ctinput. ChIP antibodies used in this study were: anti-YY1 (sc-281X), anti-HSF1 (sc-9144X) and anti-HSF2 (sc-13056X) from Santa Cruz Biotechnology; anti-H2AUb (Lys 119) (D27C4) and anti-H2BUb (Lys 120) (D11) from Cell Signaling Technology; anti-H3ac (pan-acetyl) (28612004) and anti-H3K4me3 (12613005) from Active motif.

5.5.10 Metabolic labeling of nascent transcripts. To analyze gene expression changes among the pool of nascent *UBC* mRNAs, we adopted the Click-iT Nascent RNA Capture kit (Thermo Fisher Scientific) and performed experiments essentially according to manufacturers' instructions, with slight modifications. HeLa cells transfected with the Ubwt expression construct or the empty vector pCMV-Myc were pulsed (48 h post-transfection) either with 0.5 mM 5-ethynyl Uridine for 0.5 hours or with 0.2 mM 5-ethynyl Uridine overnight (~14 hours). Cells were then collected for RNA isolation, performed with the RNeasy Plus Mini kit (Qiagen) described above. Newly synthesized transcripts were then subjected to biotinylation, which creates a biotin-based handle for capturing nascent RNA transcripts on streptavidin magnetic beads. After precipitation and quantification of RNA yield by Nanodrop, the biotinylated RNA was selected through binding to streptavidin coated beads and finally cDNA synthesis was performed "on beads". The Superscript III First-Strand cDNA synthesis system (Thermo Fisher Scientific) has been employed for reverse transcription of RNA, following the provided protocol, with the exception that the bead suspension containing the template RNA was heated 5 min at 68–70 °C before primers annealing and the reaction mixtures were gently mixed during the reverse transcriptase (RT) reaction (1 h at 50 °C) to prevent the beads from settling. The RT reaction was terminated and cDNA released from the beads by heating the mixture at 85 °C for 5 minutes. The beads were immobilized by using a DynaMag Spin magnet while collecting the supernatant containing cDNA. Undiluted cDNA was used in qPCR (2 μL cDNA were added in a 25 μL amplification reaction) executed with the SYBR Green Real-Time master mix reported above.

5.5.11 Nuclei purification and detection of unspliced transcripts. Cell nuclei were harvested by gentle lysis of the plasma membrane and low-speed centrifugation as detailed in ref. 72. Briefly, HeLa cells transfected in six well-plates were washed with ice-cold PBS and then harvested by mechanical scraping by adding 0.5 mL ice-cold PBS/well. Scraped cells were transferred to a 1.5 mL microcentrifuge tube, placed on ice, mixed by pipetting to ensure a uniform cell suspension and counted using the Countess™ II FL Automated Cell Counter (ThermoFisher Scientific). At least 10^6 cells were pelleted by centrifugation at $400 \times g$ for 4 min at 4 °C and supernatant was then discarded. The pellet was resuspended in 0.5 mL NP-40 Lysis Buffer (10 mM Tris-HCl pH 7.4, 10 mM NaCl, 3 mM MgCl2, 0.5% NP-40) and incubated on ice for 5 min. Nuclei were pelleted by centrifugation at $300 \times g$ for 4 min at 4 °C. Supernatant was saved to extract RNA from the cytosol fraction, while the nuclear pellet was resuspended in a

further 0.5 mL of NP-40 Lysis Buffer and immediately pelleted by centrifugation at $300 \times g$ for 4 min at 4 °C. After collection of the supernatant as above, the nuclear pellet was resuspended in 350 µL RLT lysis buffer for RNA extraction. In the same way, 2 volumes of RLT were added to the harvested cytosol fraction. RNA samples were purified from the nuclear and cytoplasmic fractions using the RNeasy Plus Mini kit and then analyzed by denaturing agarose gel electrophoresis. The images were captured using a gel documentation system (Bio-Rad, Hercules, CA, USA). Reverse transcription was performed with the PrimeScriptTM RT Master Mix. qPCR assays were carried out with the SYBR Green Real-Time master mix referred to above and new suitably designed primer sets for detecting nascent transcripts. These primers, named "NRO primers" (as in the reference paper of Roberts *et al.*[72] from which some sequences have been picked and slightly modified) have been designed in order to fall within introns or to span an intron-exon boundary. The sequence as well as the position of these NRO primers are reported in the Supplementary Table S1.

5.5.12 Statistics. Statistical analyses for experimental data were performed with PRISM software (GraphPad Software, La Jolla, CA, USA). Statistical significance was evaluated by the two-tailed paired Student's t test for pairwise comparisons or one-way ANOVA with Tukey-Kramer multiple comparisons test for multiple comparisons. Results were expressed as means ± SEM and differences between values were considered significant for $p < 0.05$.

Data availability
All data generated or analysed during this study are included in this published article (and its Supplementary Information Files).

5.6 Supplementary Data

	Myc	Ubwt	UbK48R	UbK63R	UbG76A	UbI44A	UbDGG
HSF2	1.00	1.05	1.50	1.05	1.55	1.45	1.70
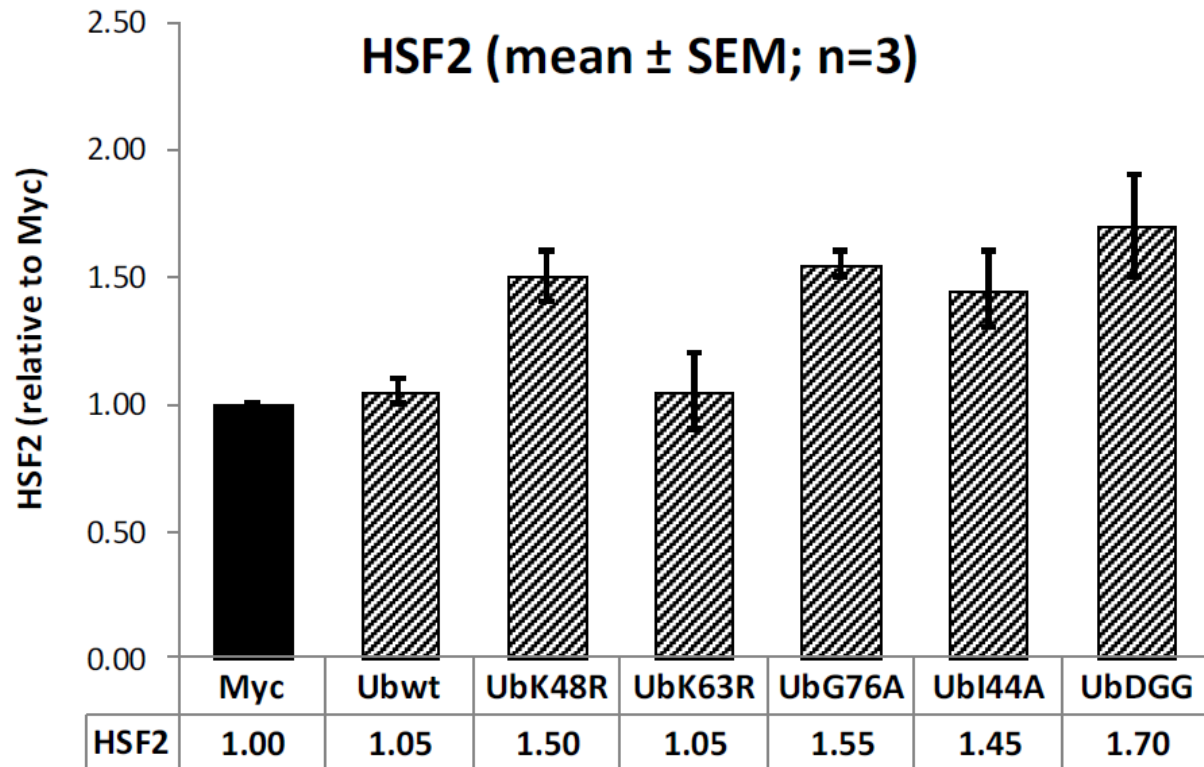
Supplementary Figure S1.
HSF2 total protein levels in HeLa cells transfected with the indicated constructs. Quantification of HSF2 protein factor in whole extracts obtained from HeLa cells transiently transfected with the indicated Ub expression vectors or the empty control vector (Myc). Relative amounts are expressed vs. the control Myc, set to 1. The histogram shows the means ± SEM of three independent experiments.
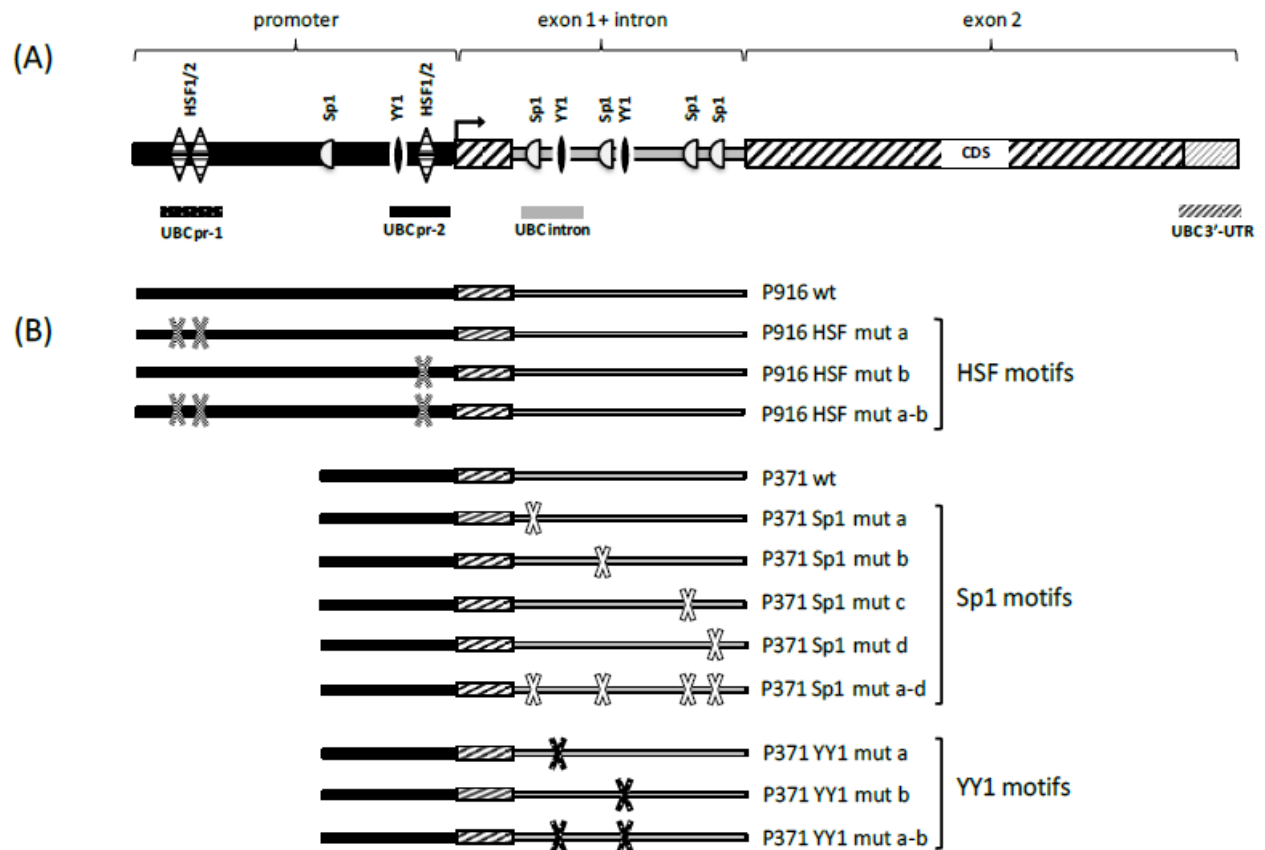
Supplementary Figure S2. Previous characterization of UBC promoter and reporter constructs used in this study.

(**A**) Schematic representation of the UBC promoter region previously investigated, with the trans-acting factors driving promoter activity under basal and stressful conditions. YY1 binding sites are present both in the intron and in the upstream promoter sequence39. Likewise, Sp1 binding sites have been identified both upstream of the TSS43 and within the intron sequence38,39. HSF1 and HSF2 interact with HSEs in the upstream promoter region16,42. (**B**) The P916 wild type reporter construct has been used as the template to mutagenize the three HSEs in the upstream promoter, alone or in combination, to generate the constructs referred to as: P916 HSF mut a, b, a-b. The P371 wild type reporter construct has been used as the template to mutagenize the Sp1 and YY1 motifs identified in the intron, alone or in combination, to generate the following constructs: P371 Sp1 mut a, b, c, d, a-d; P371 YY1 mut a, b, a-b.
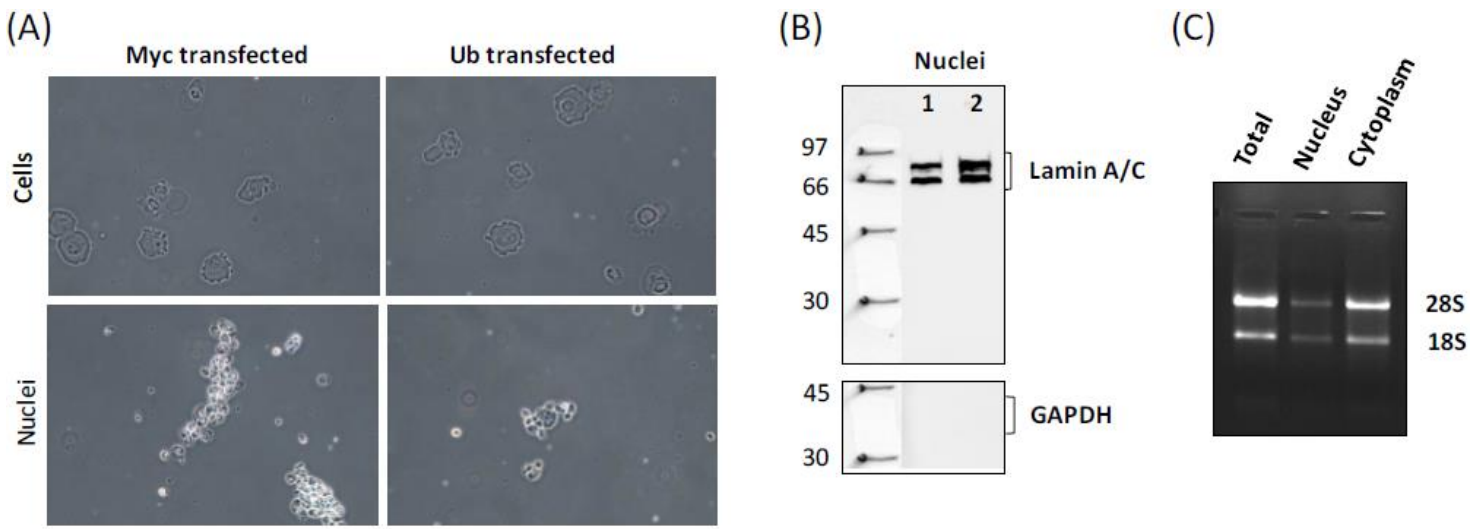
Supplementary Figure S3. Preparation and validation of nuclear extracts.
(**A**) Nuclei were harvested by gentle lysis and low speed centrifugation as described72. Whole cells and nuclear extracts from either Myc or Ub transfected samples were visualized by light microscopy (using a 40X objective). (**B**) Proteins harvested from nuclear fractions (7.5 and 15 ⦾g in lanes 1 and 2, respectively) were subjected to immunoblotting analysis with anti-Lamin A/C and anti-GAPDH antibodies. The position of molecular mass markers is indicated on the left. (**C**) RNA was extracted from whole cells (total) and from both the nuclear and cytosolic fractions. The 28S and 18S ribosomal RNAs were visualized by running 10 ⦾L of each elution (of 50 ⦾L) on a 1.3% formaldehyde-agarose gel. The image shown in (A) is representative of three independent experiments. For (B) and (C), representative gels, relative to the Myc-transfected sample, are shown. Full-length immunoblots and gel image are presented in Supplementary Figure S9.

half life ($T_{1/2}$) = ln2 /K_{decay}
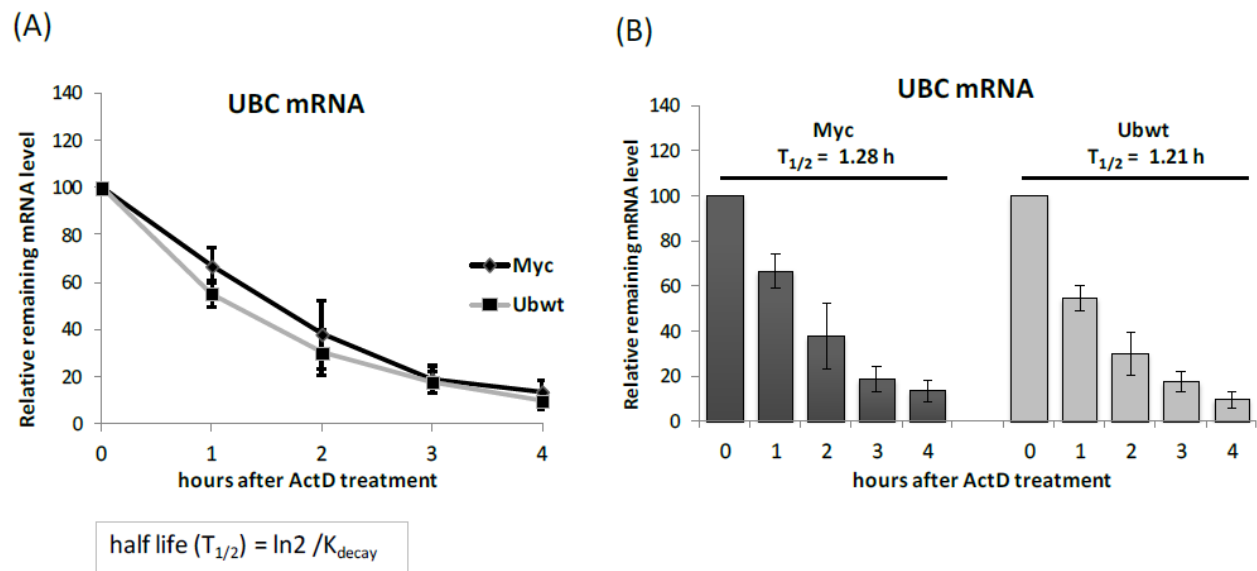
Supplementary Figure S4. Determination of *UBC* mRNA half-life.
(**A,B**) RTqPCR analysis of *UBC* mRNA in HeLa cells transfected with the Ubwt expression construct or the empty vector Myc, at indicated times after treatment with Actinomycin D (ActD). The half-life was calculated by the equation T1/2 = ln2/Kdecay. Data presented in the graphs are means ± SEM of three independent experiments; p = 0.5933 vs. Myc.

86

Fig. 2A
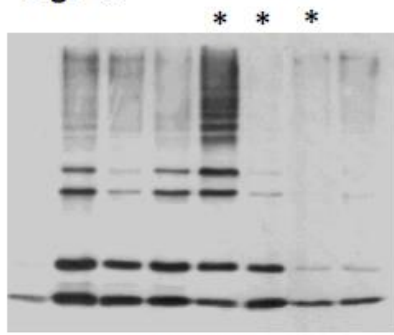
Low exposure
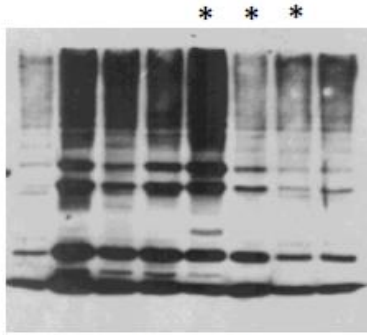
High exposure

Fig. 2B

Fig. 2C

n.s.
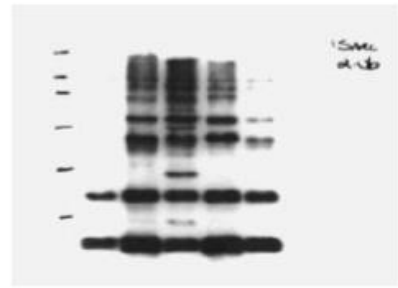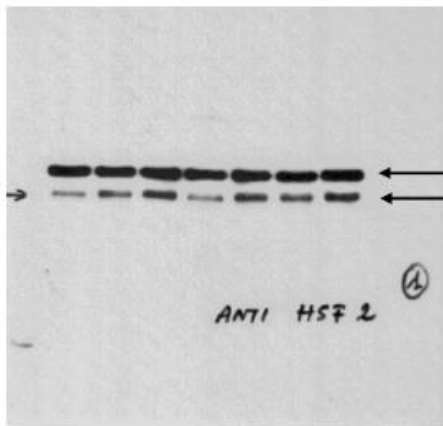
HSF2

ANTI HSF 2
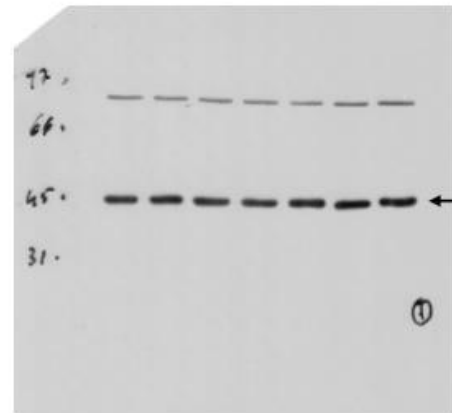
β-actin

Supplementary Figure S5. Full immunoblot exposures for results shown in Figure 2A-2B-2C.
Lanes highlighted by a star represent samples unrelated to this study.

Fig. 4A

High exposure

Low exposure
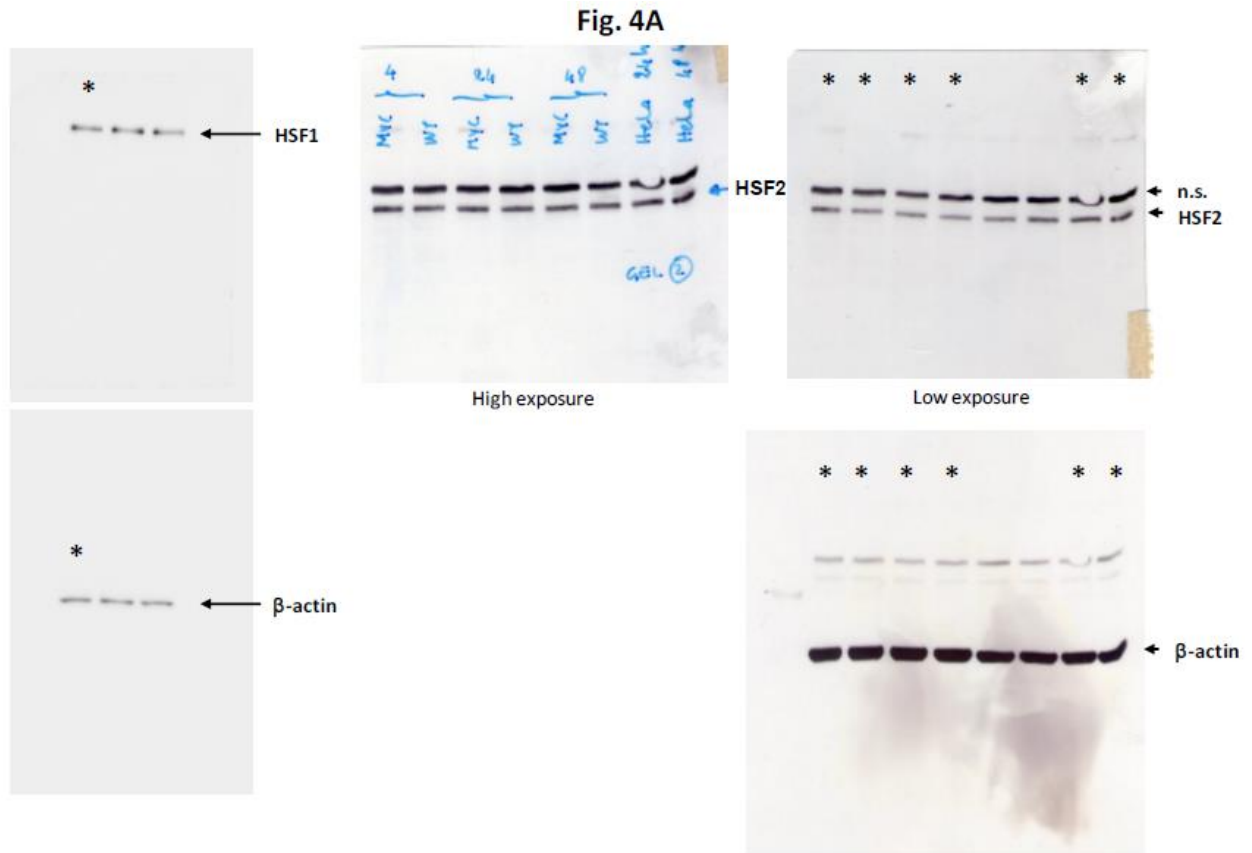
Supplementary Figure S6. Full-length immunoblots for results shown in Figure 4A.
Lanes highlighted by a star represent samples unrelated to this study.
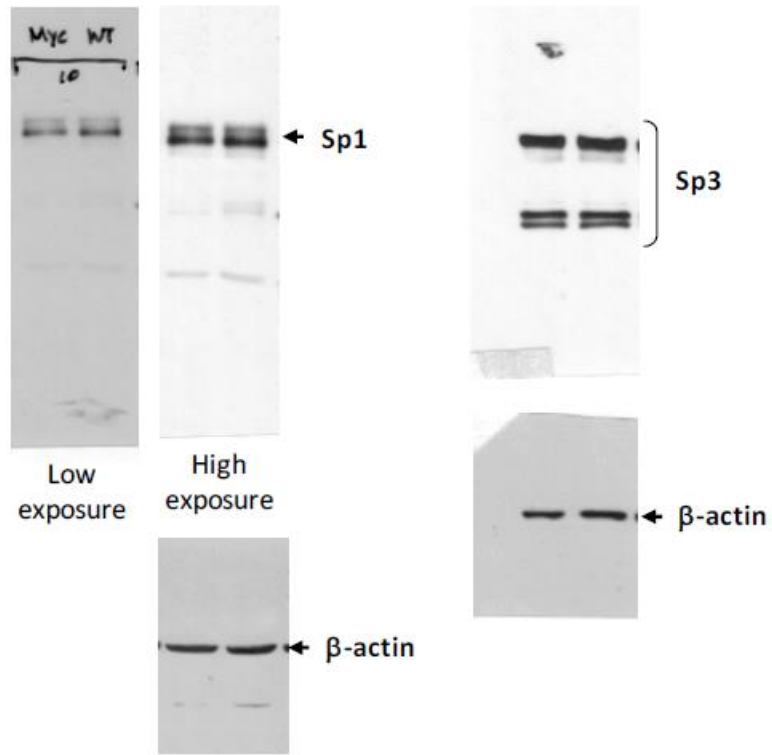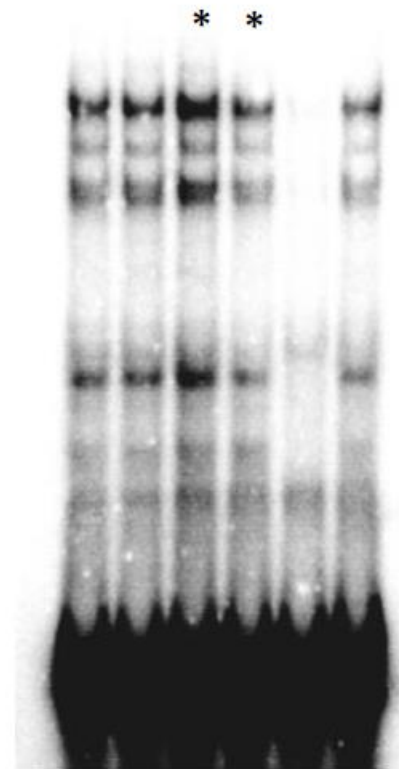
Supplementary Figure S7. Full-length immunoblots and EMSA for results shown in Figure 5A and 5B. Lanes highlighted by a star represent samples unrelated to this study.

Fig. 6A

→ YY1

→ β-actin
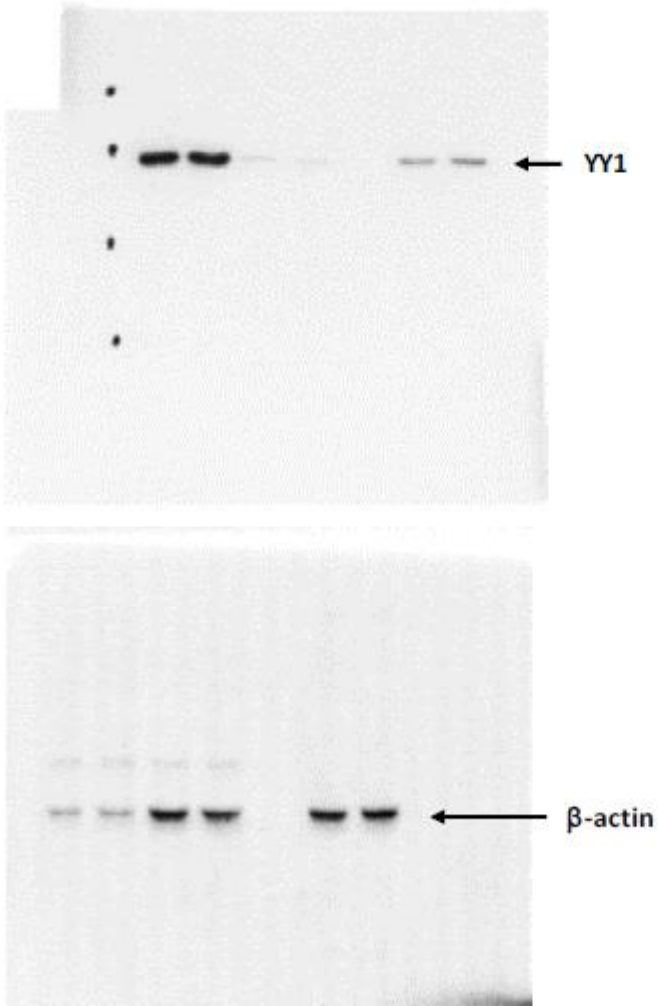
Fig. 6B
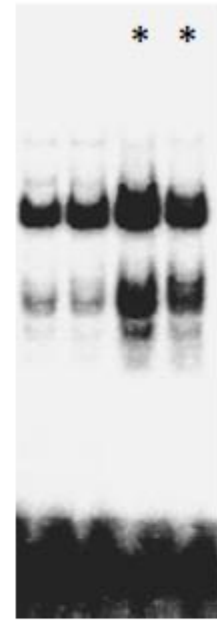
Supplementary Figure S8. Full-length immunoblots and EMSA for results shown in Figure 6A and 6B. Lanes highlighted by a star represent samples unrelated to this study.

Fig. S3B

Mw std

Lamin A/C

GAPDH

Fig. S3C

rRNA
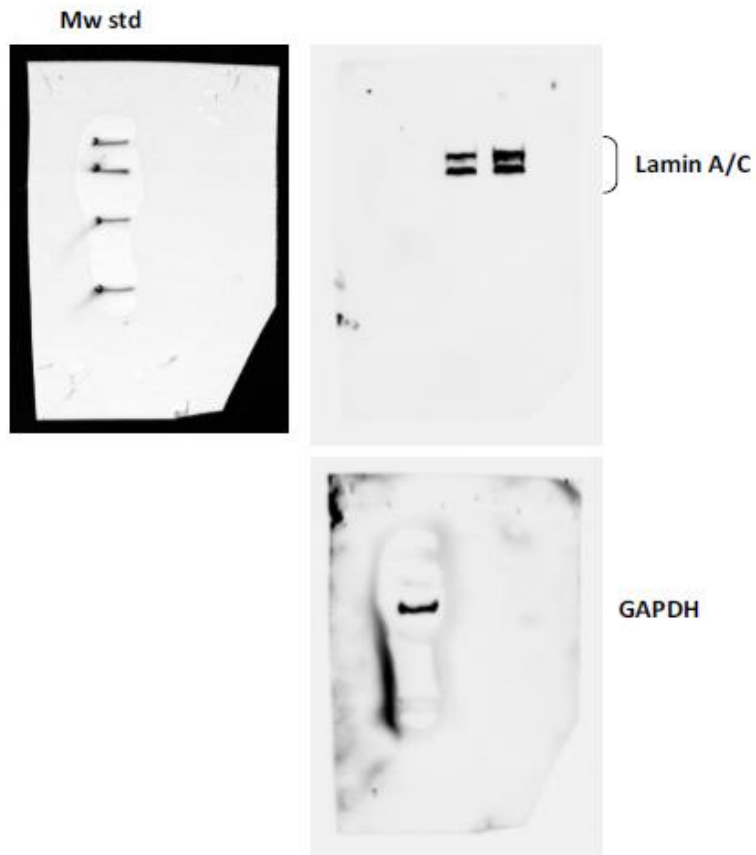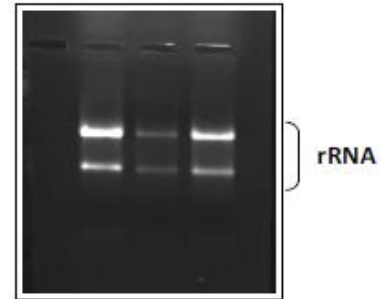
Supplementary Figure S9
Full-length immunoblots and gel image for results shown in Supplementary Figure S3B and S3C.

Supplementary Table S1. Synthetic oligonucleotides used in this study

| oligo ID_strand	SEQUENCE (5' to 3')	APPLICATION	NOTES	REFERENCE
Oligonucleotides used for reporter and ubiquitin expression constructs			*Restriction enzyme cutting site*	
hUBC (-916)_F	ggtaccGAGCTCGAGAAATTTCCATGCCTCCCTG	*cloning*	*Sac I*	*Bianchi et al., Gene 2009*
hUBC (-535)_F	caggtaccGAGCTCAGACCCGTCCATCTCGCAGG	*cloning*	*Sac I*	*Bianchi et al., Gene 2009*
hUBC (-371)_F	caggtaccGAGCTCTAAGGAACGCGGGCCGCCCA	*cloning*	*Sac I*	*Bianchi et al., Gene 2009*
hUBC (-254)_F	ggtaccGAGCTCAGCGAGCGTCCTGATCCTTC	*cloning*	*Sac I*	*This study*
hUBC (-195)_F	ggtaccGAGCTCCTCGGCCTTAGAACCCCAGTATC	*cloning*	*Sac I*	*This study*
hUBC (-123)_F	ggtaccGAGCTCTTTCTTTCCAGAGAGCGGAACAG	*cloning*	*Sac I*	*This study*
hUBC (-84)_F	caggtaccGAGCTCCCTTCTCGGCGATTCTGCGG	*cloning*	*Sac I*	*This study*
hUBC (-37)_F	ggtaccGAGCTCGATGATTATATAAGGACGCG	*cloning*	*Sac I*	*Bianchi et al., PLoS One 2013*
hUBC (+4)_R	gtccatggAAGCTTAACTAGCTGTGCCACACCCG	*cloning*	*Hind III*	*Bianchi et al., Gene 2009*
hUBC (+63)_R	agatctGCTAGCAAGTGACGATCACAGCGATCCAC	*cloning*	*Nhe I*	*Bianchi et al., Gene 2009*
hUBC (+876)_R	tggAAGCTTGTCTAACAAAAAAGCCAAAAACGGC	*cloning*	*Hind III*	*Bianchi et al., Gene 2009*
UbΔGG_F	GTACCCGCGGGCCCATGCAGATCTTCGTGAAG	*cloning*	*Apa I*	*This study*
UbΔGG_R	TTCGGCTTGGTACCTCATCTAAGACGGAGCACCAG	*cloning*	*Kpn I*	*This study*
UbK0_F	GTGGTGGGGGGGCCCATGCAGATCTTCGTCAG	*cloning*	*Apa I*	*This study*
UbK0_R	TTAGCGGCGGTACCACCACCTCTTAGTCTTAAGACAAG	*cloning*	*Kpn I*	*This study*
UbI44A_F	CCTGACCAGCAGAGGTTGGCCTTTGCTGGGAAACAGCT	*mutagenesis*		*This study*
UbI44A_R	AGCTGTTTCCCAGCAAAGGCCAACCTCTGCTGGTCAGG	*mutagenesis*		*This study*
Kozak_UbK0_F	TGCGGAATTGTACCCGCCCCACCATGCAGATCTTCGTCAG	*mutagenesis*		*This study*
Oligonucleotides used for gene expression studies by RTqPCR				
UBC_F	GTGTCTAAGTTTCCCCTTTTAAGG	*real time*		*Bianchi et al., PLoS One 2013*
UBC_R	TTGGGAATGCAACAACTTTATTG	*real time*		*Bianchi et al., PLoS One 2013*
UBB_F	CTTTGTTGGGTGAGCTTGTTTGT	*real time*		*Bianchi et al., Gene 2015*
UBB_R	GACCTGTTAGCGGATACCAGGAT	*real time*		*Bianchi et al., Gene 2015*
UBA52_F	CTGCGAGGTGGCATTATTGAG	*real time*		*Bianchi et al., Gene 2015*
UBA52_R	GTTGACAGCACGAGGGTGAAG	*real time*		*Bianchi et al., Gene 2015*
RPS27A_F	TCGTGGTGGTGCTAAGAAAAGG	*real time*		*Bianchi et al., Gene 2015*
RPS27A_R	TTCAGGACAGCCAGCTTAACCT	*real time*		*Bianchi et al., Gene 2015*
HSP70_F	AGCTGAAGAAGGGTCAAGTGAC	*real time*		*Bianchi et al., FEBS Open Bio 2018*
HSP70_R	TGGATAGGGCAAATCCTGAG	*real time*		*Bianchi et al., FEBS Open Bio 2018*
GAPDH_F	TGCACCACCAACTGCTTAG	*real time*		*Crinelli et al., PLoS One 2015*
GAPDH_R	GATGCAGGGATGATGTTC	*real time*		*Crinelli et al., PLoS One 2015*
B2M_F	GCCTGCCGTGTGAACCAT	*real time*		*Bianchi et al., PLoS One 2013*
B2M_R	CATCTTCAAACCTCCATGATGCT	*real time*		*Bianchi et al., PLoS One 2013*
LUC_F	TGTACACGTTCGTCACATCTCATCT	*real time*		*Bianchi et al., PLoS One 2013*
LUC_R	AGTGCAATTGTCTTGTCCCTATCG	*real time*		*Bianchi et al., PLoS One 2013*

Oligonucleotides used for detection of unspliced RNA			Primer position	
nro-UBC_F	GGATTTGGGTCGCAGTTCTT	real time unspliced	exon 1	This study
nro-UBC_R	TTGGCGGTCTCTCCACAC	real time unspliced	intron	This study
nro-UBB_F	GGCATTTTGAAGGAATAGTTGC	real time unspliced	intron	This study
nro-UBB_R	ACGAAGATCTGCATTTTGACCT	real time unspliced	intron-exon junction	This study
nro-GAPDH_F	AATCCCATCACCATCTTCCAG	real time unspliced	exon	This study
nro-GAPDH_R	GGAGCCACACCATCCTAGTTG	real time unspliced	intron	This study
nro-B2M_F	GACACCAAGTTAGCCCCAAG	real time unspliced	intron	This study
nro-B2M_R	AACCCAGACACATAGCAATTCAG	real time unspliced	exon	This study
Oligonucleotides used for ChIP			**Previous name**	
UBC pr1_F	GAGAAATTTCCATGCCTCCCTGTT	real time	FR1 (-916) fwd	Crinelli et al., PLoS One 2015
UBC pr1_R	AAAAGAGGCGGAAACCCCACA	real time	FR1 (-759) rev	Crinelli et al., PLoS One 2015
UBC pr2_F	ACTCGGCCTTAGAACCCCAGTA	real time	FR6 ChIP forward	Crinelli et al., PLoS One 2015
UBC pr2_R	CTCGCCTGTTCCGCTCTCT	real time	FR6 ChIP reverse	Crinelli et al., PLoS One 2015
UBC intron_F	ACCGCCAAGGGCTGTAGTCT	real time		This study
UBC intron_R	CTCACAAGCGTCTTCCATTCAAG	real time		This study
UBC 3'-UTR_F	GTGTCTAAGTTTCCCCTTTTAAGG	real time	The same used for gene expression studies (UBC_F)	Bianchi et al., PLoS One 2013
UBC 3'-UTR_R	TTGGGAATGCAACAACTTTATTG	real time	The same used for gene expression studies (UBC_R)	Bianchi et al., PLoS One 2013
Oligonucleotides used for EMSA			**Primer position**	
Sp1_wt	TTTTGGCGCCTCCCGCGGGCGCCCCCCTCCTCACGGCGAG	EMSA	human *UbC* (−319 to −280)	Marinovic et al., J. Biol. Chem. 2002
Sp1_mut	TTTTGG**AGAAT**CCCGCGGGCGCC**TACGT**CCTCACGGCGAG	EMSA	human *UbC*mut2x (−319 to −280)	Marinovic et al., J. Biol. Chem. 2002
YY1 intron probe	AGCAAAATGGCGGCTGTTCCCGAGTCT	EMSA	intron	This study

F, forward; R, reverse.

Regarding the primers used for reporter constructs: the numbers in brackets refer to the position respect to the transcription start site (TSS) of *UBC* gene identified as +1; the lower case letters stand for degenerate extra-sequences; the restriction enzyme sites are underlined.

For the nro- (Nuclear Run On) primers, the position of the binding sequence is indicated in the NOTES column. The letters in bold in the mutagenesis primers as well as in the Sp1_mut oligonucleotide used in EMSA indicate the nucleotide changes introduced.

Supplementary Table S2. Plasmids used in this study

CONSTRUCT ID_ (CURRENT NAME)	DESCRIPTION	PREVIOUS NAME	REFERENCES
Expression constructs			
Ubwt	expression of wild-type ubiquitin (Ub)	Ub-Myc[cl]	*Crinelli et al., Mol. Cell. Biochem. 2008*
UbK48R	expression of Ub carrying the $Lys^{48} \rightarrow Arg^{48}$ substitution	UbK48R	*Crinelli et al., Mol. Cell. Biochem. 2008*
UbK63R	expression of Ub carrying the $Lys^{63} \rightarrow Arg^{63}$ substitution	UbK63R	*Crinelli et al., Mol. Cell. Biochem. 2008*
UbK0	expression of Ub carrying all the Lys replaced with Arg (Lys-less Ub)		*Lim et al., J. Neurosci. 2005*
UbG76A	expression of Ub carrying the $Gly^{76} \rightarrow Ala^{76}$ substitution	UbG76A	*Palma et al., Mol. Cell. Biochem. 2009*
UbΔGG	expression of Ub lacking the Gly^{75} and Gly^{76} residues		*This study*
UbI44A	expression of Ub carrying the $Ile^{44} \rightarrow Ala^{44}$ substitution		*This study*
pCMV-Myc	empty vector	pCMV-Myc	*Crinelli et al., Mol. Cell. Biochem. 2008*
Reporter constructs			
5' and 3' serial deletions	*The cloned UBC promoter region is indicated in square brackets*		
P916	[-916/+876] intron included	P1	*Bianchi et al., Gene 2009*
P535	[-535/+876] intron included	P2	*Bianchi et al., Gene 2009*
P371	[-371/+876] intron included	P3	*Bianchi et al., Gene 2009*
P254	[-254/+876] intron included		*This study*
P195	[-195/+876] intron included		*This study*
P123	[-123/+876] intron included		*This study*
P84	[-94/+876] intron included		*This study*
P37	[-37/+876] intron included	P3 Δ[-371/-38] nt construct	*Bianchi et al., PLoS One 2013*
P916-int	[-916/+4] intron excluded	P4	*Bianchi et al., Gene 2009*
P535-int	[-535/+4] intron excluded	P5	*Bianchi et al., Gene 2009*
P371-int	[-371/+4] intron excluded	P6	*Bianchi et al., Gene 2009*
P371+chimeric int	[-371/+4] + chimeric intron	P7+chimeric intron	*Bianchi et al., Gene 2009*
pGL3-Basic	empty (promoter-less) vector	pGL3-Basic	*Bianchi et al., Gene 2009*
Mutagenized constructs			
P916 wt	wild type sequence	P1 (FR1-2-6)	*Crinelli et al., PLoS One 2015*
P916 HSF mut a	upstream HSF1/2 sites mutagenized	P1mut FR1-2	*Crinelli et al., PLoS One 2015*
P916 HSF mut b	proximal HSF1/2 site mutagenized	P1mut FR6	*Crinelli et al., PLoS One 2015*
P916 HSF mut a-b	both upstream and proximal HSF1/2 sites mutagenized		*This paper*
P371 wt	wild type sequence	P3	*Bianchi et al., Gene 2009*
P371 Sp1 mut a	first intronic Sp1 site mutagenized	Sp1 mut a	*Bianchi et al., PLoS One 2013*
P371 Sp1 mut b	second intronic Sp1 site mutagenized	Sp1 mut b	*Bianchi et al., PLoS One 2013*
P371 Sp1 mut c	third intronic Sp1 site mutagenized	Sp1 mut c	*Bianchi et al., PLoS One 2013*
P371 Sp1 mut d	fourth intronic Sp1 site mutagenized	Sp1 mut d	*Bianchi et al., PLoS One 2013*
P371 Sp1 mut a-d	all intronic Sp1 sites mutagenized	Sp1 mut a-d	*Bianchi et al., PLoS One 2013*
P371 YY1 mut a	first intronic YY1 site mutagenized	YY1 mut e	*Bianchi et al., PLoS One 2013*
P371 YY1 mut b	second intronic YY1 site mutagenized	YY1 mut f	*Bianchi et al., PLoS One 2013*
P371 YY1 mut a-b	all intronic YY1 sites mutagenized	YY1 mut e-f	*Bianchi et al., PLoS One 2013*

To make this part more understandable for readers, we have provided for each plasmid construct both the name by which it is referred to in this paper and the name used in previous publications (see REFERENCE column).

5.7 References

1. Hershko, A. & Ciechanover, A. The ubiquitin system. *Annu. Rev. Biochem.* **67**, 425–479 (1998).

2. Finley, D., Ciechanover, A. & Varshavsky, A. Ubiquitin as a central cellular regulator. *Cell* **116**, S29–32 (2004).

3. Finley, D., Bartel, B. & Varshavsky, A. The tails of ubiquitin precursors are ribosomal proteins whose fusion to ubiquitin facilitates ribosome biogenesis. *Nature* **338**, 394–401 (1989).

4. Hochstrasser, M. Origin and function of ubiquitin-like proteins. *Nature* **458**, 422–429, https://doi.org/10.1038/nature07958 (2009).

5. Reyes-Turcu, F. E., Ventii, K. H. & Wilkinson, K. D. Regulation and cellular roles of ubiquitin-specific deubiquitinating enzymes. *Annu. Rev. Biochem.* **78**, 363–397, https://doi.org/10.1146/annurev.biochem.78.082307.091526 (2009).

6. Wiborg, O. *et al*. The human ubiquitin multigene family: some genes contain multiple directly repeated ubiquitin coding sequences. *EMBO J.* **4**, 755–759 (1985).

7. Baker, R. T. & Board, P. G. The human ubiquitin-52 amino acid fusion protein gene shares several structural features with mammalian ribosomal protein genes. *Nucleic Acids Res.* **19**, 1035–1040 (1991).

8. Redman, K. & Rechsteiner, M. Identification of the long ubiquitin extension as ribosomal protein S27a. *Nature* **338**, 438–440 (1989).

9. Ryu, K. Y. *et al*. The mouse polyubiquitin gene UbC is essential for fetal liver development, cell-cycle progression and stress tolerance. *EMBO J.* **26**, 2693–2706 (2007).

10. Ryu, K. Y., Park, H., Rossi, D. J., Weissman, I. L. & Kopito, R. R. Perturbation of the hematopoietic system during embryonic liver development due to disruption of polyubiquitin gene Ubc in mice. *PLoS One* **7**, e32956, https://doi.org/10.1371/journal.pone.0032956 (2012).

11. Ryu, K. Y. *et al*. The mouse polyubiquitin gene Ubb is essential for meiotic progression. *Mol. Cell. Biol.* **28**, 1136–1146 (2008).

12. Lim, D., Park, C. W., Ryu, K. Y. & Chung, H. Disruption of the polyubiquitin gene Ubb causes retinal degeneration in mice. *Biochem. Biophys. Res. Commun.* **513**, 35–40, https://doi.org/10.1016/j.bbrc.2019.03.164 (2019).

13. Kaiser, S. E. *et al*. Protein standard absolute quantification (PSAQ) method for the measurement of cellular ubiquitin pools. *Nat. Methods* **8**, 691–696, https://doi.org/10.1038/nmeth.1649 (2011).

14. Park, C. W. & Ryu, K. Y. Cellular ubiquitin pool dynamics and homeostasis. *BMB Rep.* **47**, 475–482 (2014).

15. Kimura, Y. & Tanaka, K. Regulatory mechanisms involved in the control of ubiquitin homeostasis. *J. Biochem.* **147**, 793–798, https://doi.org/10.1093/jb/mvq044 (2010).

16. Bianchi, M., Crinelli, R., Arbore, V. & Magnani, M. Induction of ubiquitin C (UBC) gene transcription is mediated by HSF1: role of proteotoxic and oxidative stress. *FEBS Open Bio* **8**, 1471–1485, https://doi.org/10.1002/2211-5463.12484 (2018).

17. London, M. K., Keck, B. I., Ramos, P. C. & Dohmen, R. J. Regulatory mechanisms controlling biogenesis of ubiquitin and the proteasome. *FEBS Lett.* **567**, 259–264 (2004).

18. Hanna, J., Meides, A., Zhang, D. P. & Finley, D. A ubiquitin stress response induces altered proteasome composition. *Cell* **129**, 747–759 (2007).

19. Dantuma, N. P., Groothuis, T. A., Salomons, F. A. & Neefjes, J. A dynamic ubiquitin equilibrium couples proteasomal activity to chromatin remodeling. *J. Cell Biol.* **173**, 19–26 (2006).

20. Hanna, J., Leggett, D. S. & Finley, D. Ubiquitin depletion as a key mediator of toxicity by translational inhibitors. *Mol. Cell. Biol.* **23**, 9251–9261 (2003).

21. Peng, H. *et al*. Ubiquitylation of p62/sequestosome1 activates its autophagy receptor function and controls selective autophagy upon ubiquitin stress. *Cell Res.* **27**, 657–674, https://doi.org/10.1038/cr.2017.40 (2017).

22. Bond, U. & Schlesinger, M. J. Ubiquitin is a heat shock protein in chicken embryo fibroblasts. *Mol. Cell. Biol.* **5**, 949–956 (1985).

23. Gropper, R. *et al*. The ubiquitin-activating enzyme, E1, is required for stress-induced lysosomal degradation of cellular proteins. *J. Biol. Chem.* **266**, 3602–3610 (1991).

24. Oh, C., Park, S., Lee, E. K. & Yoo, Y. J. Downregulation of ubiquitin level via knockdown of polyubiquitin gene Ubb as potential cancer therapeutic intervention. *Sci. Rep.* **3**, 2623, https://doi.org/10.1038/srep02623 (2013).

25. Hallengren, J., Chen, P. C. & Wilson, S. M. Neuronal ubiquitin homeostasis. *Cell Biochem. Biophys.* **67**, 67–73, https://doi.org/10.1007/s12013-013-9634-4 (2013).

26. Han, S. W., Jung, B. K., Park, S. H. & Ryu, K. Y. Reversible Regulation of Polyubiquitin Gene UBC via Modified Inducible CRISPR/Cas9 System. *Int. J. Mol. Sci.* **20**, E3168, https://doi.org/10.3390/ijms20133168 (2019).

27. Vaden, J. H. *et al.* Chronic over-expression of ubiquitin impairs learning, reduces synaptic plasticity, and enhances GRIA receptor turnover in mice. *J. Neurochem.* **148**, 386–399, https://doi.org/10.1111/jnc.14630 (2019).

28. Crinelli, R. *et al.* Ubiquitin over-expression promotes E6AP autodegradation and reactivation of the p53/MDM2 pathway in HeLa cells. *Mol. Cell. Biochem.* **318**, 129–145, https://doi.org/10.1007/s11010-008-9864-8 (2008).

29. Akutsu, M., Dikic, I. & Bremm, A. Ubiquitin chain diversity at a glance. *J. Cell Sci.* **129**, 875–880, https://doi.org/10.1242/jcs.183954 (2016).

30. Ravid, T. & Hochstrasser, M. Diversity of degradation signals in the ubiquitin-proteasome system. *Nat. Rev. Mol. Cell. Biol.* **9**, 679–690, https://doi.org/10.1038/nrm2468 (2008).

31. Mukhopadhyay, D. & Riezman, H. Proteasome-independent functions of ubiquitin in endocytosis and signaling. *Science* **315**, 201–205 (2007).

32. Hodgins, R. R., Ellison, K. S. & Ellison, M. J. Expression of a ubiquitin derivative that conjugates to protein irreversibly produces phenotypes consistent with a ubiquitin deficiency. *J. Biol. Chem.* **267**, 8807–8812 (1992).

33. Palma, L., Crinelli, R., Bianchi, M. & Magnani, M. De-ubiquitylation is the most critical step in the ubiquitin-mediated homeostatic control of the NF-kappaB/IKK basal activity. *Mol. Cell. Biochem.* **331**, 69–80, https://doi.org/10.1007/s11010-009-0146-x (2009).

34. Amerik, A. Y., Swaminathan, S., Krantz, B. A., Wilkinson, K. D. & Hochstrasser, M. *In vivo* disassembly of free polyubiquitin chains by yeast Ubp14 modulates rates of protein degradation by the proteasome. *EMBO J.* **16**, 4826–4838, https://doi.org/10.1093/emboj/16.16.4826 (1997).

35. Sloper-Mould, K. E., Jemc, J. C., Pickart, C. M. & Hicke, L. Distinct functional surface regions on ubiquitin. *J. Biol. Chem.* **276**, 30483–30489 (2001).

36. Spence, J., Sadis, S., Haas, A. L. & Finley, D. A ubiquitin mutant with specific defects in DNA repair and multiubiquitination. *Mol. Cell. Biol.* **15**, 1265–1273 (1995).

37. Galan, J. M. & Haguenauer-Tsapis, R. Ubiquitin lys63 is involved in ubiquitination of a yeast plasma membrane protein. *EMBO J.* **16**, 5847–5854 (1997).

38. Bianchi, M., Crinelli, R., Giacomini, E., Carloni, E. & Magnani, M. A potent enhancer element in the 5'-UTR intron is crucial for transcriptional regulation of the human ubiquitin C gene. *Gene* **448**, 88–101, https://doi.org/10.1016/j.gene.2009.08.013 (2009).

39. Bianchi, M. *et al.* Yin Yang 1 intronic binding sequences and splicing elicit intron-mediated enhancement of ubiquitin C gene expression. *PLoS One* **8**, e65932, https://doi.org/10.1371/journal.pone.0065932 (2013).

40. Deroo, B. J. & Archer, T. K. Proteasome inhibitors reduce luciferase and beta-galactosidase activity in tissue culture cells. *J. Biol. Chem.* **277**, 20120–20123 (2002).

41. Becker, J. P., Clemens, J. R., Theile, D. & Weiss, J. Bortezomib and ixazomib protect firefly luciferase from degradation and can flaw respective reporter gene assays. *Anal. Biochem.* **509**, 124–129, https://doi.org/10.1016/j.ab.2016.06.015 (2016).

42. Crinelli, R. *et al.* Molecular Dissection of the Human Ubiquitin C Promoter Reveals Heat Shock Element Architectures with Activating and Repressive Functions. *PLoS One* **10**, e0136882, https://doi.org/10.1371/journal.pone.0136882 (2015).

43. Marinovic, A. C., Zheng, B., Mitch, W. E. & Price, S. R. Ubiquitin (UbC) expression in muscle cells is increased by glucocorticoids through a mechanism involving Sp1 and MEK1. *J. Biol. Chem.* **277**, 16673–16681 (2002).

44. Raychaudhuri, S. *et al.* Interplay of acetyltransferase EP300 and the proteasome system in regulating heat shock transcription factor 1. *Cell* **156**, 975–985, https://doi.org/10.1016/j.cell.2014.01.055 (2014).

45. Bonelli, M. A., Alfieri, R. R., Poli, M., Petronini, P. G. & Borghetti, A. F. Heat-induced proteasomic degradation of HSF1 in serumstarved human fibroblasts aging *in vitro*. *Exp. Cell Res.* **267**, 165–172 (2001).

46. Xing, H., Hong, Y. & Sarge, K. D. PEST sequences mediate heat shock factor 2 turnover by interacting with the Cul3 subunit of the Cul3-RING ubiquitin ligase. *Cell Stress Chaperones* **15**, 301–308, https://doi.org/10.1007/s12192-009-0144-7 (2010).

47. Jeong, H. M., Lee, S. H., Yum, J., Yeo, C. Y. & Lee, K. Y. Smurf2 regulates the degradation of YY1. *Biochim. Biophys. Acta.* **1843**, 2005–2011, https://doi.org/10.1016/j.bbamcr.2014.04.023 (2014).

48. Nakagawa, T. *et al.* Deubiquitylation of histone H2A activates transcriptional initiation via trans-histone cross-talk with H3K4 diand trimethylation. *Genes Dev.* **22**, 37–49, https://doi.org/10.1101/gad.1609708 (2008).

49. Zhou, W. *et al*. Histone H2A monoubiquitination represses transcription by inhibiting RNA polymerase II transcriptionale longation. *Mol. Cell* **29**, 69–80, https://doi.org/10.1016/j.molcel.2007.11.002 (2008).

50. Fierz, B. *et al*. Histone H2B ubiquitylation disrupts local and higher-order chromatin compaction. *Nat. Chem. Biol.* **7**, 113–119, https://doi.org/10.1038/nchembio.501 (2011).

51. Wu, L., Li, L., Zhou, B., Qin, Z. & Dou, Y. H2B ubiquitylation promotes RNA Pol II processivity via PAF1 and pTEFb. *Mol. Cell* **54**, 920–931, https://doi.org/10.1016/j.molcel.2014.04.013 (2014).

52. Bianchi, M. *et al*. Dynamic transcription of ubiquitin genes under basal and stressful conditions and new insights into the multiple UBC transcript variants. *Gene* **573**, 100–109, https://doi.org/10.1016/j.gene.2015.07.030 (2015).

53. Vihervaara, A. *et al*. Transcriptional response to stress in the dynamic chromatin environment of cycling and mitotic cells. *Proc. Natl. Acad. Sci. USA* **110**, E3388–E3397, https://doi.org/10.1073/pnas.1305275110 (2013).

54. Radici, L., Bianchi, M., Crinelli, R. & Magnani, M. Ubiquitin C gene: Structure, function, and transcriptional regulation. *Advances in Bioscience and Biotechnology* **4**, 1057–1062, https://doi.org/10.4236/abb.2013.412141 (2013).

55. Oshikawa, K., Matsumoto, M., Oyamada, K. & Nakayama, K. I. Proteome-wide identification of ubiquitylation sites by conjugation of engineered lysine-less ubiquitin. *J. Proteome Res.* **11**, 796–807, https://doi.org/10.1021/pr200668y (2012).

56. Huang, T., Li, J. & Byrd, R. A. Solution structure of lysine-free (K0) ubiquitin. *Protein Sci.* **23**, 662–667, https://doi.org/10.1002/pro.2450 (2014).

57. Björk, J. K. & Sistonen, L. Regulation of the members of the mammalian heat shock factor family. *FEBS J.* **277**, 4126–4139 (2010).

58. Dayalan Naidu, S. & Dinkova-Kostova, A. T. Regulation of the mammalian heat shock factor 1. *FEBS J.* **284**, 1606–1627, https://doi.org/10.1111/febs.13999 (2017).

59. Anckar, J. & Sistonen, L. Regulation of HSF1 function in the heat stress response: implications in aging and disease. *Annu. Rev. Biochem.* **80**, 1089–1115, https://doi.org/10.1146/annurev-biochem-060809-095203 (2011).

60. Spengler, M. L., Guo, L. W. & Brattain, M. G. Phosphorylation mediates Sp1 coupled activities of proteolytic processing, desumoylation and degradation. *Cell Cycle* **7**, 623–630 (2008).

61. Mir, R., Sharma, A., Pradhan, S. J. & Galande, S. Regulation of Transcription Factor SP1 by the β-Catenin Destruction Complex Modulates Wnt Response. *Mol. Cell. Biol.* **38**, e00188–18, https://doi.org/10.1128/MCB.00188-18 (2018).

62. Mimnaugh, E. G., Chen, H. Y., Davie, J. R., Celis, J. E. & Neckers, L. Rapid deubiquitination of nucleosomal histones in human tumor cells caused by proteasome inhibitors and stress response inducers: effects on replication, transcription, translation, and the cellular stress response. *Biochemistry* **36**, 14418–14429 (1997).

63. Ben Yehuda, A. *et al*. Ubiquitin Accumulation on Disease Associated Protein Aggregates Is Correlated with Nuclear Ubiquitin Depletion, Histone De-Ubiquitination and Impaired DNA Damage Response. *PLoS One* **12**, e0169054, https://doi.org/10.1371/journal.pone.0169054 (2017).

64. Milligan, L. *et al*. RNA polymerase II stalling at pre-mRNA splice sites is enforced by ubiquitination of the catalytic subunit. *Elife* **6**, e27082, https://doi.org/10.7554/eLife.27082.001 (2017).

65. Chanarat, S. & Mishra, S. K. Emerging Roles of Ubiquitin-like Proteins in Pre-mRNA Splicing. *Trends Biochem. Sci.* **43**, 896–907, https://doi.org/10.1016/j.tibs.2018.09.001 (2018).

66. Thakran, P. *et al*. Sde2 is an intron-specific pre-mRNA splicing regulator activated by ubiquitin-like processing. *EMBO J.* **37**, 89–101, https://doi.org/10.15252/embj.201796751 (2018).

67. Sayani, S. & Chanfreau, G. F. Sequential RNA degradation pathways provide a fail-safe mechanism to limit the accumulation of unspliced transcripts in Saccharomyces cerevisiae. *RNA* **18**, 1563–1572, https://doi.org/10.1261/rna.033779 (2012).

68. Hackmann, A. *et al*. Quality control of spliced mRNAs requires the shuttling SR proteins Gbp2 and Hrb1. *Nat. Commun.* **5**, 3123, https://doi.org/10.1038/ncomms4123 (2014).

69. Kilchert, C. *et al*. Regulation of mRNA Levels by Decay-Promoting Introns that Recruit the Exosome Specificity Factor Mmi1. *Cell Rep.* **13**, 2504–2515, https://doi.org/10.1016/j.celrep.2015.11.026 (2015).

70. Lim, K. L. *et al*. Parkin mediates nonclassical, proteasomal-independent ubiquitination of synphilin-1: implications for Lewy body formation. *J. Neurosci.* **25**, 2002–2009, https://doi.org/10.1523/JNEUROSCI.4474-04.2005 (2005).

71. Livak, K. J. & Schmittgen, T. D. Analysis of relative gene expression data using real-time quantitative PCR and the 2(-Delta Delta C(T)) Method. *Methods* **25**, 402–408 (2001).

72. Roberts, T. C. *et al*. Quantification of nascent transcription by bromouridine immunocapture nuclear run-on RT-qPCR. *Nat. Protoc.* **10**, 1198–1211, https://doi.org/10.1038/nprot.2015.076 (2015).

97

Acknowledgements

Author contributions

M.B. and R.C. conceived and designed the research. M.B., R.C., E.G., E.C., L.R., E.S.S. and F.T. performed the experiments and analyzed the data. M.M. contributed reagents/materials. M.B. wrote the paper. All authors took part in discussions, reviewed and approved the final manuscript.

Competing interests

The authors declare no competing interests.

Additional information

Supplementary information is available for this paper at https://doi.org/10.1038/s41598-019-54973-7.

Correspondence and requests for materials should be addressed to M.B.

Reprints and permissions information is available at www.nature.com/reprints.

Publisher's note Springer Nature remains neutral with regard to jurisdictional claims in published maps and institutional affiliations.

CHAPTER 6: CONCLUSIONS

Gastric cancer is one of the most lethal and common types of tumor worldwide. Late stage patients exhibit low 5-year survival rate and early detection of patients greatly improves their chances of survival. For these reasons, there is a need for new gastric cancer biomarkers and therapeutic targets; however, molecular knowledge regarding the processes of tumorigenesis and metastatization of gastric cancer are still lacking.

In light of our lab's previous background on ubiquitin studies, we compared the asset of the ubiquitin system in two gastric cancer cell lines: the primary line 23132/87 and the metastatic line MKN45.

MKN45 exhibit higher expression levels of three out of the four ubiquitin-coding genes *UBC*, *UBB* and *RPS27A*, but the total ubiquitin protein content and its distribution between the free and conjugated ubiquitin pools was similar in the two cell lines. This discrepancy could be partially explained by the higher proteasomal activity displayed by MKN45, which could therefore have an ubiquitin turnover greater than 23132/87.

The protein levels of HSF1, YY1 and SP1, three transcription factors known to regulate ubiquitin gene expression, were also examined: MKN45 displayed higher levels of YY1 and lower levels of both HSF1 and SP1. Their involvement in gastric cancer ubiquitin gene expression was however excluded, as siRNA-mediated knockdown of either transcription factor did not impact the transcript levels of any ubiquitin gene in both cell lines.

Next, siRNA-mediated knockdown of *UBC* and *UBB* was performed, singularly or in combination, as this approach has been successful in reducing tumor cell proliferation and viability as well as reducing tumor xenograph growth. All conditions tested effective and reduced the ubiquitin content in both cell lines. Interestingly, *UBC* knockdown elicited a significant *UBB* upregulation in 23132/87, which was not found in MKN45; while *UBB* knockdown did not result in *UBC* upregulation in 23132/87 nor MKN45.

Simultaneous knockdown of *UBB* and *UBC* produced a reduction in 23132/87 cell viability due to apoptosis activation, as demonstrated by the increase in Fas protein levels and the concomitant decrease of inactive caspase-3 levels. Conversely, MKN45 survivability was not affected by the double knockdown of *UBB* and *UBC*.

Based on our results, we propose a pro-survival role for *UBB* and *UBC* in the primary line 23132/87, as it is more reliant on its endogenous ubiquitin levels for survival and less resistant to ubiquitin expression impairment than the metastatic line MKN45.

CHAPTER 7: REFERENCES

Akua T, Berezin I, Shaul O. The leader intron of AtMHX can elicit, in the absence of splicing, low-level intron-mediated enhancement that depends on the internal intron sequence. BMC Plant Biol. 2010;10:93. doi:10.1186/1471-2229-10-93

Ambroggio XI, Rees DC, Deshaies RJ. JAMM: a metalloprotease-like zinc site in the proteasome and signalosome. Plos Biology. 2004;2(1):E2. doi:10.1371/journal.pbio.0020002.

American Cancer Society 2020 – Cancer Facts & Figures 2020 https://www.cancer.org/research/cancer-facts-statistics/all-cancer-facts-figures/cancer-facts-figures-2020.html

Ando T, Goto Y, Maeda O et al. Causal role of Helicobacter pylori infection in gastric cancer. World J Gastroenterol. 2006;12(2):181-186. doi:10.3748/wjg.v12.i2.181

Ang TL, Fock KM. Clinical epidemiology of gastric cancer. Singapore Med J. 2014 Dec;55(12):621-8. doi:10.11622/smedj.2014174.

Aravind L, Koonin EV. The U-box is a modified RING finger - a common domain in ubiquitination. Current Biology 2000;10(4):132-134. doi:10.1016/S0960-9822(00)00398-5

Arellano-Garcia ME, Misuno K, Tran SD et al. Interferon-γ induces immunoproteasomes and the presentation of MHC I-associated peptides on human salivary gland cells. Plos one. 2014;9(8):e102878. doi:10.1371/journal.pone.0102878.

Ayatollahi H, Tavassoli A, Jafarian AH et al. KRAS Codon 12 and 13 Mutations in Gastric Cancer in the Northeast Iran. Iran J Pathol. 2018;13(2):167-172. PMID: 30697286.

Bader M, Steller H. Regulation of cell death by the ubiquitin-proteasome system. Curr Opin Cell Biol. 2009;21(6):878-884. doi:10.1016/j.ceb.2009.09.005

Balakrishnan M, George R, Sharma A et al. Changing Trends in Stomach Cancer Throughout the World. Curr Gastroenterol Rep. 2017 Aug;19(8):36. doi:10.1007/s11894-017-0575-8.

Barchi LC, Yagi OK, Jacob CE et al. Predicting recurrence after curative resection for gastric cancer: External validation of the Italian Research Group for Gastric Cancer (GIRCG) prognostic scoring system. Euro. Jour. Surg. Onc. 2016;42(1):123-131. doi:10.1016/j.ejso.2015.08.164.

Bard JAM, Goodall EA, Greene ER et al. Structure and Function of the 26S Proteasome. Annu Rev Biochem. 2018;87:697-724. doi:10.1146/annurev-biochem-062917-011931.

Bertrand MJ, Milutinovic S, Dickson KM et al. cIAP1 and cIAP2 facilitate cancer cell survival by functioning as E3 ligases that promote RIP1 ubiquitination. Mol Cell. 2008;30(6):689-700. doi:10.1016/j.molcel.2008.05.014.

Bianchi M, Crinelli R, Arbore V et al. Induction of ubiquitin C (UBC) gene transcription is mediated by HSF1: role of proteotoxic and oxidative stress. FEBS Open Bio 2018;8:1471–1485. doi:10.1002/2211-5463.12484.

Bianchi M, Crinelli R, Giacomini E et al. A potent enhancer element in the 5'-UTR intron is crucial for transcriptional regulation of the human ubiquitin C gene. Gene. 2009 Dec 1;448(1):88-101. doi:10.1016/j.gene.2009.08.013.

Bianchi M, Crinelli R, Giacomini E et al. Yin Yang 1 intronic binding sequences and splicing elicit intron-mediated enhancement of ubiquitin C gene expression. PLoS One. 2013;8(6):e65932. doi:10.1371/journal.pone.0065932

Bianchi M, Crinelli R, Giacomini E et al. A negative feedback mechanism links UBC gene expression to ubiquitin levels by affecting RNA splicing rather than transcription. Sci Rep. 2019;9(1):18556. doi:10.1038/s41598-019-54973-7.

Bianchi M, Giacomini E, Crinelli R et al. Dynamic transcription of ubiquitin genes under basal and stressful conditions and new insights into the multiple UBC transcript variants. Gene. 2015;573(1):100-9. doi:10.1016/j.gene.2015.07.030.

Borissenko L, Groll M. 20S proteasome and its inhibitors: crystallographic knowledge for drug development. Chem Rev. 2007;107(3):687-717. doi:10.1021/cr0502504.

Bray F, Ferlay J, Soerjomataram I et al. Global cancer statistics 2018: GLOBOCAN estimates of incidence and mortality worldwide for 36 cancers in 185 countries. CA Cancer J Clin. 2018;68(6):394-424. doi:10.3322/caac.21492. Erratum in: CA Cancer J Clin. 2020 Jul;70(4):313.

Broemer M, Meier P. Ubiquitin-mediated regulation of apoptosis. Trends in Cell Biology. 2009;19(3)130-140. doi:10.1016/j.tcb.2009.01.004

Cancer Genome Atlas Research Network. Comprehensive molecular characterization of gastric adenocarcinoma. Nature. 2014; http://dx.doi.org/10.1038/nature13480.

Carneiro F. Hereditary gastric cancer. Pathologe 2012;33(Suppl. 2):231–234. doi:10.1007/s00292-012-1677-6.

Correa P. Gastric cancer: overview. Gastroenterol Clin North Am. 2013;42(2):211-7. doi:10.1016/j.gtc.2013.01.002.

Corso G, Velho S, Paredes J et al: Oncogenic mutations in gastric cancer with microsatellite instability. Eur J Cancer 2011;47:443–451. doi:10.1016/j.ejca.2010.09.008

Crinelli R, Bianchi M, Menotta M et al. Ubiquitin over-expression promotes E6AP autodegradation and reactivation of the p53/MDM2 pathway in HeLa cells. Mol Cell Biochem. 2008;318(1-2):129-45. doi:10.1007/s11010-008-9864-8.

Crinelli R, Bianchi M, Radici L et al. Molecular Dissection of the Human Ubiquitin C Promoter Reveals Heat Shock Element Architectures with Activating and Repressive Functions. PLoS One. 2015;10(8):e0136882. doi:10.1371/journal.pone.0136882.

D'Angelica M, Gonen M, Brennan M et al. Patterns of initial recurrence in completely resected gastric adenocarcinoma. Annals of Surgery. 2004;240(5):808-816. doi: 10.1097/01.sla.0000143245.28656.15.

Da Silva-Ferrada E, Torres-Ramos M, Aillet F et al. Role of monoubiquitylation on the control of IκBα degradation and NF-κB activity. PLoS One. 2011;6(10):e25397. doi:10.1371/journal.pone.0025397

Deveraux QL, Takahashi R, Salvesen GS et al. X-linked IAP is a direct inhibitor of cell-death proteases. Nature. 1997;388(6639):300-4. doi:10.1038/40901.

Duckett CS, Li F, Wang Y et al. Human IAP-like protein regulates programmed cell death downstream of Bcl-xL and cytochrome c. Mol Cell Biol. 1998;18(1):608-615. doi:10.1128/mcb.18.1.608

Duncan LM, Piper S, Dodd RB et al. Lysine-63-linked ubiquitination is required for endolysosomal degradation of class I molecules. EMBO J. 2006;25(8):1635-45. doi: 10.1038/sj.emboj.7601056.

Fang DC, Luo YH, Yang SM et al. Mutation analysis of APC gene in gastric cancer with microsatellite instability. World J Gastroenterol. 2002;8(5):787-791. doi:10.3748/wjg.v8.i5.787

Faesen AC, Luna-Vargas MP, Geurink PP et al. The differential modulation of USP activity by internal regulatory domains, interactors and eight ubiquitin chain types. Chem Biol. 2011;18(12):1550-61. doi:10.1016/j.chembiol.2011.10.017.

Feldman M, Friedman LS, Brandt LJ. Sleisenger & Fordtran's Gastrointestinal and Liver Disease: Pathophysiology/Diagnosis/Management; 11th edition, (2020); eds. ELSEVIER SAUNDERS.

Fenoglio-Preiser CM, Wang J, Stemmermann GN et al. 2003 – TP53 and gastric cancer: a review Human Mutation 2003;21(3):258–270. doi:10.1002/humu.10180

Fernandes R, Ramalho J, Pereira P. Oxidative stress upregulates ubiquitin proteasome pathway in retinal endothelial cells. Mol Vis. 2006;12:1526-35. PMID: 17167411.

Finley D. Recognition and processing of ubiquitin-protein conjugates by the proteasome. Annu Rev Biochem. 2009;78:477-513. doi:10.1146/annurev.biochem.78.081507.101607.

Finley D, Ozkaynak E, Varshavsky A. The yeast polyubiquitin gene is essential for resistance to high temperatures, starvation, and other stresses. Cell. 1987;48(6):1035-46. doi:10.1016/0092-8674(87)90711-2.

Fleisher AS, Esteller M, Wang S et al. Hypermethylation of the hMLH1 gene promoter in human gastric cancers with microsatellite instability. Cancer Res. 1999;59(5):1090-5. PMID: 10070967.

Forman D, Newell DG, Fullerton F et al. Association between infection with Helicobacter pylori and risk of gastric cancer: evidence from a prospective investigation. BMJ. 1991;302(6788):1302-1305. doi:10.1136/bmj.302.6788.1302.

Fornace AJ Jr, Alamo I Jr, Hollander MC et al. Ubiquitin mRNA is a major stress-induced transcript in mammalian cells. Nucleic Acids Res. 1989;17(3):1215-1230. doi:10.1093/nar/17.3.1215

Freedman ND, Abnet CC, Leitzmann MF et al. A Prospective Study of Tobacco, Alcohol, and the Risk of Esophageal and Gastric Cancer Subtypes. American Journal of Epidemiolog. 2007;165(12):1424–1433 doi:10.1093/aje/kwm051

Freudenthal BD, Gakhar L, Ramaswamy S et al. 2010. Structure of monoubiquitinated PCNA and implications for translesion synthesis and DNA polymerase exchange. Nat. Struct. Mol. Biol. 2010;17(4):479–484. doi:10.1038/nsmb.1776.

Gaddy JA, Radin JN, Loh JT et al. High dietary salt intake exacerbates Helicobacter pylori-induced gastric carcinogenesis. Infect Immun. 2013;81(6):2258-67. doi:10.1128/IAI.01271-12.

Gilberto S, Peter M. Dynamic ubiquitin signaling in cell cycle regulation. J Cell Biol. 2017;216(8):2259-2271. doi:10.1083/jcb.201703170.

Goldberg AL, Cascio P, Saric T et al. The importance of the proteasome and subsequent proteolytic steps in the generation of antigenic peptides. Mol Immunol. 2002;39(3-4):147-64. doi:10.1016/s0161-5890(02)00098-6.

Goldstein G, Scheid M, Hammerling U et al. Isolation of a polypeptide that has lymphocyte-differentiating properties and is probably represented universally in living cells. Proc Natl Acad Sci USA. 1975;72(1):11-5. doi:10.1073/pnas.72.1.11.

Graber TE, Holcik M. Distinct roles for the cellular inhibitors of apoptosis proteins 1 and 2. Cell Death Dis. 2011;2(3):e135. doi:10.1038/cddis.2011.20.

Grabsch H, Sivakumar S, Gray S et al. HER2 expression in gastric cancer: rare, heterogeneous and of no prognostic value – conclusions from 924 cases of two independent series. Cell Oncol 2010;32(1-2): 57–65. doi:10.3233/CLO-2009-0497.

Grabsch HI, Tan P. Gastric cancer pathology and underlying molecular mechanisms. Dig Surg. 2013;30(2):150-8. doi:10.1159/000350876.

Gravalos C, Jimeno A. HER2 in gastric cancer: a new prognostic factor and a novel therapeutic target. Ann Oncol 2008;19(9):1523-9. doi:10.1093/annonc/mdn169.

Green D (2011). Means to an End: Apoptosis and other Cell Death Mechanisms. Cold Spring Harbor, NY: Cold Spring Harbor Laboratory Press. ISBN 978-0-87969-888-1.

Groll M, Ditzel L, Löwe J et al. Structure of 20S proteasome from yeast at 2.4 A resolution. Nature. 1997;386(6624):463-71. doi:10.1038/386463a0.

Grossman SR, Deato ME, Brignone C et al. Polyubiquitination of p53 by a ubiquitin ligase activity of p300. Science. 2003;300(5617):342-4. doi:10.1126/science.1080386

Guo HJ, Tadi P. Biochemistry, ubiquitination. NCBI Bookshelf. A service of the National Library of Medicine, National Institutes of Health. StatPearls Publishing. 2020.

Gylling A, Abdel-Rahman WM, Juhola M, et al. Is gastric cancer part of the tumour spectrum of hereditary non-polyposis colorectal cancer? A molecular genetic study. Gut. 2007;56(7):926-933. doi:10.1136/gut.2006.114876

Hanna J, Leggett DS, Finley D. Ubiquitin depletion as a key mediator of toxicity by translational inhibitors. Mol Cell Biol. 2003;23(24):9251-9261. doi:10.1128/mcb.23.24.9251-9261.2003

Hirano T. Chromosome Dynamics during Mitosis. Cold Spring Harb Perspect Biol. 2015;7(6):a015792. doi:10.1101/cshperspect.a015792.

Horii A, Nakatsuru S, Miyoshi Y et al. The APC gene, responsible for familial adenomatous polyposis, is mutated in human gastric cancer. Cancer Res. 1992;52(11):3231-3. PMID: 1317264.

Hu B, El Hajj N, Sittler S et al. Gastric cancer: classification, histology and application of molecular pathology. Journ. Gastroint. Onc. 2012;3(3). doi:10.3978/j.issn.2078-6891.2012.021

Huang TT, Nijman SM, Mirchandani KD et al. 2006. Regulation of monoubiquitinated PCNA by DUB autocleavage. Nat. Cell Biol. 2006;8(4):339–47 doi:10.1038/ncb1378.

Hudler P. Genetic aspects of gastric cancer instability. Scientific World Journal. 2012;2012:761909. doi:10.1100/2012/761909.

IARC Working Group on the Evaluation of Carcinogenic Risk to Humans; 1994 - IARC Monographs on the Evaluation of Carcinogenic Risks to Humans, No. 61 - Schistosomes, Liver Flukes and Helicobacter pylori.

IARC Working Group on the Evaluation of Carcinogenic Risk to Humans; 2012 - IARC Monographs on the Evaluation of Carcinogenic Risks to Humans, No. 100 – personal habits and indoor combustion.

Iizasa H, Nanbo A, Nishikawa J et al. Epstein-Barr Virus (EBV)-associated gastric carcinoma. Viruses. 2012;4(12):3420-39. doi:10.3390/v4123420.

Iwamatsu H, Nishikura K, Watanabe H et al. Heterogeneity of p53 mutational status in the superficial spreading type of early gastric carcinoma. Gastric Cancer. 2001;4(1):20–26. doi:10.1007/s101200100012.

Jackson SP, Durocher D. Regulation of DNA damage responses by ubiquitin and SUMO. Mol Cell. 2013;49(5):795-807. doi: 10.1016/j.molcel.2013.01.017.

Jin HS, Lee DH, Kim DH et al. cIAP1, cIAP2, and XIAP act cooperatively via nonredundant pathways to regulate genotoxic stress-induced nuclear factor-kappaB activation. Cancer Res. 2009;69(5):1782-91. doi:10.1158/0008-5472.CAN-08-2256.

Johnson ES, Ma PC, Ota IM et al. A proteolytic pathway that recognizes ubiquitin as a degradation signal. J. Biol. Chem. 1995;270:17442–56. doi:10.1074/jbc.270.29.17442

Kaiser S, Riley B, Shaler T et al. Protein standard absolute quantification (PSAQ) method for the measurement of cellular ubiquitin pools. Nat Methods 8, 691–696 (2011). doi:10.1038/nmeth.1649

Karimi P, Islami F, Anandasabapathy S et al. Gastric cancer: descriptive epidemiology, risk factors, screening, and prevention. Cancer Epidemiol Biomarkers Prev. 2014;23(5):700-13. doi:10.1158/1055-9965.EPI-13-1057.

Katai H, Ishikawa T, Akazawa K. Registration Committee of the Japanese Gastric Cancer Association. Five-year survival analysis of surgically resected gastric cancer cases in Japan: a retrospective analysis of more than 100,000 patients from the nationwide registry of the Japanese Gastric Cancer Association (2001-2007). Gastric Cancer. 2018;21(1):144-154. doi:10.1007/s10120-017-0716-7.

Keller I, Vosyka O, Takenaka S et al. Regulation of Immunoproteasome Function in the Lung. Sci Rep. 2015;5:10230. doi:10.1038/srep10230

Koegl M, Hoppe T, Schlenker S et al. A novel ubiquitination factor, E4, is involved in multiubiquitin chain assembly. Cell. 1999;96(5):635-44. doi:10.1016/s0092-8674(00)80574-7.

Kerscher O, Felberbaum R, Hochstrasser M. Modification of proteins by ubiquitin and ubiquitin-like proteins. Annu Rev Cell Dev Biol. 2006;22:159-80. doi:10.1146/annurev.cellbio.22.010605.093503.

Keusekotten K, Elliott PR, Glockner L et al. OTULIN antagonizes LUBAC signaling by specifically hydrolyzing Met1-linked polyubiquitin. Cell. 2013;153(6):1312–26. doi:10.1016/j.cell.2013.05.014.

Kim HC, Huibregtse HM. Polyubiquitination by HECT E3s and the Determinants of chain type specificity. Molecular and Cellular Biology. 2009;29(12):3307-3318. doi:10.1128/mcb.00240-09.

Kimura HJ, Chen CY, Tzou SC et al. Immunoproteasome overexpression underlies the pathogenesis of thyroid oncocytes and primary hypothyroidism: studies in humans and mice. PLoS One. 2009;4(11):e7857. doi:10.1371/journal.pone.0007857.

Kimura Y, Tanaka K. Regulatory mechanisms involved in the control of ubiquitin homeostasis. Jour. Biochem. 2010;147(6):793-798. doi:10.1093/jb/mvq044

Komander D, Rape M. The ubiquitin code. Annu Rev Biochem. 2012;81:203-29. doi:10.1146/annurev-biochem-060310-170328.

Kloetzel P. Antigen processing by the proteasome. Nat Rev Mol Cell Biol. 2001;2: 179–188. doi:10.1038/35056572

Kravtsova-Ivantsiv Y, Cohen S, Ciechanover A. Modification by single ubiquitin moieties rather than polyubiquitination is sufficient for proteasomal processing of the p105 NF-kappaB precursor. Mol Cell. 2009;33(4):496-504. doi:10.1016/j.molcel.2009.01.023.

Lam YA, Xu W, DeMartino G et al. Editing of ubiquitin conjugates by an isopeptidase in the 26S proteasome. Nature. 1997;385:737–740. doi:10.1038/385737a0

Lazăr DC, Tăban S, Cornianu M et al. New advances in targeted gastric cancer treatment. World J Gastroenterol. 2016;22(30):6776-6799. doi:10.3748/wjg.v22.i30.6776

Lee BH, Lu Y, Prado M et al. USP14 deubiquitinates proteasome-bound substrates that are ubiquitinated at multiple sites. Nature. 2016;532:398–401. doi:10.1038/nature17433

Lee C, Prakash S, Matouschek A. Concurrent translocation of multiple polypeptide chains through the proteasomal degradation channel. J Biol Chem. 2002;277(38):34760-5. doi:10.1074/jbc.M204750200.

Lee KH, Lee JS, Suh C et al. Clinicopathologic significance of the K-ras gene codon 12 point mutation in stomach cancer. An analysis of 140 cases. Cancer. 1995;75(12):2794–2801. doi:10.1002/1097-0142(19950615)75:12<2794::aid-cncr2820751203>3.0.co;2-f.

Lee MJ, Lee BH, Hanna J et al. Trimming of ubiquitin chains by proteasome-associated deubiquitinating enzymes. Mol Cell Proteomics. 2011;10(5):R110.003871. doi:10.1074/mcp.R110.003871

Ley R, Balmanno K, Hadfield K et al. Activation of the ERK1/2 signaling pathway promotes phosphorylation and proteasome-dependent degradation of the BH3-only protein, Bim. J Biol Chem. 2003;278(21):18811-6. doi:10.1074/jbc.M301010200.

Li K, Luo H, Huang L et al. Microsatellite instability: a review of what the oncologist should know. Cancer Cell Int. 2020;20:16. doi:10.1186/s12935-019-1091-8.

Lim D, Park CW, Ryu KY et al. Disruption of the polyubiquitin gene Ubb causes retinal degeneration in mice. Biochem. Biophys. Res. Commun. 2019;513:35–40. doi:10.1016/j.bbrc.2019.03.164

Liu J, Shaik S, Dai X et al. Targeting the ubiquitin pathway for cancer treatment. Biochim Biophys Acta. 2015;1855(1):50-60. doi:10.1016/j.bbcan.2014.11.005.

Liu JB, Wu XM, Cai J et al. CpG island methylator phenotype and Helicobacter pylori infection associated with gastric cancer. World J Gastroenterol. 2012;18(36):5129-5134. doi:10.3748/wjg.v18.i36.5129

Liu XP, Tsushimi K, Tsushimi M et al. Expression of p53 protein as a prognostic indicator of reduced survival time in diffuse-type gastric carcinoma. Pathology International. 2001;51(6):440–444. doi:10.1046/j.1440-1827.2001.01216.x.

López-Mosqueda J, Dikic I. Deciphering functions of branched ubiquitin chains. Cell. 2014;157(4):767-9. doi:10.1016/j.cell.2014.04.026. PMID: 24813601.

Marinovic AC, Zheng B, Mitch WE et al. Ubiquitin (UbC) expression in muscle cells is in- creased by glucocorticoids through a mechanism involv- ing Sp1 and MEK1. J. Biol. Chem. 2002;277:16673 doi:10.1074/jbc.M200501200

Marrelli D, De Stefano A, de Manzoni G et al. Prediction of recurrence after radical surgery for gastric cancer: a scoring system obtained from a prospective multicenter study. Ann Surg. 2005;241(2):247-55. doi:10.1097/01.sla.0000152019.14741.97.

Matsumoto ML, Wickliffe KE, Dong KC et al. K11-Linked Polyubiquitination in Cell Cycle Control Revealed by a K11 Linkage-Specific Antibody. Molecular Cell. 2010;39(3):477-484. doi.org/10.1016/j.molcel.2010.07.001

McLean MH, El-Omar EM. Genetics of gastric cancer. Nat Rev Gastroenterol Hepatol. 2014;11(11):664-74. doi:10.1038/nrgastro.2014.143.

Metzger MB, Hristova VA, Weissman AM. HECT and RING finger families of E3 ubiquitin ligases at a glance. Journal of Cell Science. 2012;125: 531-537. doi:10.1242/jcs.091777

Mevissen TET, Komander D. Mechanisms of Deubiquitinase Specificity and Regulation. Annu Rev Biochem. 2017;86:159-192. doi:10.1146/annurev-biochem-061516-044916.

Moll UM, Petrenko U. The MDM2-p53 interaction. Mol Cancer Res. 2003;1(14):1001-1008. PMID: 14707283

Mukhopadhyay D, Riezman H. 2007. Proteasome-independent functions of ubiquitin in endocytosis and signaling. Science. 2007;315(5809):201-205. doi:10.1126/science.1127085.

Nakagawa T, Nakayama K. Protein monoubiquitylation: targets and diverse functions. Genes Cells. 2015;20(7):543-562. doi:10.1111/gtc.12250

Navon A, Goldberg AL. Proteins Are Unfolded on the Surface of the ATPase Ring before Transport into the Proteasome, Mol Cell. 2001;8:1339–49. doi:10.1016/S1097-2765(01)00407-5.

Nenoi M. Induced accumulation of polyubiquitin gene transcripts in HeLa cells after UV-irradiation and TPA-treatment. Int J Radiat Biol. 1992;61(2):205-11. doi:10.1080/09553009214550831.

Nijman SM, Luna-Vargas MP, Velds A, Brummelkamp TR, Dirac AM, Sixma TK, Bernards R. A genomic and functional inventory of deubiquitinating enzymes. Cell. 2005;123(5):773-86. doi:10.1016/j.cell.2005.11.007.

Nishimura K, Yokozaki H, Haruma K et al. Alterations of the APC gene in carcinoma cell-lines and precancerous lesions of the stomach. Int J Oncol 1995;7:587–592. doi:10.3892/ijo.7.3.587.

Oh C, Park S, Lee EK et al. Downregulation of ubiquitin level via knockdown of polyubiquitin gene Ubb as potential cancer therapeutic intervention. Sci Rep. 2013;3:2623. doi:10.1038/srep02623.

Okines AF, Thompson LC, Cunningham D et al. Effect of HER2 on prognosis and benefit from peri-operative chemotherapy in early oesophago-gastric adenocarcinoma in the MAGIC trial. Ann Oncol 2013;24(5):1253–1261. doi:10.1093/annonc/mds622.

Oliveira C, Pinheiro H, Figueiredo J et al. E-cadherin-alterations in hereditary disorders with emphasis on dereditary diffuse gastric cancer. Prog. Mol. Biol. Transl. Sci. 2013;116:337–359. doi:10.1016/B978-0-12-394311-8.00015-7

Oliveira C, Seruca R, Seixas M et al. The clinicopathological features of gastric carcinomas with microsatellite instability may be mediated by mutations of different "target genes": a study of the TGFbeta RII, IGFII R, and BAX genes. Am J Pathol. 1998;153(4):1211-9. doi:10.1016/s0002-9440(10)65665-9.

Park CW, Ryu KY. Cellular ubiquitin pool dynamics and homeostasis. BMB Rep. 2014;47(9):475-82. doi:10.5483/bmbrep.2014.47.9.128.

Paredes J Figuereido J, Albergaria A et al. Epithelial E- and P-cadherins: role and clinical significance in cancer. Biochim. Biophys. Acta 2012;1826(2):297–311. doi:10.1016/j.bbcan.2012.05.002.

Petroski MD, Deshaies RJ. Mechanism of lysine 48-linked ubiquitin-chain synthesis by the cullin-RING ubiquitin-ligase complex SCF-Cdc34. Cell. 2005;123(6):1107-20. doi:10.1016/j.cell.2005.09.033.

Pickart CM, Eddins MJ. Ubiquitin: structures, functions, mechanisms. Biochim Biophys Acta. 2004;1695(1-3):55-72. doi:10.1016/j.bbamcr.2004.09.019.

Radici L, Bianchi M, Crinelli R et al. Ubiquitin C gene: structure, function and transcriptional regulation. Advances in Bioscience and Biotechnology 2013;4:1057-1062 doi:10.4236/abb.2013.412141.

Raj A, Mayberry JF, Podas T. Occupation and gastric cancer. Postgrad Med J. 2003;79(931):252-258. doi:10.1136/pmj.79.931.252

Rawla P, Barsouk A. Epidemiology of gastric cancer: global trends, risk factors and prevention. Prz Gastroenterol. 2019;14(1):26-38. doi:10.5114/pg.2018.80001.

ResSeq NG_027722.2, NCBI reference sequence, GenBank database; 14 Oct. 2020

Rehman ASA, Kristariyanto YA et al. MINDY-1 Is a Member of an Evolutionarily Conserved and Structurally Distinct New Family of Deubiquitinating Enzymes. Molecular Cell. 2016;63. doi:10.1016/j.molcel.2016.05.009.

Renovanz M, Kim EL. Intratumoral heterogeneity, its contribution to therapy resistance and methodological caveats to assessment. Front. Oncol. 2014;4:142 doi:10.3389/fonc.2014.00142

Reyes-Turcu FE, Ventii KH, Wilkinson KD. Regulation and cellular roles of ubiquitin-specific deubiquitinating enzymes. Annu Rev Biochem. 2009;78:363-97. doi:10.1146/annurev.biochem.78.082307.091526.

Ryu KY, Baker RT, Kopito RR. Ubiquitin-specific protease 2 as a tool for quantification of total ubiquitin levels in biological specimens. Anal Biochem. 2006;353(1):153-5. doi:10.1016/j.ab.2006.03.038.

Ryu KY, Maehr R, Gilchrist CA et al. The mouse polyubiquitin gene UbC is essential for fetal liver development, cell-cycle progression and stress tolerance. EMBO J. 2007;26(11):2693-2706. doi:10.1038/sj.emboj.7601722

Ryu KY, Sinnar SA, Reinholdt LG et al. The mouse polyubiquitin gene Ubb is essential for meiotic progression. Mol Cell Biol. 2008;28(3):1136-1146. doi:10.1128/MCB.01566-07

Ryu KY, Garza JC, Lu XY et al. Hypothalamic neurodegeneration and adult-onset obesity in mice lacking the Ubb polyubiquitin gene. Proc Natl Acad Sci USA. 2008;105(10):4016-4021. doi:10.1073/pnas.0800096105

Sackton KL, Dimova N, Zeng X et al. Synergistic blockade of mitotic exit by two chemical inhibitors of the APC/C. Nature. 2014;514(7524):646-649. doi:10.1038/nature13660.

Saeki Y, Kudo T, Sone T et al. Lysine 63-linked polyubiquitin chain may serve as a targeting signal for the 26S proteasome. EMBO J. 2009;28:359–71. doi:10.1038/emboj.2008.305.

Sahtoe DD, Sixma TK. Layers of DUB regulation. Trends Biochem Sci. 2015;40(8):456-67. doi:10.1016/j.tibs.2015.05.002.

Santibañez M, Alguacil J, de la Hera MG et al. Occupational exposures and risk of stomach cancer by histological type. Occup Environ Med. 2012;69(4):268-75. doi:10.1136/oemed-2011-100071.

Shi D, Pop MS, Kulikov R et al. CBP and p300 are cytoplasmic E4 polyubiquitin ligases for p53. Proc Natl Acad Sci U S A. 2009;106(38):16275-16280. doi:10.1073/pnas.0904305106

Shin CH, Lee WY, Hong SW et al. Characteristics of gastric cancer recurrence five or more years after curative gastrectomy. Chinese Journal of Cancer Research 2016;28(5). doi:10.21147/j.issn.1000-9604.2016.05.05.

Skalniak L, Kocik J, Polak J et al. Prolonged Idasanutlin (RG7388) Treatment Leads to the Generation of p53-Mutated Cells. Cancers (Basel). 2018;10(11):396. doi:10.3390/cancers10110396

Singh K, Ghoshal UC. Causal role of Helicobacter pylori infection in gastric cancer: an Asian enigma. World J Gastroenterol. 2006;12(9):1346-1351. doi:10.3748/wjg.v12.i9.1346

Sitarz R, Skierucha M, Mielko J et al. Gastric cancer: epidemiology, prevention, classification, and treatment. Cancer Manag Res. 2018; 10:239-248. doi:10.2147/CMAR.S149619.

Sivamani E, Qu R. Expression Enhancement of a Rice Polyubiquitin Gene Promoter. Plant. Mol. Biol. 2006;60:225–239. doi:10.1007/s11103-005-3853-z

Sjodahl K, Lu Y, Nilsen TI et al. Smoking and alcohol drinking in relation to risk of gastric cancer: a population-based, prospective cohort study. Int. J. Cancer, 2007;120:128-132. doi:10.1002/ijc.22157

Tang Y, Geng Y, Luo J et al. Downregulation of ubiquitin inhibits the proliferation and radioresistance of non-small cell lung cancer cells in vitro and in vivo. Sci Rep. 2015;5:9476. doi:10.1038/srep09476

Smyth EC, Verheij M, Allum W et al. Gastric cancer: ESMO Clinical Practice Guidelines for diagnosis, treatment and follow-up. Annals of Oncology 2016;27(5):v38-v39. doi:10.1093/annonc/mdw350.

Teixeira LK, Reed SI. Ubiquitin ligases and cell cycle control. Annu Rev Biochem. 2013;82:387-414. doi:10.1146/annurev-biochem-060410-105307.

Thrower JS, Hoffman L, Rechsteiner M et al. Recognition of the polyubiquitin proteolytic signal. EMBO J. 2000;19(1):94-102. doi:10.1093/emboj/19.1.94

Tomioka N, Morita K, Kobayashi N et al. Array comparative genomic hybridization analysis revealed four genomic prognostic biomarkers for primary gastric cancers. Cancer Genet Cytogenet. 2010;201(1):6-14. doi:10.1016/j.cancergencyto.2010.04.017. PMID: 20633762.

Toyota M, Ahuja N, Suzuki H et al. Aberrant methylation in gastric cancer associated with the CpG island methylator phenotype. Cancer Res. 1999;59(21):5438-42. PMID: 10554013.

Toyota M, Ahuja N, Suzuki H et al. Aberrant methylation in gastric cancer associated with the CpG island methylator phenotype. Cancer Res. 1999;59(21):5438-5442. PMID: 10554013.

Tredaniel J, Boffetta P, Buiatti E et al. Tobacco smoking and gastric cancer: review and meta-analysis. Int. J. Cancer, 1999;72:565-573. doi:10.1002/(SICI)1097-0215(19970807)72:4<565::AID-IJC3>3.0.CO;2-O

Tsukamoto Y, Uchida T, Karnan S et al. Genome-wide analysis of DNA copy number alterations and gene expression in gastric cancer. J Pathol. 2008;216(4):471-482. doi:10.1002/path.2424. PMID: 18798223.

van Grieken NC, Aoyama T, Chambers PA et al. KRAS and BRAF mutations are rare and related to DNA mismatch repair deficiency in gastric cancer from the East and the West: results from a large international multicentre study. Br J Cancer. 2013;108(7):1495-1501. doi:10.1038/bjc.2013.109

Vassilev LT. Small-molecule antagonists of p53-MDM2 binding: research tools and potential therapeutics. Cell Cycle. 2004;3(4):419-21. PMID: 15004525.

Vihervaara A, Sergelius C, Vasara J et al. Transcriptional response to stress in the dynamic chromatin environment of cycling and mitotic cells. Proc Natl Acad Sci USA. 2013;110(36):E3388-E3397. doi:10.1073/pnas.1305275110.

Vermeulen K, Van Bockstaele DR, Berneman ZN. The cell cycle: a review of regulation, deregulation and therapeutic targets in cancer. Cell Prolif. 2003;36(3):131-49. doi:10.1046/j.1365-2184.2003.00266.x.

Voges D, Zwickl P, Baumeister W. The 26S proteasome: a molecular machine designed for controlled proteolysis. Annu Rev Biochem. 1999;68:1015-1068. doi:10.1146/annurev.biochem.68.1.1015.

Wang J, Maldonado MA. The ubiquitin-proteasome system and its role in inflammatory and autoimmune diseases. Cell Mol Immunol. 2006;3(4):255-61. PMID: 16978533.

Watson P, Vasen HFA, Mecklin JP et al. The risk of extra-colonic, extra-endometrial cancer in the Lynch syndrome. Int J Cancer. 2008;123(2):444-449. doi:10.1002/ijc.23508.

Wiborg O, Pedersen MS, Wind A et al. The human ubiquitin multigene family: some genes contain multiple directly repeated ubiquitin coding sequences. EMBO J. 1985;4(3):755-759. PMID: 2988935

World Cancer Research Fund/American Institute for Cancer Research (WCRF/AICR). Continuous Update Project Report: Diet, Nutrition, Physical Activity and Stomach Cancer 2016. Revised 2018.

Wu M, Semba S, Oue N et al. BRAF/K-ras mutation, microsatellite instability, and promoter hypermethylation of hMLH1/MGMT in human gastric carcinomas. Gastric Cancer 2004;7:246–253. https://doi.org/10.1007/s10120-004-0300-9

Yang W, Xia Y, Cao Y et al. EGFR-induced and PKCepsilon monoubiquitylation-dependent NF-kappaB activation upregulates PKM2 expression and promotes tumorigenesis. Mol. Cell. 2012;48: 771-784. doi:10.1016/j.molcel.2012.09.028

Yao T, Cohen RE. A cryptic protease couples deubiquitination and degradation by the proteasome. Nature. 2002;419(6905):403-407. doi:10.1038/nature01071.

Ye Y, Blaser G, Horrocks MH et al. Ubiquitin chain conformation regulates recognition and activity of interacting proteins. Nature. 2012;492(7428):266-270. doi:10.1038/nature11722

Youn HS, Baik SC, Cho YK et al. Comparison of Helicobacter pylori Infection between Fukuoka, Japan and Chinju, Korea. Helicobacter 1998;3:9-14. doi:10.1046/j.1523-5378.1998.08011.x

Zeng X, Sigoillot F, Gaur S et al. Pharmacologic inhibition of the anaphase-promoting complex induces a spindle checkpoint-dependent mitotic arrest in the absence of spindle damage. Cancer Cell. 2010;18(4):382-395. doi:10.1016/j.ccr.2010.08.010

Zeng X, King RW. An APC/C inhibitor stabilizes cyclin B1 by prematurely terminating ubiquitination. Nat Chem Biol. 2012;8(4):383-392. doi:10.1038/nchembio.801

Zhu L, Li Z, Wang Y et al. Microsatellite instability and survival in gastric cancer: A systematic review and meta-analysis. Mol Clin Oncol. 2015;3(3):699-705. doi:10.3892/mco.2015.506.